

1-1-2009

Effect of residual stresses and cold-straightening on the compressive resistance of solid round steel columns

Jin Xu

Ryerson University

Follow this and additional works at: <http://digitalcommons.ryerson.ca/dissertations>



Part of the [Civil Engineering Commons](#)

Recommended Citation

Xu, Jin, "Effect of residual stresses and cold-straightening on the compressive resistance of solid round steel columns" (2009). *Theses and dissertations*. Paper 897.

**EFFECT OF RESIDUAL STRESSES AND COLD-
STRAIGHTENING ON THE COMPRESSIVE RESISTANCE
OF SOLID ROUND STEEL COLUMNS**

By

Jin Xu, B.Eng

Ryerson University, 2007

A Thesis
Presented to Ryerson University
In partial fulfillment of the
Requirement for the degree of
Master of Applied Science
In the Program of
Civil Engineering
Toronto, Ontario, Canada, 2009
Jin Xu 2009©

Author's Declaration

I hereby declare that I am the sole author of this thesis.

I authorize Ryerson to lend this document to other institutions or individuals for the purpose of scholarly research.

Jin Xu

I further authorize Ryerson University to reproduce the document by photocopying or by other means, in total or part, at the request of other institutions or individuals for the purpose of scholarly research.

Jin Xu

Effect of Residual Stresses and Cold-Straightening
on the Compressive Resistance of
Solid Round Steel Columns
Jin Xu, 2009
Civil Engineering, Ryerson University
Toronto, ON, Canada

ABSTRACT

The objective of this research is to study the effects of residual stresses and cold-straightening on the compressive resistance of solid round steel columns. Thermal residual stresses in selected solid round sizes were determined from experimental study, finite element analysis, and previous research. In the experimental investigation, classical boring-out method using water-jet technology was applied on four samples with different diameters. Finite element models were constructed for the determination of thermal residual stresses for columns with 12 different diameters. The results were then compared with results obtained from a recent study on the prediction of symmetrical residual stresses in solid rounds using X-ray diffraction method. For the non-symmetrical residual stresses arising from cold-straightening, the equation developed by Nitta and Thurlimann was adopted in the finite element modeling to study the effect of non-symmetrical residual stresses on the compressive resistance of solid round steel columns. The Finite Element Analysis has been conducted on different bar diameter (1.5 inch to 12 inch diameter) and length, as well as initial out-of-straightness.

ACKNOWLEDGEMENTS

I wish to express my deep appreciation to my advisor Dr. Khaled Sennah at Ryerson University, for his constant support and valuable supervision during the development of this research. Dr. Sennah devoted his time and effort to make this study a success. His most helpful guidance is greatly appreciated.

The author wishes to greatly appreciate Mr. Dan Peneff for his continuous assistance throughout the experimental work.

Special thanks are due to Viking Engineering and Tool Company for supplying experimental equipment. Mr Guangzhao Wen, the technician in the company, is also acknowledged for his help in the experimental work.

TABLE OF CONTENT

ABSTRACT	iii
ACKNOWLEDGEMENTS.....	iv
TABLE OF CONTENTS	v
NOTATIONS.....	viii
LIST OF FIGURES.....	x
LIST OF TABLES.....	xiv
CHAPTER 1 INTRODUCTION.....	1
1.1 General	1
1.2 Need for Investigation	2
1.3 Objective of Study	3
1.4 Organization of Thesis	4
CHAPTER 2 LITERATURE REVIEW	5
2.1 General	5
2.2 Critical-Load Theory and Theory of Imperfect Column	5
2.2.1 Critical-Load Theory	5
2.2.2 Theory of Imperfect Column	7
2.3 Previous Study on Compressive Resistance of Steel Columns.....	8
2.3.1 Column Ultimate Strength Determined Theoretically and Experimentally	8
2.3.2 Influence of Residual Stress.....	10
2.3.3 Influence of Out-of-Straightness.....	11
2.3.4 Influence of Cold-Straightening	12
2.4 Available Standards for Solid Round Steel Column Design.....	13
2.4.1 Structural Stability Research Council (SSRC) Column Strength Curves.....	13
2.4.2 Canadian Standard (CSA-S37-01)	15
2.4.3 Eurocode 3.....	16
2.4.4 Proposed Equation by Sennah et al.	17

CHAPTER 3 EXPERIMENTAL PROGRAM	18
3.1 General	18
3.2 Material Properties	18
3.3 Methods.....	19
3.4 Test Set-Up.....	19
3.4.1 Water-jet Machine.....	20
3.4.2 Strain Gauges.....	20
3.4.3 Surface Preparation	21
3.4.4 Gage Installation	21
3.5 Test Procedures.....	22
3.6 Determination of Longitudinal Residual Stress.....	23
3.7 Finite Element Model	24
3.8 Residual Stress Distribution	25
3.9 Observations	26
3.10 Error Analysis	27
CHAPTER 4 FEA MODELS FOR RESIDUAL STRESS SIMULATION	28
4.1 General	28
4.2 Geometry and Model	28
4.2.1 Steel Properties.....	28
4.2.2 Analysis Procedure.....	29
4.2.3 Analysis Parameters.....	31
4.3 Results and Discussions	32
CHAPTER 5 COMPRESSIVE RESISTANCE OF SOLID ROUND STEEL COLUMNS WITH THE EFFECT OF INITIAL OUT-OF-STRAIGHTNESS	33
5.1 General	33
5.2 Geometry and Model	33
5.2.1 Slenderness Parameter	33
5.2.2 Initial Out-of-Straightness	34
5.2.3 Steel Properties.....	35

5.3	Analysis Procedure	36
5.4	Sensitivity Study	36
5.5	Results and Discussions	38
CHAPTER 6 COMPRESSIVE RESISTANCE OF SOLID ROUND STEEL COLUMNS WITH THE EFFECT OF SYMMETRICAL RESIDUAL STRESS		40
6.1	General	40
6.2	Geometry and Model	40
6.3	Symmetrical Residual Stress	40
6.4	Sensitivity Study	41
6.5	Results and Discussions	42
CHAPTER 7 COMPRESSIVE RESISTANCE OF SOLID ROUND STEEL COLUMNS WITH THE EFFECT OF NON-SYMMETRICAL RESIDUAL STRESS.....		44
7.1	General	44
7.2	Geometry and Model	44
7.3	Non-Symmetrical Residual Stress.....	44
7.4	Sensitivity Study	45
7.5	Results and Discussions	46
CHAPTER 8 CONCLUSIONS.....		48
REFERENCES.....		51
APPENDIX.....		112

NOTATIONS

A	Cross-sectional area of member
A_i	Cross-sectional area of the specimen after boring
C_r	Compressive resistance of a member
D	Diameter of Solid Steel Column
D_i	Diameter of the hole bored
d_o	Deflection at the mid-height of the column
E	Modulus of elasticity
EI	Elastic stiffness
E_r	Reduced modulus
E_t	Tangent modulus
F_u	Ultimate Compressive Strength
F_y	Yield stress
I	Moment of inertia of a section
K	Effective buckling length factor
L	Length of the solid round bar
N	Design value of axial compressive force
P_E	Euler buckling load
P_r	Reduced modulus load
P_t	Tangent modulus load
r	Radius of gyration about the plane of buckling
z	Distance from the bottom of column to where the lateral deflection is measured
α	Imperfection factor

β	Ratio of the cold-bending moment to the full plastic moment
Δ	Column displacement
ε	Strain
ε_i	average axial strain
φ	Resistance factor for compression
χ	Reduction factor according to the standard and buckling curves as used in Europe
λ	Slenderness parameter
σ_y	Yield stress of the material

LIST OF FIGURES

Figure 2-1: Behaviours of Perfect and Imperfect Columns.....	55
Figure 2-2: General Stress-Strain Relationship	55
Figure 3-1: A 2mm slice cut from specimen 1 for determination of elastic modulus and Poisson's ratio by ultrasound.....	56
Figure 3-2: Specimen Held in the Bed of Water-Jet Drilling Machine by a Special Holder.....	56
Figure 3-3: Water-Jet Machining System.....	57
Figure 3-4: Four Strain Gauges Attached to Specimen and Connected to Data-Acquisition System.....	57
Figure 3-5: Specimens after Installation of Strain Gauges and Application of Coating.....	58
Figure 3-6: Side View of Solid Steel Column	58
Figure 3-7: Side View of the Specimen Clamped by a Special Made Holder	58
Figure 3-8: View of a Steel Specimen with the Centre Part Drilled Through.....	59
Figure 3-9: View of a Steel Specimen Drilled up to Biggest Possible Diameter	59
Figure 3-10: View of Steel Specimens after Drilling Using Water-Jet Technology.....	60
Figure 3-11: View of FEA Model for Strain Calculation	61
Figure 3-12: Strain Variation on the Surface at the Mid-Height of Specimen 1 under 1 kN Internal Force	61
Figure 3-13: Strain Variation on the Surface at the Mid-Height of Specimen 2 under 1 kN Internal Force	62
Figure 3-14: Strain Variation on the Surface at the Mid-Height of Specimen 3 under 1 kN Internal Force	62
Figure 3-15: Strain Variation on the Surface at the Mid-Height of Specimen 4 under 1 kN Internal Force	63
Figure 3-16: Residual Stress Distribution for Sample 1 (D=1.5 inch, H=3 inch)	63
Figure 3-17: Residual Stress Distribution for Sample 2 (D=2.0 inch, H=3 inch)	64
Figure 3-18: Residual Stress Distribution for Sample 3 (D=2.5 inch, H=3 inch)	64
Figure 3-19: Residual Stress Distribution for Sample 4 (D=4.25 inch, H=3 inch)	65
Figure 4-1: Yield Stress vs. Temperature Relationship.....	66
Figure 4-2: Residual Stress History for 1.5 inch Diameter Steel Bar	66
Figure 4-3: Residual Stress History for 2.0 inch Diameter Steel Bar	67

Figure 4-4: Residual Stress History for 2.5 inch Diameter Steel Bar	67
Figure 4-5: Residual Stress History for 3.0 inch Diameter Steel Bar	68
Figure 4-6: Residual Stress History for 3.5 inch Diameter Steel Bar	68
Figure 4-7: Residual Stress History for 4.0 inch Diameter Steel Bar	69
Figure 4-8: Residual Stress History for 5.0 inch Diameter Steel Bar	69
Figure 4-9: Residual Stress History for 6.0 inch Diameter Steel Bar	70
Figure 4-10: Residual Stress History for 7.0 inch Diameter Steel Bar.....	70
Figure 4-11: Residual Stress History for 8.0 inch Diameter Steel Bar.....	71
Figure 4-12: Residual Stress History for 10.0 inch Diameter Steel Bar.....	71
Figure 4-13: Residual Stress History for 12.0 inch Diameter Steel Bar.....	72
Figure 5-1: Column with Initial Out-of-Straightness.....	73
Figure 5-2: ABAQUS Model Meshing for Steel Columns without Residual Stress or with Symmetrical Residual Stress	73
Figure 5-3: Effect of Number of Circles in the Cross Section on the Ultimate Load	74
Figure 5-4: Ultimate Load v.s Slenderness Parameter for 1.5 inch Diameter Column without Residual Stress	74
Figure 5-5: Ultimate Load v.s Slenderness Parameter for 2.0 inch Diameter Column without Residual Stress	75
Figure 5-6: Ultimate Load v.s Slenderness Parameter for 2.5 inch Diameter Column without Residual Stress	75
Figure 5-7: Ultimate Load v.s Slenderness Parameter for 3.0 inch Diameter Column without Residual Stress	76
Figure 5-8: Ultimate Load v.s Slenderness Parameter for 3.5 inch Diameter Column without Residual Stress	76
Figure 5-9: Ultimate Load v.s Slenderness Parameter for 4.0 inch Diameter Column without Residual Stress	77
Figure 5-10: Ultimate Load v.s Slenderness Parameter for 5.0 inch Diameter Column without Residual Stress	77
Figure 5-11: Ultimate Load v.s Slenderness Parameter for 6.0 inch Diameter Column without Residual Stress	78
Figure 5-12: Ultimate Load v.s Slenderness Parameter for 7.0 inch Diameter Column without Residual Stress	78
Figure 5-13: Ultimate Load v.s Slenderness Parameter for 8.0 inch Diameter Column without Residual Stress	79

Figure 5-14: Ultimate Load v.s Slenderness Parameter for 10 inch Diameter Column without Residual Stress	79
Figure 5-15: Ultimate Load v.s Slenderness Parameter for 12 inch Diameter Column without Residual Stress	80
Figure 5-16: Ultimate Load v.s Slenderness Parameter curves for Columns without Residual Stress and L/500 Initial Out-of-Straightness	80
Figure 6-1: Variations of axial residual stress along the radii	81
Figure 6-2: Variations of residual stress across the 4.25-inch diameter	81
Figure 6-3: Ultimate Load v.s Slenderness Parameter for 1.5 inch Diameter Column with Symmetrical Residual Stress	82
Figure 6-4: Ultimate Load v.s Slenderness Parameter for 2.0 inch Diameter Column with Symmetrical Residual Stress	82
Figure 6-5: Ultimate Load v.s Slenderness Parameter for 2.5 inch Diameter Column with Symmetrical Residual Stress	83
Figure 6-6: Ultimate Load v.s Slenderness Parameter for 3.0 inch Diameter Column with Symmetrical Residual Stress	83
Figure 6-7: Ultimate Load v.s Slenderness Parameter for 3.5 inch Diameter Column with Symmetrical Residual Stress	84
Figure 6-8: Ultimate Load v.s Slenderness Parameter for 4.0 inch Diameter Column with Symmetrical Residual Stress	84
Figure 6-9: Ultimate Load v.s Slenderness Parameter for 5.0 inch Diameter Column with Symmetrical Residual Stress	85
Figure 6-10: Ultimate Load v.s Slenderness Parameter for 6.0 inch Diameter Column with Symmetrical Residual Stress	85
Figure 6-11: Ultimate Load v.s Slenderness Parameter for 7.0 inch Diameter Column with Symmetrical Residual Stress	86
Figure 6-12: Ultimate Load v.s Slenderness Parameter for 8.0 inch Diameter Column with Symmetrical Residual Stress	86
Figure 6-13: Ultimate Load v.s Slenderness Parameter for 10 inch Diameter Column with Symmetrical Residual Stress	87
Figure 6-14: Ultimate Load v.s Slenderness Parameter for 12 inch Diameter Column with Symmetrical Residual Stress	87
Figure 6-15: Ultimate Load v.s Slenderness Parameter Curves for Columns with Symmetrical Residual Stress and L/500 Initial Out-of-Straightness	88
Figure 7-1: ABAQUS Model Meshing for Steel Columns with Non-Symmetrical Residual	

Stress	89
Figure 7-2: Non-Symmetrical Residual Stress Distribution along the Radius of Column	89
Figure 7-3: Ultimate Load v.s Slenderness Parameter for 1.5 inch Diameter Column with Non-Symmetrical Residual Stress	90
Figure 7-4: Ultimate Load v.s Slenderness Parameter for 2.0 inch Diameter Column with Non-Symmetrical Residual Stress	90
Figure 7-5: Ultimate Load v.s Slenderness Parameter for 2.5 inch Diameter Column with Non-Symmetrical Residual Stress	91
Figure 7-6: Ultimate Load v.s Slenderness Parameter for 3.0 inch Diameter Column with Non-Symmetrical Residual Stress	91
Figure 7-7: Ultimate Load v.s Slenderness Parameter for 3.5 inch Diameter Column with Non-Symmetrical Residual Stress	92
Figure 7-8: Ultimate Load v.s Slenderness Parameter for 4.0 inch Diameter Column with Non-Symmetrical Residual Stress	92
Figure 7-9: Ultimate Load v.s Slenderness Parameter for 5.0 inch Diameter Column with Non-Symmetrical Residual Stress	93
Figure 7-10: Ultimate Load v.s Slenderness Parameter for 6.0 inch Diameter Column with Non-Symmetrical Residual Stress	93
Figure 7-11: Ultimate Load v.s Slenderness Parameter for 7.0 inch Diameter Column with Non-Symmetrical Residual Stress	94
Figure 7-12: Ultimate Load v.s Slenderness Parameter for 8.0 inch Diameter Column with Non-Symmetrical Residual Stress	94
Figure 7-13: Ultimate Load v.s Slenderness Parameter for 10 inch Diameter Column with Non-Symmetrical Residual Stress	95
Figure 7-14: Ultimate Load v.s Slenderness Parameter for 12 inch Diameter Column with Non-Symmetrical Residual Stress	95
Figure 8-1: Comparison of Ultimate Strenth of Column without Residual Stress, with Symmetrical Residual Stress and Non-Symmetrical Residual Stress for 3" Diameter, 60" Length Column	96
Figure 8-2: Comparison of Ultimate Strenth of Column with Different Initial Deflection for 3" Diameter, 60" Length Column with Symmetrical Residual Stress	96
Figure 8-3: Comparison of Ultimate Strenth of Column with Different Slenderness Parameter for 3" Diameter with Symmetrical Residual Stress and L/500 Initial Deflection	97
Figure 8-4: Comparison of Ultimate Strenth of Column with Different Diameter for 60" Length, With Symmetrical Residual Stress and L/2000 Initial Deflection.....	97

LIST OF TABLES

Table 3-1: Dimensions of Specimens.....	98
Table 3-2: Strain Readings for Specimen 1	98
Table 3-3: Strain Readings for Specimen 2	99
Table 3-4: Strain Readings for Specimen 3	99
Table 3-5: Strain Readings for Specimen 4	100
Table 3-6: Strain Variation on the Surface at the Mid-Height of Specimen 1 under 1 kN Interl Force.....	100
Table 3-7: Strain Variation on the Surface at the Mid-Height of Specimen 2 under 1 kN Interl Force.....	101
Table 3-8: Strain Variation on the Surface at the Mid-Height of Specimen 3 under 1 kN Interl Force.....	101
Table 3-9: Strain Variation on the Surface at the Mid-Height of Specimen 4 under 1 kN Interl Force.....	102
Table 3-10: Residual Stress Distribution for Sample 1 (D=1.5 inch, H=3 inch)	103
Table 3-11: Residual Stress Distribution for Sample 2 (D=2.0 inch, H=3 inch)	104
Table 3-12: Residual Stress Distribution for Sample 3 (D=2.5 inch, H=3 inch)	105
Table 3-13: Residual Stress Distribution for Sample 4 (D=4.25 inch, H=3 inch).....	106
Table 5-1: Number of Circles on the Cross Section vs. Ultimate Load for Columns without Residual Stress	107
Table 5-2: Number of Elements in the Longitudinal Direction vs. Ultimate Load for Columns without Residual Stress	107
Table 6-1: Number of Circles in the Cross Section vs. Ultimate Load for Columns with Symmetrical Residual Stress.....	108
Table 6-2: Number of Elements in Longitudinal Direction vs. Ultimate Load for Columns with Symmetrical Residual Stress.....	108
Table 7-1: Ultimate Strenght to Yield Strength Ratio for 3 inch Diameter Column.....	109
Table 7-2: Number of Slices in the Cross Section vs. Ultimate Load for Columns with Non-Symmetrical Residual Stress	110
Table 7-3: Number of Elements in Longitudinal Direction vs. Ultimate Load for Columns	

CHAPTER 1

INTRODUCTION

1.1 General

Antenna towers are used throughout the world by the communications and other industries. From radio to high-speed wireless internet, mobile phones to navigation system, antenna towers are a critical part of modern wireless communication and other industries. Antenna towers are the best choice because they are relatively economical and effective for remote transmission, especially in North America where land area is large and distances among cities and towns are great. There are a variety of major types of antenna towers, including self-supporting, bracketed, guyed and rigid tube towers. Self-supporting towers are supported entirely by the tower structure and a solid cement or concrete base. They are usually with heights up to 120 m. Bracketed and guyed towers use either brackets or guy wires attached to adjacent buildings or anchors in order to provide support to the tower. Such type of antenna towers can be as high as up to 620 m. Rigid tube towers make use of a "lattice-style" rigid tube structure to provide internal support in a cross-bracing pattern for the entire height of the tower. While the most common use for antenna towers is mounting of communications devices, the same construction technologies are used for many other tower fixtures ranging from renewable energy to light fixtures. Rigid tube tower structures are popular for low sodium lighting installed at outdoor sporting fields and stadiums, and guyed or rigid tube construction is a popular method for remote installation of wind turbines or other alternative energy systems.

Solid round steel columns are commonly used as legs and also as diagonal and horizontal members of antenna towers. Steel bars with varying diameters are connected together by the joints welded or bolted. The towers are subjected to self-weight, snow load, wind load and also earthquake load in seismic area. Although the behaviour of a whole tower is rather complicated when subjected to these loads, the resultant forces in the members are mainly axial tension or compression. Therefore, the ultimate strength of solid round steel column is the most important consideration in the tower design. It should be noted that, the residual stresses in the steel columns, which may introduced during rolling, hear treatment, rotary straightening or other process, and may have significant influence on the behaviour of these members. For this reason, the properties of the members with residual stresses must be studied in order to get an optimized design while satisfying the safety requirements.

1.2 Need for Investigation

The behavior of members in tension is relatively simple compared to that of those in compression. The mostly used philosophy for steel compression member design at the present time is based on the ultimate compressive resistance of the members. Steel columns are conventionally classified as short, intermediate, or long members, and each category has an associated characteristic behavior. A short column is one, which can resist a load equal to the yield load. A long column fails by elastic buckling on which the maximum load depends only on the bending stiffness (EI) and length of the member. Columns in the intermediate range are most common in tower design. Failure is characterized by inelastic buckling and there are many factors affecting the compressive resistance of the members, such as, the properties of steel, the slenderness of the member,

the end constraints, the shape of the cross-section, initial deflection of the column, residual stress, etc.

Among all factors, initial thermal residual stress has critical effect on the behavior of compression members and a lot of work has been done about this topic. However, most of the work is about wide flange members. Few research has been done on solid round steel members. In compression members with initial residual stresses, early localized yielding occurs at some part of the cross section when the loading increases and the ultimate strength is appreciably reduced. Furthermore, the fatigue life will be shortened due to the presence residual stresses when the tower is subjected to dynamic loads such as wind load. Nitta and Thurlimann [1962a] has done some research in this area in 1960's at Lehigh University. Also, Ding [2000] and Mull [1999] recently carried out research work on residual stresses measurements and their effects on the compressive resistance of solid rounds. However, they did not study the whole range of column diameters and yield stress. Most recently, Sennah et al. (2009, 2008) proposed revised compressive resistance equation for solid rounds based on an extensive experimental study on 64 solid rounds between 1.5 inch to 4.5 inch in diameter. This proposed equation needed to be extended for solid rounds of diameters up to 12 inch as used in practice.

As a result, there is an urgent need to study the effect of residual stress and cold-straightening on the compressive strength of solid round steel columns. The present study uses both experimental and numerical techniques to estimate the residual stresses in solid round bars as well as the associated ultimate strength.

1.3 Objectives of Study

The objective of this research includes:

- Determination of residual stresses on solid round steel bars by the boring-out test using water-jet technology. Comparison of the results with available data on the same specimens using X-ray diffraction method (Roy, 2008).
- Simulation of formation of thermal residual stresses by the finite element method and comparison between experimental results and those from finite element modeling.
- Studying the effect of residual stresses and cold-straightening on the ultimate strength of solid round columns of different slenderness parameters.

1.4 Organization of Thesis

This thesis consists of eight chapters. In Chapter 1, the need for the study and the objectives of the research are presented. In Chapter 2, related literature on this research topic is reviewed for better understanding of the problem. Chapter 3 presents the experimental investigation of residual stress on solid round steel bars using boring-out method with water-jet technology. In Chapter 4, finite element models are used to simulate the residual stress development during the air cooling of hot-rolled steel bars. In Chapter 5, effect of cold-straightening on ultimate strength of columns is studied by utilizing the FEA models. The steel members are considered with no existing residual stress. In Chapter 6 and 7, the effect of symmetrical and non-symmetrical residual stress on the ultimate strength of columns is examined respectively. Finally, conclusions and recommendations for further research are given in Chapter 8.

CHAPTER 2

LITERATURE REVIEW

2.1 General

This chapter summarizes the previous study pertained to compressive resistance of axially loaded steel members emphasizing on solid steel columns. The literature review consists of critical-load theory, inelastic buckling of columns, imperfect columns, compressive strength of columns with influence of residual stress, out-of-straightness and cold-straightening, and prediction of compressive strength with respective of American Specification, Canadian Standard and European Code.

2.2 Critical-Load Theory and Theory of Imperfect Column

Column strength can be approximated by considering theoretically either (1) a column with mathematically perfect geometry and perfect centroidal loading: critical load theory, and (2) a column in which the geometry and/or the loading deviate slightly from the perfect: theory of imperfect columns. For practical purposes, some types of columns (eg., cold-formed steel columns) can be idealized as perfect, while for other columns (eg., hot-rolled or welded built-up structural steel columns), it is necessary to consider the effects of the imperfections.

2.2.1 Critical-Load Theory

The strength of a perfectly straight prismatic column with perfect central loading and well-defined end restraints is Euler load, P_E , as long as the material is still elastic when buckling occurs (Galambos, 1998):

$$P_E = \frac{\pi^2 EI}{(KL)^2} \quad (2-1)$$

Where,

EI is the elastic stiffness

L is the length of the column

K is the effective length factor

When the axial load attains P_E , a stable equilibrium configuration is possible even in the presence of lateral deflection (Figure 2.1a) while the load remains essentially constant (Figure 2.1b path OAB). Even if an initial deflection, and/or an initial load eccentricity is present, the maximum load will approach the Euler load asymptotically as long as the material remains elastic (curve C in Figure 2.1b)

Many practical columns are in a range of slenderness where at buckling portions of the columns are no longer elastic. The stiffness of the column is reduced by yielding, which may be a result of the nonlinearity in the material itself or it may be due to partial yielding of the cross section at points of compressive residual stress. The post-buckling behavior of such a column is radically different from the elastic column. Bifurcation bulking occurs at the tangent modulus load, point D in Figure 2.1c,

$$P_t = \frac{\pi^2 E_t I}{(KL)^2} \quad (2-2)$$

Where, E_t is the tangent modulus, which is the slope of the stress-strain curve at a load level (Figure 2.2) when the material is non-linear.

Further lateral deflection is possible only if the load increases. If there are no further changes in stiffness due to yielding, the load would asymptotically approach the reduced modulus load as the deflection becomes large, (Point E in Figure 2.1c):

$$P_r = \frac{\pi^2 E_r I}{(KL)^2} \quad (2-3)$$

Where, E_r is the reduced modulus.

The increase in load is due to the elastic unloading of some fibers in the cross section, which results in an increase in stiffness. In presence of residual stress, E_t and E_r depend on the shape of the cross-section. Since increased loading beyond the tangent modulus load results in further yielding, stiffness continues to be reduced and the load-deflection curve achieves a peak (P_{max}) point E in Figure 2.1c beyond which it falls off.

2.2.2 Theory of Imperfect Column

Geometric imperfections, in the form of tolerable but unavoidable out-of-straightness of the column and/ or eccentricity of the axial load, will introduce bending moment from the onset of loading, and curve G in Figure 2.1c characterizes the performance of such a column. Lateral deflection exists from the start of loading, and the maximum load is reached when the internal moment capacity at the critical section is equal to the external moment caused by the product of the load and the deflection. The maximum load is thus a function of the imperfection. For some types of columns the nature of the problem is such that the maximum capacity of the imperfect column is closely approximated by the tangent modulus load of the perfect column, but for many types of columns the imperfections must be included to give a realistic maximum load. In

general, the strength of columns must be determined by including the imperfections and the material nonlinearity and/or the residual stress effects. The effect of residual stress and out-of straightness are two major considerations and the study results about this area are presented in the following section.

2.3 Previous Study on Compressive Resistance of Steel Columns

2.3.1 Column Ultimate Strength Determined Theoretically and Experimentally

Steel columns are conventionally classified as short, intermediate, or long members, and each category has an associated characteristic type of behavior. A short column is one, which can resist a load equal to the yield load. A long column fails by elastic buckling on which the maximum load depends only on the bending stiffness and length of the member. Columns in the intermediate range are most common in steel structures. Failure is characterized by inelastic buckling and is greatly influenced by the magnitude and pattern of residual stresses, the magnitude and shape of the initial imperfections and end restraints. These effects lessen for both shorter and longer columns.

To take into account these effects, a computerized maximum strength analysis was performed at Lehigh University on W-shaped and hollow column section. Next, a set of 112 column curves was generated for members whose residual-stress distributions were available, assuming an initial crookedness of 1/1000 of the column length and zero end restraint. Bjorhovde grouped the whole spectrum of column behavior to three column curves known as Structural Stability Research Council (SSRC) Column Strength Curves 1, 2 and 3 (Galambos, 1998).

In a pilot investigation conducted from 1954 to 1956, the behavior of 70 mm diameter stress-relieved bars was studied experimentally (Fujita and Driscoll 1962). Nine axially loaded column tests were performed. The slenderness ratios of these columns ranged from 30 to 73. Comparison with the tangent modulus concept for axially loaded columns, and with an inelastic strength theory for the eccentrically loaded columns, showed that the ultimate strength of solid round columns might be predicted adequately by theory.

Latter, Galambos and Ueda (1962) reported testing four axially loaded solid round columns of 190.5 mm diameter and slenderness ratios of 52, 61, 66 and 67, respectively. All four columns were free of thermal residual stresses. However, one column of each steel contained relatively high cold-straightening residual stresses, whereas the second column of each steel was essentially free of residual stresses. Then, Galambos (1965) added the results of the experimental ultimate axial compressive strength of thirteen solid rounds with diameter 70 mm and slenderness ratios ranging from 30 to 62. Four columns were made of stress-relieved steel, while the other nine columns had residual stresses from the manufacturing process and/or cold-straightening.

Most recently, Mull (1999) experimentally determined the compressive resistance of forty steel solid round specimens for five different diameters ranging from 31.75 mm to 57.15 mm. Results showed that only sixteen of the forty specimens had load eccentricities less than or equal to 1/500th of the effective length of the specimen. For these sixteen specimens, the ratio of the resistance computed from the superseded Canadian Standard "Limit States Design of Steel Structures", CAN/CSA-S16.1-94 (CSA, 1994) to the experimental failure loads ranged from 0.98 to 0.79 and, for resistances

computed from AISC-LRFD Specification (1993), the ratios ranged from 1.10 to 0.89. Sennah and Wahba (2002) tested six solid rounds of 109.5 mm diameter and 762 mm length of slenderness ratio of 20. Three of these columns were typical and made of stress-relieved steel. The other three columns were similar but made of non-stress-relieved steel. They concluded that CSA-S37-01(CSA, 2001) specifies the compressive resistance of solid round columns, which is conservative by about 20% in case of non-stress-relieved steel and 23% in case of stress-relieved steel. Also, they concluded that AISC-LRFD Standard is conservative by about 14% in case of non-stress-relieved solid rounds and by 24% in case of stress-relieved solid rounds.

2.3.2 Influence of Residual Stress

Residual stresses in structural steel shapes and plates result primarily from uneven cooling after rolling of hot-rolled steel column. The quick cooling parts of sections when solidified resist further shortening, while those parts that are still hot tend to shorten further as they cool. The net result is that the area that cooled more quickly has residual compressive stresses, while the slower cooling areas have residual tensile stresses. In the elastic region, residual stresses and initial crookedness have a significant influence on the strength of solid round bars. These stresses are of particular importance for columns with slenderness ratio varying from approximately 40 to 120, a range that includes a very large percentage of real-world columns. For materials which are quenched without stress relieving, the effect of residual stresses is significant (Galambos 1965). A few authors (among them: Hetenyi, 1957; Watanabe et al., 1955; Bühler, 1954; Ding, 2000) measured experimentally the residual stress in cylindrical steel columns by the boring-out technique.

According to the study by Nitta and Thürlimann (1962b) on the effect of thermal residual stress caused by water quenching, for example, carry approximately a 10 to 20% lower load than air-cooled or stress-relieved steel columns, provided that the generalized slenderness ratio and initial deflections are the same. Most recently, Ding (2000) used the classical boring-out method to determine residual stresses on fourteen samples of hot-rolled solid round steel bars of diameters ranging from 38.1 to 152.4mm. He reached the conclusion that initial residual stress can result in remarkable loss of ultimate strength of a column, especially when the slenderness parameter of the column is greater than 0.88. A few authors utilized analytical and numerical simulation techniques, such as the finite-element method, to predict residual stresses produce by the manufacturing process (Jahanian, 1995; Toparli and Aksoy, 1991; Kamamoto et al., 1985; Weiner and Huddleston, 1959).

Fujita and Driscoll (1962) solved graphically the ultimate strength of H-shape and built-up columns including the effect of residual stresses due to welding. Since these particular solutions are not applicable to any other cross sectional shapes in which the magnitude and the distribution pattern of residual stresses are different, further studies are necessary in order to visualize the true column behavior until failure occurs.

2.3.3 Influence of Out-of-Straightness

The initial out-of-straightness (also referred to as initial crookedness or initial curvature) also affects the primary column strength. The analysis of the strength of inelastic, initially curved columns has either made use of assumed values and shapes of the initial out-of-straightness, or can use actually measured data. The former is the most common, mostly because the measurements that are available for columns are rare. This

applies in particular to the magnitude of the maximum out-of-straightness, normally assumed to occur at mid-height of the member. The latter is usually thought to that of half-sine wave (Batterman and Johnston, 1967; Bjorhovde and Tall, 1971). The results obtained by the studies of Batterman and Johnston (1967) showed that the separate effects of residual stress and initial curvature cannot be added to give a good approximation of the combined effects on the maximum column strength. Residual stresses have little effect on the maximum strength of very slender columns, either straight or initially crooked, which have strength approaching the Euler load. However, such columns made of high-strength steel can tolerate much greater lateral deflection before yielding or becoming unstable. The differences in column strength, caused by variations in the shape of the residual stress pattern, are smaller for initially curved columns than for initially straight columns.

2.3.4 Influence of Cold-Straightening

The strength of cold-straightened columns is, in general, greater than that of the corresponding as-rolled members because of the improved straightness and redistribution of residual stress (Alpsten 1970). According to the study by Nitta and Thürlimann (1962a) on the effect of cold-straightening on the ultimate strength of circular columns, the tangent modulus concept cannot be used for prediction of cold-straightening columns, as there exists no bifurcation point in the load-deflection curve of cold-straightened column, which contains antisymmetric residual stress. The strength depends upon the magnitude of the cold-straightening residual stresses and the out-of-straightness remaining after cold-straightening operation. Fujita and Driscoll (1962) tested nine axially loaded bars and two eccentrically loaded bars (eight USS "T-1" constructional alloy steel bars and

one structural carbon steel bars and one structural carbon steel bar). The bars were of 70mm in diameter, with slenderness ratio (KL/r) ranging from 30 to 73. The bars were cold straightened and subsequently stress-relieved, followed by air-cooling. Comparison with the theory based on the “tangent modulus” concept for axially loaded column, and with an inelastic strength theory for the eccentrically loaded columns shows that the ultimate strength of solid round columns may be predicted adequately by the tangent modulus concept.

2.4 Available Standards for Solid Round Steel Column Design

2.4.1 Structural Stability Research Council (SSRC) Column Strength Curves

Bjorhovde (1972) examined the deterministic and probabilistic characteristics of column strength in general and developed an extensive database for the maximum strengths of centrally loaded compression members, covering the full practical range of shapes, steel grades, and manufacturing methods. This study resulted in a collection of 112 maximum-strength column curves. Then, these curves were subdivided into groups of curves with a mean or similar curve for each group. The latter defines the Multiple Column Curve Concept (Bjorhovde and Tall, 1971; Bjorhovde, 1972). This resulted in three curves known as SSRC column strength curves 1, 2 and 3. None of these column curves covered solid round columns. However, based on limited experimental research on the compressive resistance of solid rounds carried out as far back as to 1965 (Galambos, 1965), the superseded version of the Canadian Standard for Antennas, Towers, and Antenna-Supporting Structures, CSA-S37-94, assumed the applicability of Column Strength Curve 2 of the Structural Stability Research Council (Galambos, 1998) to hot-rolled solid round bars 51 mm in diameter and less and to hot-rolled solid rounds

greater than 51 mm in diameter that are stress-relieved to manufacturer's recommendations after initial cold-straightening at the mill.

It should be noted that the resulting equations of the SSRC Column Strength Curve 2, equations 1 to 5 listed below, were obtained for W-shapes and hollow structural sections as follows:

$$0 \leq \lambda \leq 0.15 \quad C_r = \phi \cdot A \cdot F_y \quad (2-4)$$

$$0.15 < \lambda \leq 1.0 \quad C_r = \phi \cdot A \cdot F_y [1.035 - 0.202\lambda - 0.222\lambda^2] \quad (2-5)$$

$$1.0 < \lambda \leq 2.0 \quad C_r = \phi \cdot A \cdot F_y [-0.111 + 0.636\lambda^{-1} + 0.087\lambda^{-2}] \quad (2-6)$$

$$2.0 < \lambda \leq 3.6 \quad C_r = \phi \cdot A \cdot F_y [0.009 + 0.087\lambda^{-2}] \quad (2-7)$$

$$3.6 < \lambda \leq 5.0 \quad C_r = \phi \cdot A \cdot F_y [\lambda^{-2}] \quad (2-8)$$

where:

$$\lambda = \frac{KL}{r} \sqrt{\frac{F_y}{\pi^2 E}}; \quad F_y = \text{yield stress}; \quad \phi = \text{resistance factor}; \quad A = \text{cross-sectional area}; \quad \lambda =$$

slenderness function; L = length of member; r = radius of gyration; K = effective length factor; E = modulus of elasticity.

Also, the CSA-S37-94 presented expressions of the compressive resistance of solid round bars greater than 51 mm in diameter and not stress-relieved after cold straightening, based on Column Strength Curve 3 of the Structural Stability Research Council (Galambos 1998).

$$0 < \lambda \leq 0.8 \quad C_r = \phi \cdot A \cdot F_y [1.093 - 0.622\lambda] \quad (2-9)$$

$$0.8 < \lambda \leq 2.3 \quad C_r = \phi \cdot A \cdot F_y [-0.128 + 0.707\lambda^{-1} - 0.102\lambda^{-2}] \quad (2-10)$$

$$2.3 < \lambda \leq 5.0 \quad C_r = \phi \cdot A \cdot F_y [0.008 + 0.792\lambda^{-2}] \quad (2-11)$$

2.4.2 Canadian Standard (CSA-S37-01)

Most recently, the Canadian Standard for Antennas, Towers, and Antenna Supporting Structures, CSA-S37-01, introduced some modifications to the expressions found in the superseded version of 1994 for compressive resistance of solid rounds. These modifications were based on results of testing a limited number of solid rounds back to 1965. The factored axial compressive resistance, C_r , of a member is determined by the following formula:

$$C_r = \phi \frac{AF_y}{[1 + \lambda^{2n}]^{1/n}} \quad (2-12)$$

where:

$n = 1.34$ for hot-rolled round bars 51 mm in diameter and less, and hot-rolled solid round bars greater than 51 mm in diameter and stress relieved to manufacturer's recommendations after initial cold straightening at the mill.

$n = 0.93$ for hot-rolled solid round bars greater than 51 mm in diameter and not stress relieved after cold straightening.

It should be noted that earlier versions of the Canadian Standard "Limit States Design of Steel Structures" adopted Equations 2-4 to 2-11 for solid round columns until the 1994 version of the standard. However, the current standard "CAN/CSA-S16-01" (2003) omitted these equations due to insufficient data in the literature that supports them for the design of solid rounds. According to the AISC-LRFD, "Load and Resistance Factor Design Specifications for Structural Steel Buildings", the compressive resistance of structural steel members of different shapes is given by:

$$C_r = \phi \cdot A \cdot F_{cr} \quad (2-13)$$

where,

$$F_{cr} = \left[0.658^{\lambda^2} \right] F_y \quad \text{for } \lambda \leq 1.5, \text{ and} \quad (2-14)$$

$$F_{cr} = \left[\frac{0.877}{\lambda^2} \right] F_y \quad \text{for } \lambda > 1.5 \quad (2-15)$$

It should be noted that equations 2-14 and 2-15 represent SSRC Column Strength Curve 2 and assumed applicable for solid round steel columns by the American Standard for Antenna Supporting Structures and Antennas, TIA-222-G.2005 (ANSI, 2005).

2.4.3 Eurocode 3

The European Standard for the design of steel structures, Eurocode 3, (CEN, 2003) specifies rules relating to ultimate limit state analysis of the buckling resistance of steel linear members and frames susceptible to loss of stability in which buckling will take place, using the following equation:

$$\frac{N_{Ed}}{N_{b,Rd}} \leq 1 \quad (2-16)$$

where N_{Ed} is design value of the compressive force, $N_{b,Rd}$ is the design buckling resistance of the compression member as obtained from the following equation:

$$N_{b,Rd} = \frac{\chi \cdot A \cdot F_y}{\gamma_{M1}} \quad (2-17)$$

where A is the column cross-sectional area, F_y is the steel yield strength, γ_{M1} is a partial safety factor of 1.1, and χ is a reduction factor for the relevant buckling mode. The value

χ for the appropriate non-dimensional slenderness parameter, λ_K , should be determined from the relevant buckling curve according to:

$$\text{if } \bar{\lambda}_k \leq 0.2; \quad \chi = 1 \quad (2-18)$$

$$\text{if } \bar{\lambda}_k > 0.2; \quad \chi = \frac{1}{k + \sqrt{k^2 - \bar{\lambda}_k^2}} \quad (2-19)$$

where $k = 0.5[1 + \alpha(\bar{\lambda}_k - 0.2) + \bar{\lambda}_k^2]$ and α is the imperfection factor being taken as 0.49 for solid round columns. It should be noted that Eurocode 3 specifies that buckling effects may be ignored (i.e. $\chi = 1$) and only cross sectional check applies if slenderness parameter $\lambda_K \leq 0.2$.

2.4.4 Proposed Equation by Sennah et al.(Sennah et al., 2007a and Sennah et al., 2007b)

Dr. Sennah from Ryerson University and his group has recently conducted a test program on the compressive resistance of non-stress-relieved and stress-relieved steel solid rounds. Thirty-three non-stress-relieved steel bars and twenty stress-relieved bars have been tested to collapse. A proposed compressive resistance equation for economical design of such columns has been concluded. The equation is similar to CSA-S37-01 Equation but with the parameter n of 1.7.

$$C_r = \phi \frac{AF_y}{[1 + \lambda^{2n}]^{1/n}} \quad (2-20)$$

where n=1.7 for non-stress relieved solid rounds of diameter 190mm and less and stress-relieved solid rounds.

CHAPTER 3

EXPERIMENTAL PROGRAM

3.1 General

Thermal residual stresses of round steel columns with four different diameters were determined by experimental investigation. The specimens were supplied by Electronic Research Inc; (ERI), Sioux City, IA, USA. The dimensions of each specimen are shown in Table 3-1.

3.2 Material Properties

The elastic properties of the specimens were measured previously by Dr. George Roy from Ministry of Natural Resources (Roy, 2008). Two elastic material properties, modulus of elasticity, E , and Poisson's ratio, ν , were measured on a stress-annealed, round, and thin specimen, see Figure 3-1. The stress annealing was carried out through heat treatment as follows (Roy, 2008):

1. Place all the specimens in the furnace at room temperature.
2. Evacuate air and replace with Argon (to avoid oxidation).
3. Raise the furnace temperature to 690°C.
4. Maintain the temperature for 30 minutes.
5. Furnace-cool in Argon until room temperature.

The elastic properties were determined non-destructively by ultrasonic measurements of pitch-and-catch time for longitudinal and shear waves and density measurements of the steel; shear waves were launched along the 1-3 and 2-4 directions

showed in Figure 3-1. Analysis of the measurements indicated that E and ν are 200 GPa and 0.3, respectively. Also, the yield stress, F_y , of specimens is 345MPa.

3.3 Test Methods for Residual Stress Measurements

There is an abundance of different methods, but a few of them merit a particular attention in determining stress states in structural components: 1) X-ray Diffraction Method 2) Hole Drilling Method, and 3) Slitting Method. A few other methods, such as 4) Magnetic Barkhausen Noise Method, 5) Ultrasonic Method and 6) Neutron Diffraction Method, can be considered as well. However, methods 1 to 3 can be applied to measure stresses in small areas and on site, in particular at weld stress concentration, whereas methods 4 to 6 can be used to measure either stresses averaged over a large volume of material, or equipment that is not transportable at all. Since in the majority of engineering structures, the degradation of material originates in small areas at the surface, methods in 1 to 3 will be mainly considered. Among them, the water-jet drilling method was chosen in this study for the determination of residual stresses in the solid round steel columns. The philosophy of hole drilling method is that, after taking out some part of the material with residual stresses, the stresses will be released and the stresses in the remaining part will change to a new equilibrium. By measuring the strain changes, the residual stresses in the taken-out part can be calculated.

3.4 Test Set-Up

The tests were conducted at the workshop of Viking Engineering and Tool Company of Toronto, Ontario. The specimens were held in the bed of a water-jet drilling

machine (Figure 3-2). Four strain gauges were attached to each specimen and connected to a data-acquisition system.

3.4.1 Water-jet Machine

The water-jet drilling technique has been in use since 1970. Nowadays, water-jets are widely used in the automobile, aerospace, and glass industries, to name a few, to create precision parts from hard-to-cut materials. A water jet machining system (Figure 3-3) uses water that is pressurized to 40, 000 psi or even higher pressure and then forced through a small orifice. Garnet abrasive is then pulled into this high-speed stream of water and mixed with the water in long carbide mixing tube. A stream of abrasive-laden water moving more than 1000 feet per second (300m/s), exits the carbide mixing tube. This jet of water and abrasive is then directed at the material to be machined. The main advantage of water-jets over other machining methods is that no heat generated during machining process. Water-jets abrade material at room temperatures. As a result, there are no heat-affected areas or structural changes in material.

3.4.2 Strain Gauges

Electric resistance strain gauges, type C2A-06-250LW-120, with a gage length of 5 mm, electric resistance of 120 Ω , and a gage factor of 2.075, were chosen to measure the strains on the outer surface of the specimen. A properly polished, cleaned surface was prepared for each strain gage before fixing it to the specimen. For each specimen, four strain gages were installed on the cylinder surface as shown in Figure 3-4. The four strain

gages were 90° apart on the transverse plane in the middle of the sample. The strains were recorded with quarter-bridge circuit.

3.4.3 Surface Preparation

The steel surface preparation is meant to develop a chemically clean surface having a roughness appropriate to the gage installation requirements, a surface alkalinity corresponding to a pH of 7 or so, and visible gage layout lines for locating and orienting the strain gages. First of all, the surface of each specimen was abraded by grinder machine and a series of different grid sanding paper to remove the rust, oxides and any residual material on the surface; and to develop a surface texture suitable for bonding. Solvent degreasing was performed following to remove oils, greases, organic contaminants and soluble chemical residues. The acetone was applied by low lint wipe paper on an area of approximately 1 in². After degreasing, the gage-location layout lines was marked on the surface of specimen with a pair of crossed reference lines at the point where the strain gage is to be attached. The lines were made perpendicular to each other, with one line oriented in the direction of strain measurement, which is the longitudinal direction of steel specimen. After the layout lines were marked, M-Prep Conditioner A was applied repeatedly, and the surface scrubbed with cotton-tipped applicators until a clean tip is no longer discolored by the scrubbing. The neutralizer was applied the same manner in advance.

3.4.4 Strain Gage Installation

After the surface of sample has been properly polished and prepared, the strain gages were attached to the outer surface of the sample with special adhesive at the

specific locations. It should be noticed that the catalyst has been used to stimulate the hardening of adhesive. A special water resistance coating was also applied after the adhesive was hardened and was left for at least 24 hours before submerging in water, in order to avoid water disturbance to strain readings during successive drilling steps. The samples after installation of strain gages are shown in Figure 3-5.

3.5 Test Procedures

- Surface Preparation: Use grinder machine and abrasive papers to polish the steel column surface where the strain gages are to be attached.
- For each steel column, four strain gages were attached with special adhesive. The strain gages were located as 90 degree apart on the transverse plane in the middle of the specimen as shown in Figure 3-6.
- After the adhesive and coating completely hardened, the steel column was properly clamped in the bed of water-jet machine by special made holders as shown in Figure 3-7. The two holders were of the same height as the specimens, which were 3 inch height. The reason of leaving the middle part of V-shape arms open is to avoid pressure applied on strain gages by holders. Also, the wires can go through the holders and to be connected on DataScan System.
- The strain gages were then connected to the DataScan system with shielded wires. The strain readings of the four gauges were set to zero when the readings become stable after installation.
- Drill the specimen at the centre (Figure 3-8) up to the possible biggest diameter (Figure 3-9), following the diameters in tables Table 3-2 to 3-5 for specimen 1 to

4 respectively. After each drilling, wait for 3 to 5 minutes until the strain becomes steady, and then take the readings of each strain gage. The readings of the four strain gages should be set to zero again before the next drilling. The measured strains of gages 1 to 4 are also shown in Table 3-2 to 3-5 respectively. Pictures of samples after drilling was taken and one of them is shown in Figure 3-10.

3. 6 Determination of Longitudinal Residual Stress Distribution

For solid round columns with large length-diameter ratio (>20) used in structures, the residual stresses in longitudinal direction are more important than those in other directions. Therefore for simplicity, only longitudinal residual stresses are considered when analyzing such structures. In this study, the focus is on longitudinal stresses and radial and tangential stresses are ignored.

For a solid cylinder with outer diameter of D , the diameter of inner co-axial hole bored is D_i , and the average axial strain is ε_i . The force released by the inner drilled part is

$$F_i = A_i \cdot \varepsilon_i \cdot E \quad (3-1)$$

Where A_i is the cross-sectional area of the specimen after boring,

$$A_i = \frac{\pi}{4}(D^2 - D_i^2) \quad (3-2)$$

E is the modulus of elasticity of steel.

If a slightly larger hole of diameter D_{i+1} is drilled and ε_{i+1} is the measured strain after drilling, the force released by the part between D_i and D_{i+1} is

$$\Delta F_{i+1} = F_{i+1} - F_i = E \cdot (A_{i+1} \cdot \varepsilon_{i+1} - A_i \cdot \varepsilon_i) \quad (3-3)$$

The average residual stress in axial direction is

$$\sigma_{i+1} = \frac{\Delta F_{i+1}}{\Delta A_{i+1}} \quad (3-4)$$

in which $\Delta A_{i+1} = A_i - A_{i+1}$

The formula for longitudinal residual stress calculation is hence

$$\sigma_{i+1} = \frac{E \cdot (A_{i+1} \cdot \varepsilon_{i+1} - A_i \cdot \varepsilon_i)}{A_i - A_{i+1}} \quad (3-5)$$

Equation (3-5) assumes that the strain ε_i is uniform over the remaining cross-section. However, this is not true and a more accurate relationship between the force released and the strain measured at mid-height of the specimen can only be obtained by finite element analysis. For this reason, finite element modeling for each drilling step was used to determine the force released.

The formula (3-1) turns to be

$$F_i = \varepsilon_i / \varepsilon_{oi} \quad (3-6a)$$

$$\text{and } F_{i+1} = \varepsilon_{i+1} / \varepsilon_{oi+1} \quad (3-6b)$$

where ε_{oi} is the strain when unit internal force is applied to the specimen after *i*th boring.

Then the residual stress will be

$$\sigma_{i+1} = (F_{i+1} - F_i) / (A_i - A_{i+1}) \quad (3-7)$$

3.7 Finite Element Model

For specimen with different diameters, different models were established for the analysis. For the axisymmetry of the cylinders (Figure 3-6), the analysis was carried out using 8-node axisymmetric element type (CAX8R) with reduced integration scheme provided by ABAQUS software (Hibbett et al, 2008). The element mesh is shown in

Figure 3-11. Distributed surface forces were applied on the inner surface to simulate the interaction between the drilled-out part and remaining part. The strains at the middle of outer surface were obtained for the finite element analysis. In order to reduce the total number of nodes, only a quarter of the total area was modeled for analysis by applying proper boundary conditions. To reduce the shear locking problem in finite elements, the second-order elements with reduced integration were used. Appendix A is an example of input file for ABAQUS analysis. The results for specimens are shown in Table 3-6 to 3-9 and Figure 3-12 to 3-15. It is noted that, for the 4.25 inch diameter specimen, the strains are negative when the inner diameters are not big enough though the forces applied are drag. This is due to the moment effect when the forces are not at the center of geometry.

3.8 Residual Stress Distribution

The procedure for analyzing the data obtained is as follows,

1. The strains for each drilling step were the difference between the step readings and the original ones when no hole was drilled.
2. Four strains for each drilling were averaged and this averaged strain was selected for the calculation of residual stresses.
3. For every averaged strain, the force released by the total area taken out was computed by using the finite element simulation results.
4. The difference between two successive forces was the force released by the area bored out in the step.
5. Finally, the residual stress was calculated by dividing the force released by the area bored.

6. The residual stress distribution was obtained by correlating the residual stress with corresponding normalized radius.

The residual stress distribution calculated from the tests are shown in Table 3-10 to Table 3-14 and Figure 3-16 to 3-19. The details of calculations are shown in Appendix B: Sample Calculation for Residual Stress Distribution. It should be noted that, the readings of gage 3 of Sample 3, gage 3 of Sample 4 were not selected for the calculation of averaged strains. The reason is that these readings are negative, which are obviously unrealistic since the samples are under compression. The error may be caused by the water leakage during the drilling which can damage the strain gage. The readings of gage 4 of Sample 3 were not available due to the improper installation of strain gage.

3.9 Observations

From the results above, it is observed that,

1. For Samples 1, 2 and 3, the residual stress distributions are similar. The inner part of the solid is in tension and the outside part is in compression.
2. For Sample 4, the calculated residual stress shows erroneous oscillations when the diameter of the hole is large compared to the specimen diameter ($R_i/R > 0.6$).
3. The specimens with larger diameter have relatively greater residual stress than those with smaller diameters.
4. The compressive residual stress at the outer surface is very small compared with the tension at the inner surface. This is because the drilling was not performed for larger diameter due to the technical limitation: the thickness of the hollow

cylinder was too thin to maintain the holding condition. If the drilling can be continued up to specimen diameter, the trend line of residual stress should go down more to the negative zone and shows larger compression stress.

3.10 Error Analysis

The final result of residual stress distribution depends mainly on the accuracy of strain readings. There are several factors affecting the strain readings:

1. The holding of specimen inevitably introduces new stresses due to the clamping load. Although only the top and bottom part of specimen were touched by holder, the stress generated may still be transferred to middle part where the strain gage attached and affect the reading of strain gage.
2. The water-jet drilling method was chosen to avoid the heat generation during the classical drilling process. However, this may cause a new problem: the water might damage the strain gage which is highly sensitive to liquid. Although the water-resistance coating was adopted, two of the strain gages still showed erroneous reading during the test. So, it can be suggested using weldable-strain gages that are not affected by water.
3. The accuracy of the DataScan system is certainly very good; but the connection between the sample and the system may be disturbed. The strain readings are very sensitive to the environment.
4. The drilling out part cannot be perfectly centered due to the technical limitation of water-jet machine and the residual stress might not be axisymmetric. Therefore, the four strain readings sometimes vary widely.

CHAPTER 4

FEA MODELS FOR RESIDUAL STRESS SIMULATION

4.1 General

When structural steel members are heat-treated, two different types of stresses, namely thermal and transformation stresses (due to plastic flow during rolling or other operations), will be produced inside the material. Whenever the strains due to non-uniformity of the temperature in steel go over the elastic limit of the material, residual stresses will stay there after cooling stops. Generally, the formation of such residual stresses is mainly influenced by several conditions: the initial temperature, the cooling method, the size and shape of the steel member, and the properties of the material. In this chapter, a model is developed to predict the residual stresses caused by hot rolling and cooling in homogeneous long solid steel.

4.2 Geometry and Model

In hot rolling and straightening, the modulus of elasticity and the yield stress are very low at high temperature; the stresses in the material are therefore small. Most of the residual stress is produced during the cooling period. Hence only the thermal stress is modeled in this chapter. This is an uncoupled heat transfer and subsequent thermal stress analysis problem.

4.2.1 Steel Properties

The following assumptions are made to model the cooling process of hot-rolled steel:

- The initial temperature of 1038°C (1900°F) is uniformly distributed in the steel.
- Cooling process takes place in the polar-symmetrical way.
- There is no variation in temperature along the length of the cylinder.
- The thermal properties of the material are independent of temperature.
- The Newton's cooling law applies.

The thermal properties of steel were as follows:

- Density: 7832 kg/m³
- Specific heat: 0.6 kJ/kg °C
- Thermal conductivity: 58.8 W/m °C
- The film coefficient on the surface of the steel: 193.1 W/m² °C

The steel is considered as an elastic, perfectly plastic material, with a yield stress that drops linearly with temperature above 121°C, as shown in Figure 4-1. The steel is initially at a uniform temperature, near its melting point and its yield stress is small. It is assumed to be stress-free in this condition.

The steel has the following properties:

- Young's modulus: 200 GPa
- Poisson's Ratio: 0.3
- Yield Stress: 345 MPa for $T \leq 121^\circ$ and $345 [(1-(T-121)/1111)]$ MPa for $T \geq 121^\circ\text{C}$.

4.2.2 Analysis Procedure

The steel is initially at a uniform high temperature; then the surface is cooled in air at room temperature. Cooling is allowed to continue until all the steel reaches the room temperature. During the heat transfer analysis, the temperature distribution is recorded in the ABAQUS results file.

The temperature-time history recorded during the heat transfer analysis was used as input file to the thermal stress analysis. The transient stresses are large enough to cause significant plastic flow; so residual stresses will remain after the steel reaches room temperature.

The two-dimensional axisymmetric element was chosen to minimize the size of analysis. The length of the steel column was assumed to be 3 inch and the solid element was used to simulate the property of steel. 2401 first order elements are used in the model. The elements of type DCAX4 (axisymmetric 4-node linear element for heat transfer) were used for heat transfer analysis; element type CAX4 (axisymmetric 4-node linear element) was selected for the thermal stress analysis. The boundary conditions ensure that the cross-section plane remains a plane during the history of cooling.

The analysis consists of a transient heat transfer analysis, followed by a thermal stress analysis in which the temperature distribution predicted by the heat transfer analysis is used as the loading condition in the problem. ABAQUS makes it very simple to transfer temperature data in this way. After running the heat transfer input analysis, ABAQUS writes the temperature distribution result in the output database file. Then, in the thermal stress analysis, the file parameter following the *TEMPERATURE option is used to automatically read these temperatures back into the stress analysis model. This

mode of transferring the temperature is based on node numbers; the heat transfer and thermal stress analysis models have identical nodal identification number.

4.2.3 Analysis Parameters

In the heat transfer analysis, the DELTMAX parameter limits the maximum temperature change that may occur in an increment, thus determines the accuracy with which the transient temperature solution is integrated in time. It also implies the use of automatic time increment, which is desirable in a case where we wish to carry the analysis through to steady-state conditions, so that large time increments are used towards the end of the solution. In this problem, DELTMX is set to 5.56°C . This choice should provide sufficient accuracy in the heat transfer solution to define the residual stress correctly. The initial time increment is suggested to be 20 seconds, and the total time period used is 4×10^6 seconds. Since the solution should reach steady state, the time period specification is rather arbitrary: it has to be long enough to reach steady state. The END=SS parameter is also used on the HEAT TRANSFER option, which indicates that the analysis should terminate when steady-state conditions are reached. The steady-state condition is decided when the time rate of changing of temperature at all nodes falls below a specified value: in this analysis, this value is set to be $0.556 \times 10^{-6}^{\circ}\text{C}$. The solution terminates when this steady-state condition is satisfied. The specification of total time period (assumed 4×10^6 seconds in this study) should be large enough to achieve the steady-state condition. The minimum time increment should also be specified to avoid too small increment that may cause initial oscillations in the solution.

4.3 Results and Discussions

The analysis was carried out for different diameters of specimens ranging from 1.5 inch to 12 inch. Examples of ABAQUS input files for the heat transfer and thermal stress analysis are given in Appendix C and Appendix D, respectively. The time histories of the stress through the radius are shown in Figures 4-2 to 4-13. The solid line which corresponds to the last time point is considered as thermal residual stress distribution.

Based on results listed in Figures 4-2 to 4-13, the following observations are drawn:

- For all sizes of samples, the calculated residual stress histories are similar to each other, and the residual stress patterns are also alike: tension at centre of steel column, compression at outer surface of steel column.
- The bigger the diameter of steel bar, the greater the residual stresses both in tension and in compression.
- For solid round steel columns with diameter bigger than 4 inch, the tension stress at the centre are more than yield stress, which is 345 MPa. This is unrealistic since the steel column will fail beyond this stress. This error may be due to the improper modeling in ABAQUS input file. It seems that only the compression yield stress limitation is recognized by the program, but not yield stress in tension.

CHAPTER 5

Compressive Resistance of Solid Round Steel Columns with the Effect of Initial Out-of-Straightness

5.1 General

In order to evaluate the influence of residual stress on the behavior of columns, non-linear material and geometric analysis, with and without presence of residual stress, was carried out for columns with different slenderness parameters. In this chapter, the compressive resistance of solid round steel columns without the presence of residual stresses was studied.

Although there might be other factors affecting the ultimate load-carrying capacity of concentrically loaded columns, the effect of initial out-of-straightness of members would be of major importance. For this reason, the effect of initial deflection was considered and investigation was done with FEA model.

5.2 Geometry and Model

The solid round steel columns with 12 different diameters ranging from 1.5 inch to 12 inch were investigated. For each diameter, the slenderness ratio (length/radius of gyration) varies from 20 to 180, which includes most of the ratios of columns used in practice. For each slenderness ratio, three different initial deflections was considered, they were assumed to be $L/2000$, $L/1000$ and $L/500$ respectively, where L is the length of column.

5.2.1 Slenderness Parameter

The slenderness ratio is defined as below:

$$\text{slenderness ratio} = \frac{KL}{R/2} \quad (5-1)$$

And the normalized slenderness parameter of a column, λ_c , is defined as

$$\lambda_c = \frac{KL}{R/2} \sqrt{\frac{F_y}{\pi^2 E}} \quad (5-2)$$

where

K is the effective length factor of the column. In this study, both column ends were considered pinned, where $K=1$.

L is the length of the column.

R is the radius of the cross-section of the column.

F_y is the yield stress of steel.

E is the elastic modulus of steel.

In this study, FEA model of steel columns with eight slenderness ratio, meaning eight different lengths were established, corresponding to eight different λ_c ranging from 0.26 to 2.38.

5.2.2 Initial Out-of-Straightness

The geometric characteristics of the columns analyzed are shown in Figure 5-1. For non-linear material and geometric analysis, there is an initial deflection to the column

in the form of a half sine curve. The lateral deflection at different location can be calculated as below:

$$u(z) = d_0 \cdot \sin\left(\frac{\pi \cdot z}{L}\right) \quad (5-3)$$

where

z is the distance from the bottom of column to where the lateral deflection is measured

$u(z)$ is the lateral deflection at location z .

d_0 is the deflection at the mid-height of the column.

L is the length of the column.

In this study, three different d_0 values were assumed, namely: $L/2000$, $L/1000$ and $L/500$.

According to Equation 5-3, the deflection at different location of the column can be obtained based on this initial deflection.

5.2.3 Steel Properties

The properties of the steel are as follows:

- Young's Modulus: 200 GPa
- Poisson's Ratio: 0.3
- Yield Stress: 345 MPa

The steel is assumed to be a perfectly elastic-plastic material. Von Mises' yield condition defines the yielding of the material.

5.3 Analysis Procedure

Based on the presented column sizes and values of initial out-of-straightness, 324 models were constructed for geometric non-linearity analysis (12 diameters, 9 lengths for each diameter, and 3 different initial deflection for each length). The geometric non-linearity analysis utilized RIKS method provided by ABAQUS software to predict the ultimate strength of round steel columns. The RIKS method solves loads and displacement simultaneously by using the load magnitude as an additional unknown. An initial load has to be assigned to both ends of the column, and the loading during a RIKS step is always proportional to this initial load. Since the loading magnitude is part of the solution, a method need to be specified when the step is completed. This stopping criterion can be either the value of load proportionality factor or a maximum displacement value at a specified degree of freedom. In the finite element meshes, first-order 3D solid element types were chosen. From the postbuckling analysis, the load-deflection history and the ultimate strength for the columns were obtained. Appendix E gives an example input file for this analysis.

5.4 Sensitivity Study

Sensitivity study was conducted in order to determine the meshing size of the model (Figure 5-2) both in longitudinal and lateral direction.

During ABAQUS modeling, the initial load was applied evenly on all the nodes at the bottom and top of the column. After the RIKS analysis, the load-deflection history was obtained for each node and the maximum load sustained by each node was

determined by the load-deflection history curve, which was the node load value of the optimum point on the curve.

In the radial direction, the cross-section of the round column was divided into several sections for the meshing purpose. In order to optimize the analysis effect in terms of running effort and accuracy of the result, different meshing numbers (number of circles in radial direction) has been tested and the result is shown in Table 5-1 and Figure 5-3. The steel column used for this sensitivity study was of 1.5 inch diameter and 30 inch length. It can be seen that the ultimate load became stable after using more than 8 circles in radial direction. However, the cross-section with 5 circles gave very close result to higher meshing size while saving lots of analysis effort. Therefore, the cross-section with five circles (as shown in Figure 5-3) in radial direction was chosen for ABAQUS modeling in this study.

For the longitudinal direction, the number of elements showed some effect on analysis result. By increasing the number of elements, the ultimate strength was kept decreasing as shown in Table 5-2. It can be found that the reduction in the ultimate load was less than 5% for element number more than 25. Because of restriction on running time for large meshing sizes, 25 elements were chosen to minimize the analysis time.

The other consideration about longitudinal meshing number is the width to length ratio for each element. It is known that in the finite element analysis, the length-width ratio of any rectangular element should be maintained less than 4 to increase accuracy. Therefore, for longer steel column, the element number in the longitudinal direction was adjusted to meet this requirement. For column with slenderness ratio of 120, 35 elements were used for meshing purpose, and for column with slenderness ratio of 140, 35

elements were adopted. For higher slenderness ratio, 40 elements were selected to give more accurate result.

5.5 Results and Discussions

In the Finite element modeling, 324 models were constructed for postbuckling analysis, and 324 ultimate compression strength values were obtained from the load history curves.

For each diameter, the result of the ultimate load with respect to different slenderness parameter is summarized. They are shown in Figure 5-4 through 5-15. The ultimate resistance load is presented in the manner of maximum load to yield strength ratio. It can be observed that, with more initial deflection, the column can carry less load. And with higher slenderness ratio, means the column is more slender, the capacity of the column will be decreased. The compressive resistance for the column of the same diameter can drop dramatically from more than 90% of the yield strength for shortest length to less than 40% for longest length. The Euler Curve is also included in the figures to establish the sense on the obtained ultimate load as compared to Euler critical buckling load. It can be observed that Euler buckling load follows the trend of the FEA results for slenderness ratios more than 1.25.

The Ultimate load-slenderness parameter curves for different diameters with $L/500$ initial deflection are also summarized together in Figure 5-16. It can be observed that all the figures give similar trend and almost coincide with each others. Hence, it can be concluded that the column diameter does not have an effect on the ultimate strength and that only the slenderness parameter affects the ultimate to yield strength ratio (P_u/P_y).

At the same time, Sennah et al. (2008) proposed column curve for the compressive resistance of stress-relieved solid round steel columns is also shown in Figure 5-16. One may conclude that the proposed column equation by Sennah et al. (2008) which is similar to equation 2-20 but with $n=1.7$, can be applied with confidence on column sizes between 125 and 300mm (5" and 12") in diameter.

6.2 Numerical Analysis

The numerical analysis of the steel columns was done using the finite element method (FEM) using the software ABAQUS. The only difference was the inclusion of stress-relief in the steel material. In ABAQUS, the stress-relief was achieved by using the "release" option in the material definition. From the center of the steel column, the stress-relief was done using the full of each specimen but distributed symmetrically along the length of the column. Hence, the steel column was modeled as in Figure 6-2. The stress-relief was done by an expanding cylindrical residual stress.

6.3 Numerical Results

CHAPTER 6

Compressive Resistance of Solid Round Steel Columns with the Effect of Symmetrical Residual Stress

6.1 General

Symmetrical residual stress results mainly from uneven cooling after rolling of hot-rolled steel column. The influence of symmetrical residual stresses on the compressive resistance of solid round steel columns is addressed in this chapter. Since the importance of the effect of initial deflection of members, investigation on the combined effects of internal and external imperfections, that is symmetrical residual stress and out-of-straightness, was done with FEA method.

6.2 Geometry and Model

The geometry and properties of the steel columns were both identical with the ones presented in the previous chapter. The only difference was the inclusion of symmetrical residual stress in the analysis. In ABAQUS, this alternation can be achieved by editing the model keyword. The symmetrical residual stress varies from the centre of the steel column to the external surface along the radii of each specimen, but distributes symmetrically around the vertical z-axis. Hence, the steel column was meshed as in Figure 5-2, and each section has been assigned by corresponding symmetrical residual stress.

6.3 Symmetrical Residual Stress

The symmetrical residual stress distribution imported to ABAQUS model was obtained from Roy's study (Roy, 2008) about determination of residual stress in axisymmetric rods. In this research, X-ray diffraction and slitting method was applied successfully to determine residual stress in four solid round bars of diameters 1.5, 2.0, 2.5 and 4.25 inch and lengths 295, 300, 280 and 360mm. The axial stress distribution along the radii is plotted in Figure 6-1. The profile of stress variation across the diameter was assembled from two copies of the stress variations in Figure 6-1 and distributed symmetrically around the vertical z-axis as presented in Figure 6-2.

Based on Roy's result, some modifications were made to predict the symmetrical residual stress for variety of diameters and the procedure of calculation is provided in Appendix F. For the ABAQUS analysis, these commands have to be added into original input file (Appendix E) by keyword editing function to simulate the symmetrical residual stress:

```
*INITIAL CONDITIONS,TYPE=STRESS  
ELSET1,0,0,14310.87,0,0,0  
ELSET2,0,0,17713.46,0,0,0  
ELSET3,0,0,14177.44,0,0,0  
ELSET4,0,0,3702.82,0,0,0  
ELSET5,0,0,-13710.4,0,0,0
```

6.4 Sensitivity Study

As for columns without residual stresses, the meshing size was also tested along lateral and longitudinal direction for columns with symmetrical residual stresses. For the cross-section, the result is shown in Table 6-1. It should be noted that the steel column used for this sensitivity study was of 1.5 inch diameter and 30 inch length.

By comparing 5 circles meshing method with higher meshing size, the result gives fairly close ultimate load of column. Therefore, the model would be meshed in this manner in order to produce consistent results.

For longitudinal direction, the effect of total element number is shown in Table 6-2 and the 25 elements were selected for model analysis. This number was also adjusted for longer columns with the consideration of length-width ratio for each element.

6.5 Results and Discussions

In the finite element modeling, 324 models were constructed for postbuckling analysis of columns with symmetrical residual stress with which 324 ultimate compression resistance values were obtained from the load history curves.

For each diameter, the result of ultimate load for different slenderness parameter is plotted and shown through Figure 6-3 to 6-14. It was observed, just as expected, that with increase in initial deflection, the column has lower compressive resistance. Also the more slender the column, the lower the ultimate strength. With the inclusion of Euler Curve on every figure, it can be seen that Euler Buckling loads are close to those obtained from the FEA for columns with slenderness parameter more than 1.25.

The Ultimate load-slenderness parameter curves for different diameters with $L/500$ initial deflection are also summarized in Figure 6-15. It can be observed that all the figures give similar trend and almost coincide with others. Hence, it can be concluded that the column diameter does not have an effect on the ultimate strength but the slenderness parameter has.

At the same time, Sennah et al. (2008) proposed column curve for the compressive resistance of non-stress-relieved solid round steel columns is also shown in Figure 6-15. One may conclude that the proposed column equation by Sennah et al. (2008) which is similar to equation 2-20 but with $n=1.7$, can be applied with confidence on column sizes between 125 and 300mm (5" and 12") in diameter.

CHAPTER 7

Compressive Resistance of Solid Round Steel Columns with the Effect of Non-Symmetrical Residual Stress

7.1 General

Non-symmetrical residual stress is produced by the handling and transport of steel members during the manufacture process. It can also be resulted from the cold-straightening process. The effect of non-symmetrical residual stress on the ultimate strength of solid steel columns is discussed in this chapter. The effect of initial deflection will be included simultaneously by FEA using ABAQUS software.

7.2 Geometry and Model

In order to apply the non-symmetrical residual stress on steel member, the model has to be meshed orthogonally as shown in Figure 7-1. The non-symmetrical residual stress varies from one side of the steel column to the other side along the radii of each specimen. Therefore, each vertical slice has been assigned by corresponding non-symmetrical residual stress. Appendix G gives an example input file for this analysis.

7.3 Non-Symmetrical Residual Stress

The non-symmetrical residual stress is calculated by Equation 7-1. This equation is developed by Nitta and Thurlimann in their research about ultimate strength of high-yield strength constructional-alloy circular columns (Nitta and Thurlimann, 1962). The axial residual stress σ_z at a distance x from the centre of solid round column is given by:

$$\begin{aligned}
\frac{\sigma_z(\xi)}{\sigma_y} &= \frac{16}{3\pi} \beta \xi + 1 && \text{(for } -1 \leq \xi \leq -\frac{1}{F(\beta)} \text{)} \\
&= \frac{16}{3\pi} \beta \xi - F(\beta) \xi && \text{(for } -\frac{1}{F(\beta)} \leq \xi \leq \frac{1}{F(\beta)} \text{)} \\
&= \frac{16}{3\pi} \beta \xi - 1 && \text{(for } \frac{1}{F(\beta)} \leq \xi \leq 1 \text{)}
\end{aligned} \tag{7-1}$$

Where σ_y is yield stress of the material, and $\xi = x/R$. β is the ratio of the cold-bending moment M_0 to the full plastic moment M_p , and is assumed to be 0.7, 0.8 and 0.9 respectively. For these three different β , distribution of non-symmetrical residual stress along the radius of steel column are plotted based on Equation 7-1 and showed in Figure 7-2. The non-symmetrical value for each vertical slide of model can be obtained by this chart for different β value.

For the ABAQUS analysis, the values of non-symmetrical residual stress have to be added into original input file (Appendix G) by keyword editing function to simulate the non-symmetrical residual stress:

```

*INITIAL CONDITIONS, TYPE=STRESS
ELSET1,0,0,-16858,0,0,0
ELSET2,0,0,2255,0,0,0
ELSET3,0,0,12612,0,0,0
ELSET4,0,0,4204,0,0,0
ELSET5,0,0,-4204,0,0,0
ELSET6,0,0,-12612,0,0,0
ELSET7,0,0,-2255,0,0,0
ELSET8,0,0,16858,0,0,0

```

7.4 Sensitivity Study

The 3 inch diameter round steel column with lengths from 15 inch up to 120 inch has been modeled for sensitivity study purpose. For each length, three different initial deflections were considered, namely: $0.0005L$, $0.001L$ and $0.002L$ respectively, which L is the length of steel column. The influence of β value has also been examined simultaneously in the sense that the non-symmetrical residual stress calculated from three different β value has been applied to same size column by turn. The result of this sensitivity study is shown in Table 7-1. It indicates that the column with initial deflection of $0.002L$ and non-symmetrical residual stress calculated from $\beta=0.9$ is the most critical model since it gives the lowest compressive resistance.

Meanwhile, the meshing size has been tested along lateral and longitudinal direction for columns with non-symmetrical residual stress. For cross-section, the result is shown in Table 7-2. It should be noted that the steel column used for this sensitivity study is with 1.5 inch diameter and 30 inch length. By comparing 8 slices meshing method with higher meshing size, the result gives fairly close ultimate load of column. Therefore, the model would be meshed in this manner in order to produce optimum result in terms of result satisfaction and running effort. For longitudinal direction, the effect of total element number is shown in Table 7-3 and the 25 elements were selected for model analysis. This number was also adjusted to 30, 35 and 40 for longer columns with the consideration of length-width ratio for each element.

7.5 Results and Discussions

In the finite element analysis, 96 models were constructed for postbuckling analysis of columns with non-symmetrical residual stress (12 diameters, 8 lengths for each diameter). The initial deflections of these bars were all $1/2000$ of the length. The

residual stress applied on these bars are calculated from Equation 7-1 by using $\beta=0.9$. The results of ultimate load with respect to slenderness parameter for different size solid round steel columns are shown in Table 7-2 and Figures 7-3 to 7-14. From these figures, it can be concluded that all columns of different diameters show very similar trend (the ultimate load decreases when slenderness parameter increases).

CHAPTER 8

Conclusions

In this thesis, experimental investigations on the residual stresses were carried out using boring-out method. Additionally FEA models for the formation of residual stresses in hot-rolled solid round steel columns were developed. At the same time, the symmetrical and non-symmetrical residual stress predicted by previous research was studied and their results have been adopted for learning the effect of residual stress on compressive resistance of solid round steel column. The influence of cold-straightening was also considered as they introduce non-symmetrical residual stress. Comparisons were made in different aspect and the details are presented below.

Based on the data generated from this research, the following conclusions can be drawn:

1. First of all, for same size steel column with same initial deflection, the comparison of ultimate compressive resistance was made among the members without any residual stresses, with symmetrical residual stress and with non-symmetrical residual stress. As stated above, the initial deflection is identical for each column and is equal to $1/500$ length. It was observed that, the steel column without any residual stress has the highest compressive resistance. The steel column with symmetrical residual stress has the second highest compressive resistance whereas the one with non-symmetrical residual stress has the lowest. It can be concluded that when

there are residual stresses in the columns, the capacity of the column will considerably decreased.

2. Comparison was made for columns with different initial deflection, while maintaining all other conditions. It is clearly shown that columns with more initial deflection have lower compressive resistance as expected.
3. The effect of slenderness parameter is studied while maintaining the values of symmetrical residual stress and initial deflection. By increasing the length of steel columns and hence increasing the slenderness parameter, the ultimate strength significantly decreases.
4. The residual stress, calculated from the data obtained from tests, are extremely sensitive to the accuracy of the strain reading. This factor should be taken into account in the interpretation of results.
5. Comparison between experimental and numerical results indicated that the FEA model for formation of residual stress gave reasonable results for small diameter bars. The difference for bigger diameter bars may result from the high sensitivity of experimental strain data.
6. From the postbuckling analysis of columns, it can be concluded that the initial deflection and residual stress can result in remarkable loss of ultimate strength of a column. The residual stress releasing and straightening operations are worth using for columns with this range of sizes.

7. FEA results showed that the compressive strength equation with $n=1.7$ as proposed by Sennah et al. (2009, 2008) is applicable up to 300 mm (12") column diameters.

REFERENCES

- Alpsten, G. (1970). **Residual Stresses and Strength of Cold-Straightened Wide-Flange Shapes**. Jernkontorets Ann., Vol. 154.
- American Institute of Steel Construction, Inc. (1993). **Load and Resistance Factor Design Specification for Structural Steel Buildings**. Chicago, Illinois, USA.
- American National Standards Institute, ANSI. (2005). **Structural Standard for Steel Antenna Supporting Structures and Antenna**, ANSI/TIA-222-G.2005. Telecommunication Industry Association, Arlington, VA.
- Batterman, R., and Johanston, B. (1967). **Behaviour and Maximum Strength of Metal Columns**. Journal of the Structural Division, ASCE, Vol. 93, No.ST2, pp.205-230.
- Bjorhovde, R. (1972). **Deterministic and Probabilistic Approaches to the Strength of Steel Columns**. Ph.D. Dissertation, Lehigh University, Bethlehem, Pa.
- Bjorhovde, R., and Tall, L. (1971). **Maximum Column Strength and the Multiple Column Curve Concept**. Report No. 337.29, Lehigh University, Fritz Eng. Lab, Bethlehem, PA.
- Bühler, H. (1954). **Complete Determination of the State of Residual Stress in Solid and Hollow Metal Cylinders, Residual Stresses, Residual Stresses in Metals and Metal Construction**. Edited by W. R. Osgood, Reinhold Publishing Corporation, New York, N. Y., PP. 305-329.

- Canadian Standards Association. (2001). **Antenna, Towers and Antenna-Supporting Structures**. CAN/CSA-S37-01, Rexdale, Ontario, Canada.
- Canadian Standards Association. (1994). **Antenna, Towers and Antenna-Supporting Structures**. CAN/CSA-S16.1-94, Rexdale, Ontario, Canada.
- Canadian Standards Association. (2003). **Limit States Design of Steel Structures**. CAN/CSA-S16-01, Rexdale, Ontario, Canada.
- CEN. (2003). Eurocode 3 part 1.1: **General Rules and Rules for Steel Buildings**. CEN, European Committee for Standardization, Brussels, Belgium.
- Ding, Y. (2000). **Residual Stresses in Hot-Rolled Solid Round Steel Bars and their Effect on the Compressive Resistance of Members**. M.A.Sc. Thesis, Civil and Environmental Engineering, University of Windsor, Windsor, Ontario, Canada.
- Fujita, Y, and Driscoll, G. (1962). **Strength of Round Columns**. Journal of the Structural Division, ASCE, Vol. 88, No. ST2, pp. 43-59.
- Galambos, T. V. (1998). **Guide to Stability Design Criteria for Metal Structures, 5th Edition**. Structural Stability Research Council, John Wiley & Sons Inc., New York, N. Y.
- Galambos, T. V. (1965). **Strength of Round Steel Columns**. ASCE Journal of the Structural Division, 91(ST1): 121-140.
- Galambos, T. V., and Ueda, Yukio. (1962). **Column Tests on 7¹/₂ in. Round Solid Bars**. ASCE, Journal of the Structural Division, 88(ST4):1-17.

- Hetenyi, M. (1957). **Handbook of Experimental Stress Analysis**. Third Edition, John Wiley & Sons Inc., New York, N. Y.
- Hibbett, D., Kavlsson, I., and Sorenson, J. (2008). ABAQUS User's Manual Version 6.7, Hibbett, Kavlsson and Sorenson, Inc., providence, RI., USA.
- Jahanian, S. (1995). **Residual and Thermo-elasto-plastic Stress Distribution in a Heat Treated Solid Cylinder**. *Materials at High Temperatures*, 13(2):103-110.
- Kamamoto, S., Nihimori T., and Kinoshita, S. (1985). **Analysis of Residual Stress and Distortion Resulting from Quenching in Large Low-Alloy Steel Shafts**. *Journal of Material Science and Technology*, 1:798-804.
- Mull, N. C. (1999). **Compressive Resistance of Solid Rounds**. M.Sc. Thesis, Civil & Environmental Engineering, University of Windsor, Windsor, Ontario, Canada.
- Nitta, A. and Thürlimann, B. (1962a). **Ultimate Strength of High Yield Strength Constructional-Alloy Circular Columns – Effect of Cold-Straightening**. Publication, IABSE, 22: 265-288.
- Nitta, A. and Thürlimann, B. (1962b). **Ultimate Strength of High Yield Strength Constructional-Alloy Circular Columns – Effect of Thermal Residual Stresses**. Publication, IABSE, 22: 231-264.
- OMAX User's Guide (2008). Part # 302316 Revision G.
- Roy, G. (2008). **Determination of Residual Stress in Axisymmetric Rods**. Second Draft. CANMET/MTL. Ministry of Natural Resources, Ottawa, Ontario, Canada.

- Sennah, K. and Wahba, J. (2002). **Compression Tests on Large Solid Steel Round Bars**. ASCE Journal of Structural Engineering, 130 (1): 147-150.
- Sennah, K., Saliba, M., Jaalouk, N., and Wahba, J. (2008) **Experimental Study of the Compressive Resistance of Stress-Relieved Solid Round Steel Members**. Journal of Constructional Steel Research, 65 (2009): 1034-1042.
- Sennah, K., Saliba, M., Al-Hashimy, M., and Wahba, J. (2008) **Experimental Evaluation of the Compressive Resistance of Non-Stress-Relieved Steel Solid Round Columns**. Canadian Journal of Civil Engineering, 35: 1221-1238.
- Toparli, M. and Aksoy, T. (1991). **Calculation of Residual Stress in Cylindrical Steel Bars Quenched in Water from 600°C**. Proceeding of AMSE Conference, New Delhi, India, 4:93-104.
- Watanabe, M., Sato, K., and Goda, S. (1955). **Thermal and Residual Stress of Circular Cylinders Suddenly Cooled from the Uniformly Heated Conditions**. Journal of the Society of Naval Architects of Japan, 88: 155-164.
- Weiner, J. H. and Huddleston, J. V. (1959). **Transient and Residual Stress in Heat-Treated Cylinders**. Journal of Applied Mechanics, 26E(1): 31-39.

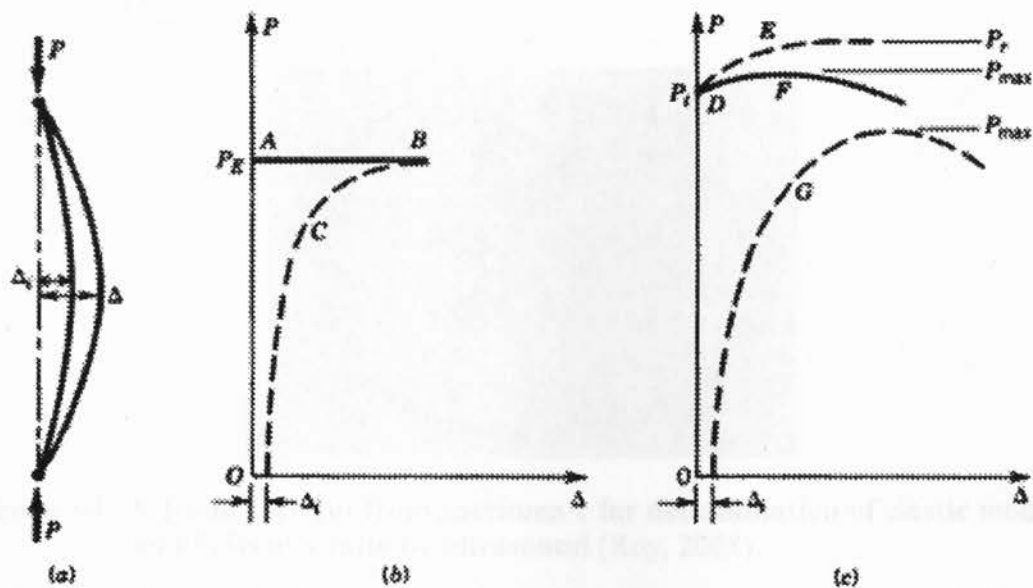


Figure 2-1: Behavior of Perfect and Imperfect Columns

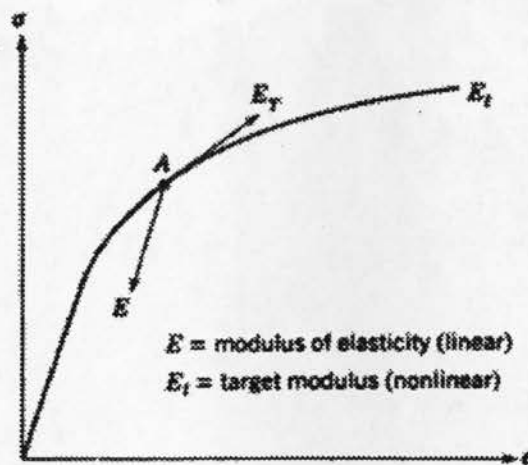


Figure 2-2: General Stress-Strain Relationship

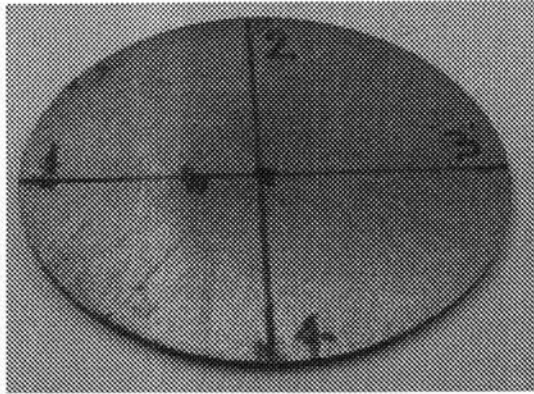


Figure 3-1: A 2-mm slice cut from specimen 1 for determination of elastic modulus and Poisson's ratio by ultrasound (Roy, 2008)

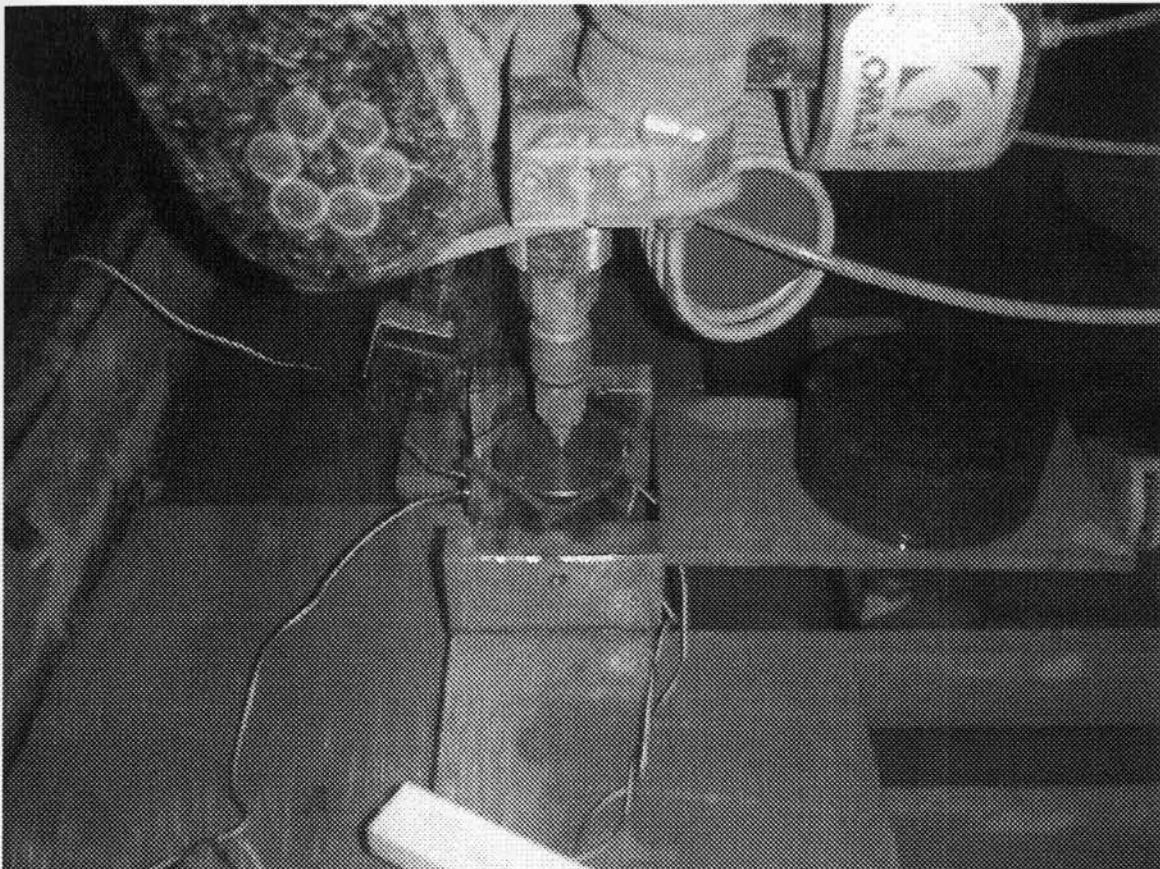


Figure 3-2: Specimen Held in the Bed of Water-Jet Drilling Machine by a Special Holder

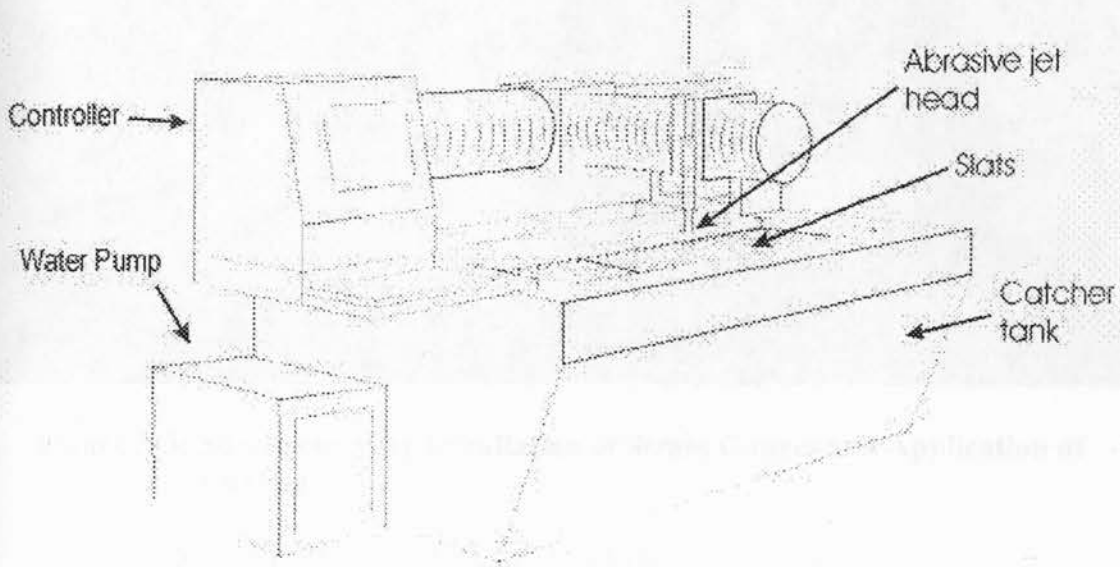


Figure 3-3: Water-Jet Machining System (OMAX User's Guide, 2008)

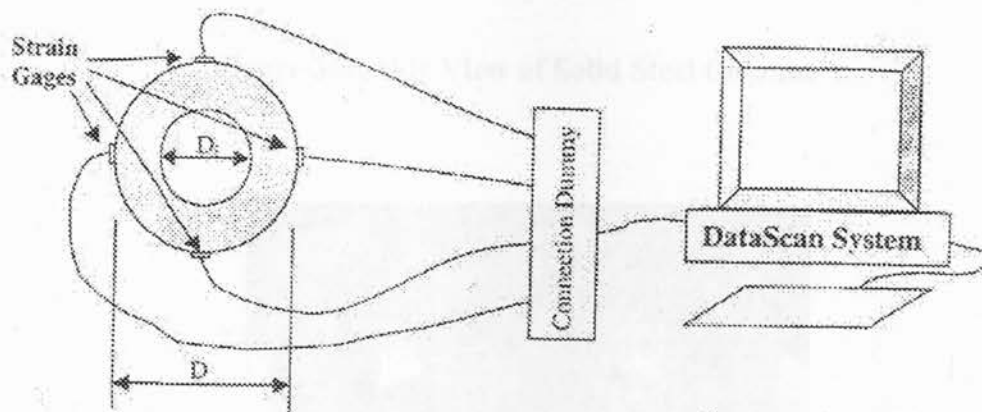


Figure 3-4: Four Strain Gauges Attached to Specimen and Connected to Data-Acquisition System

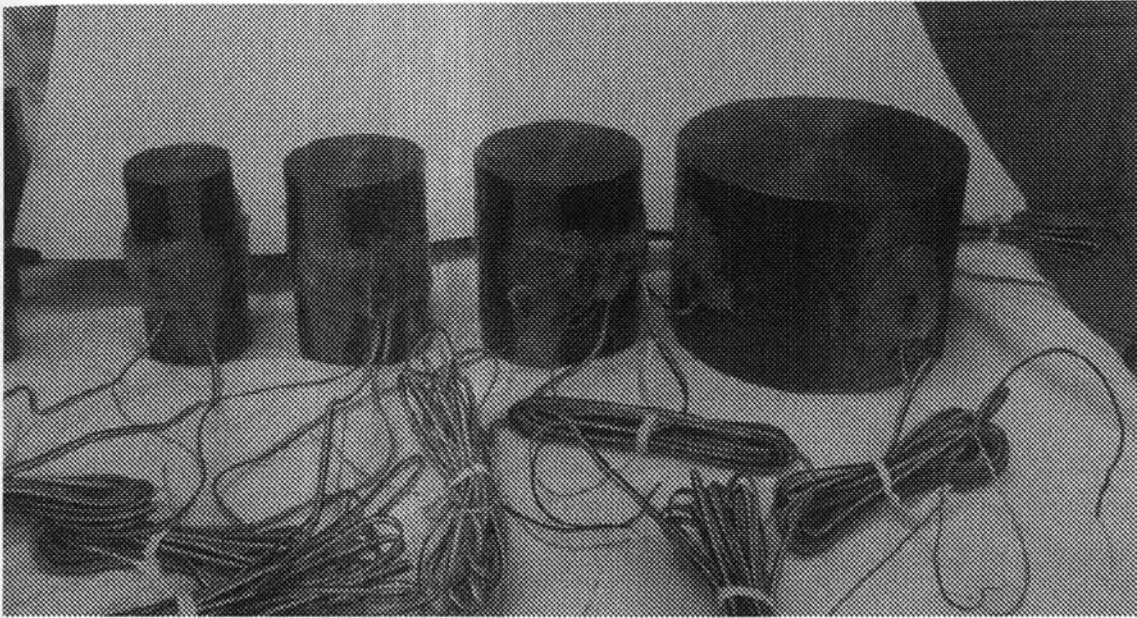


Figure 3-5: Specimens after Installation of Strain Gauges and Application of Coating

Figure 3-6: Side View of a Steel Specimen with the Gauge Part Drilled Through

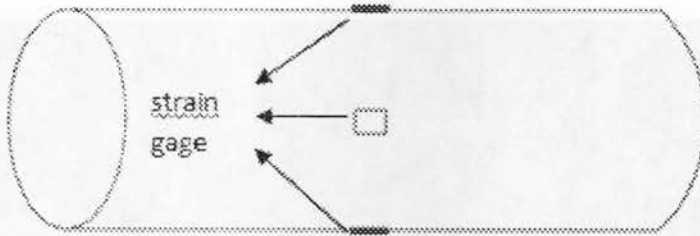


Figure 3-6: Side View of Solid Steel Column

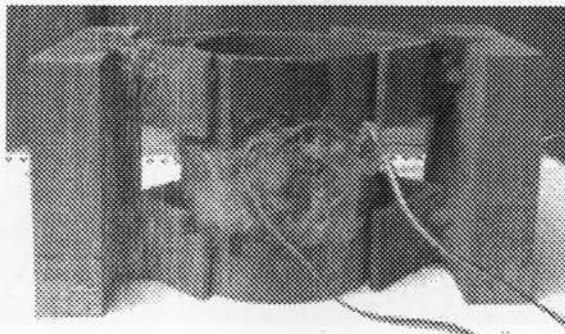


Figure 3-7: Side View of a Steel Specimen Drilled up to Biggest Possible Diameter

Figure 3-7: Side View of the Specimen Clamped by a Special Made Holder

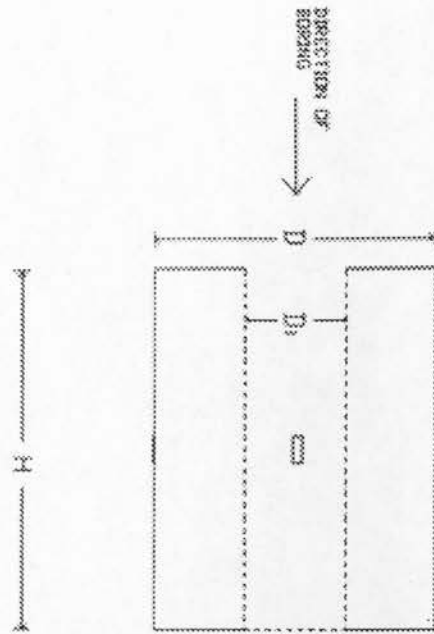


Figure 3-8: View of a Steel Specimen with the Centre Part Drilled Through

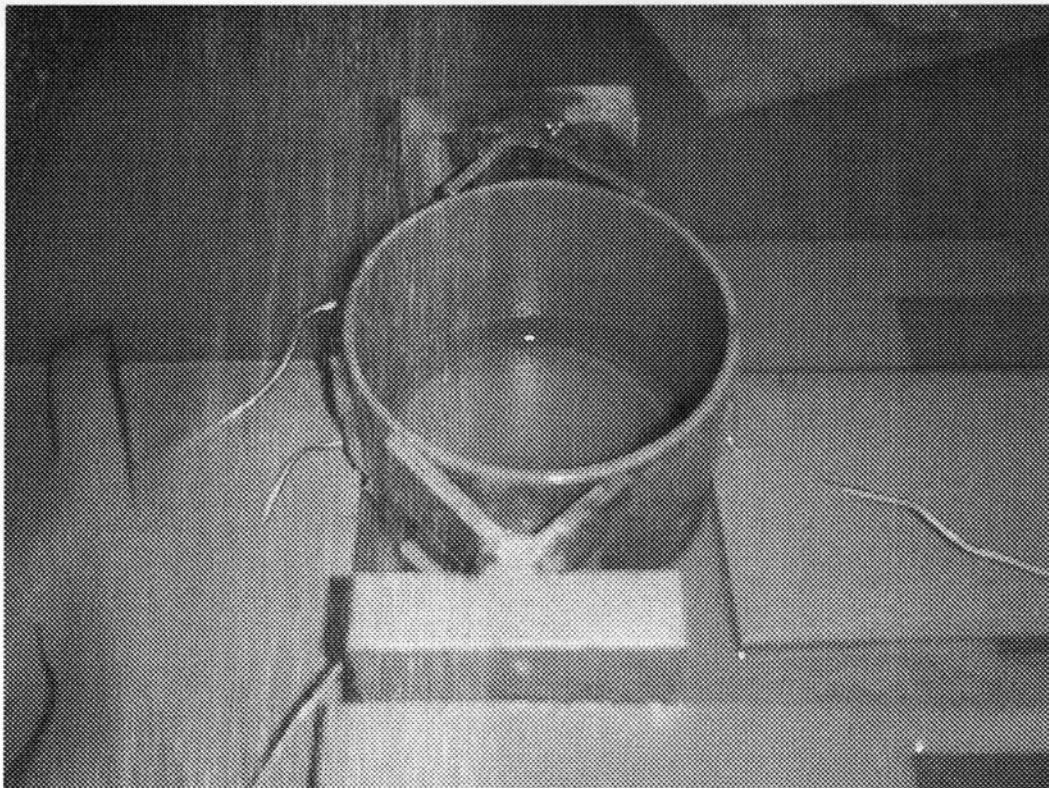


Figure 3-9: View of a Steel Specimen Drilled up to Biggest Possible Diameter

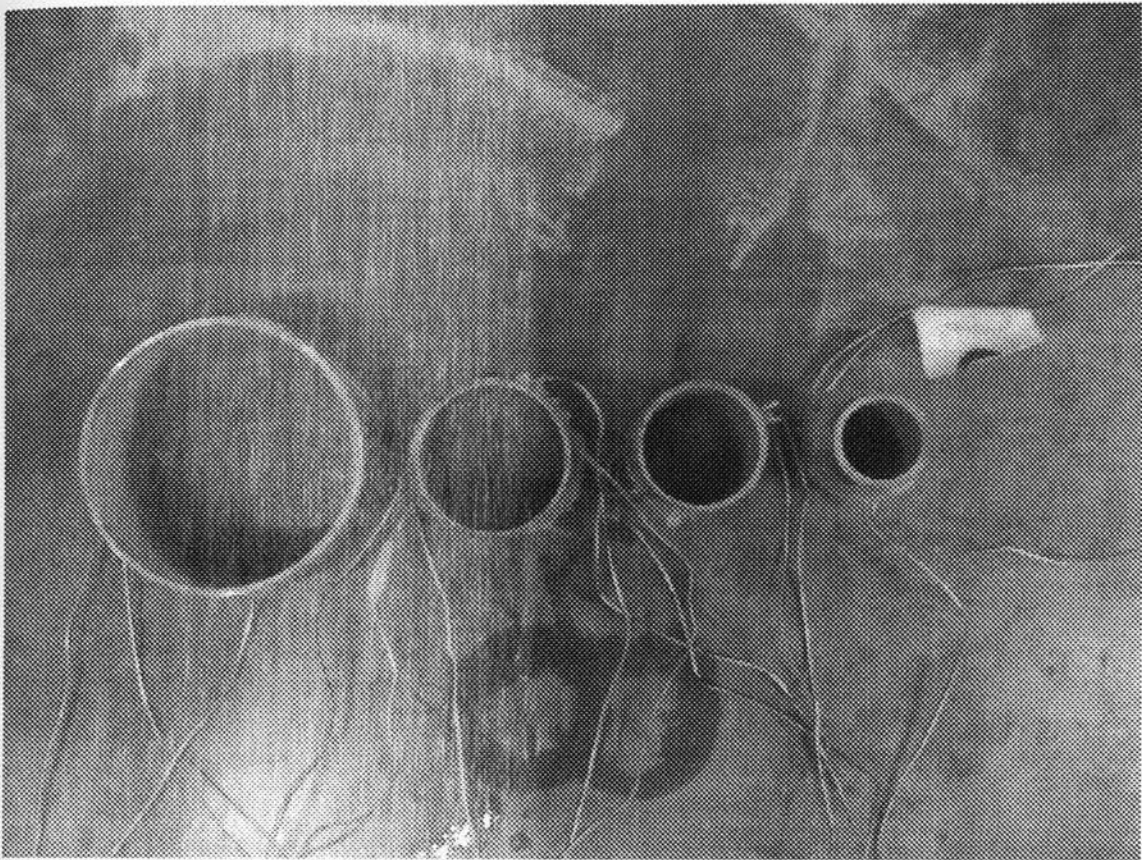


Figure 3-10: View of Steel Specimens after Drilling Using Water-Jet Technology



Figure 3-12: Lateral Deflection vs. Load at the Mid-Height of Specimen 1 under 1 kN Interval Load

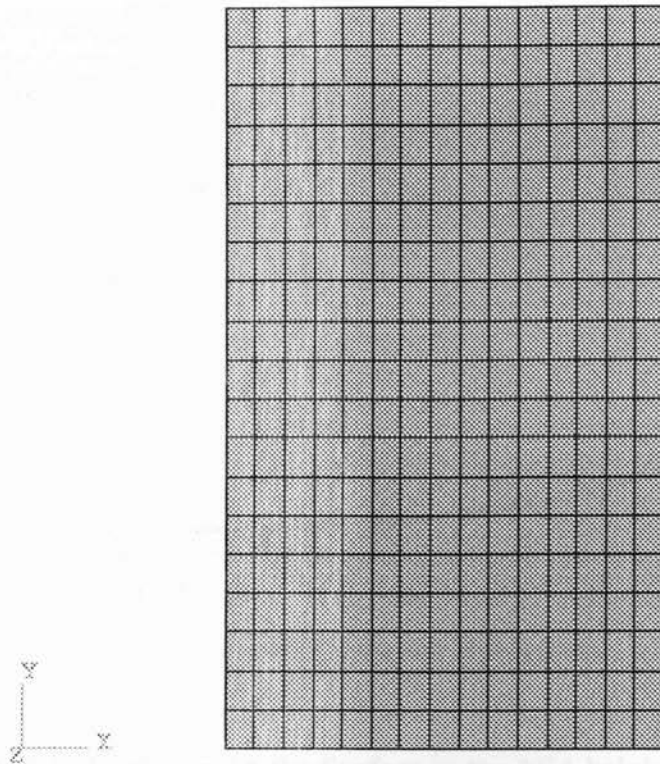


Figure 3-11: View of FEA Model for Strain Calculation

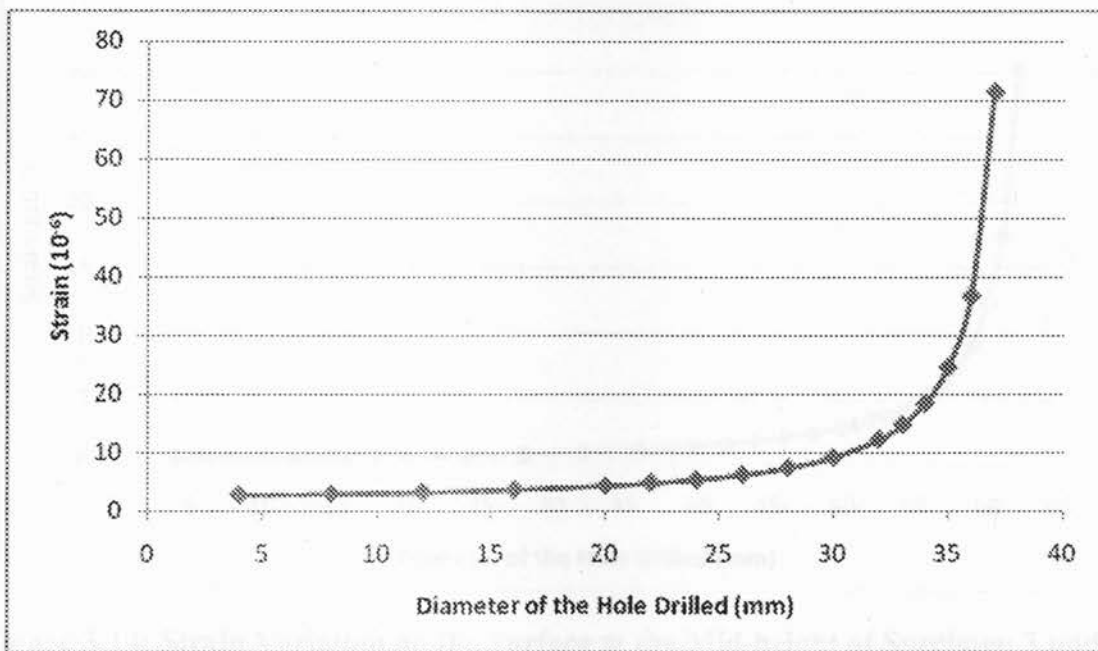


Figure 3-12: Strain Variation on the Surface at the Mid-Height of Specimen 1 under 1 kN Internal Force

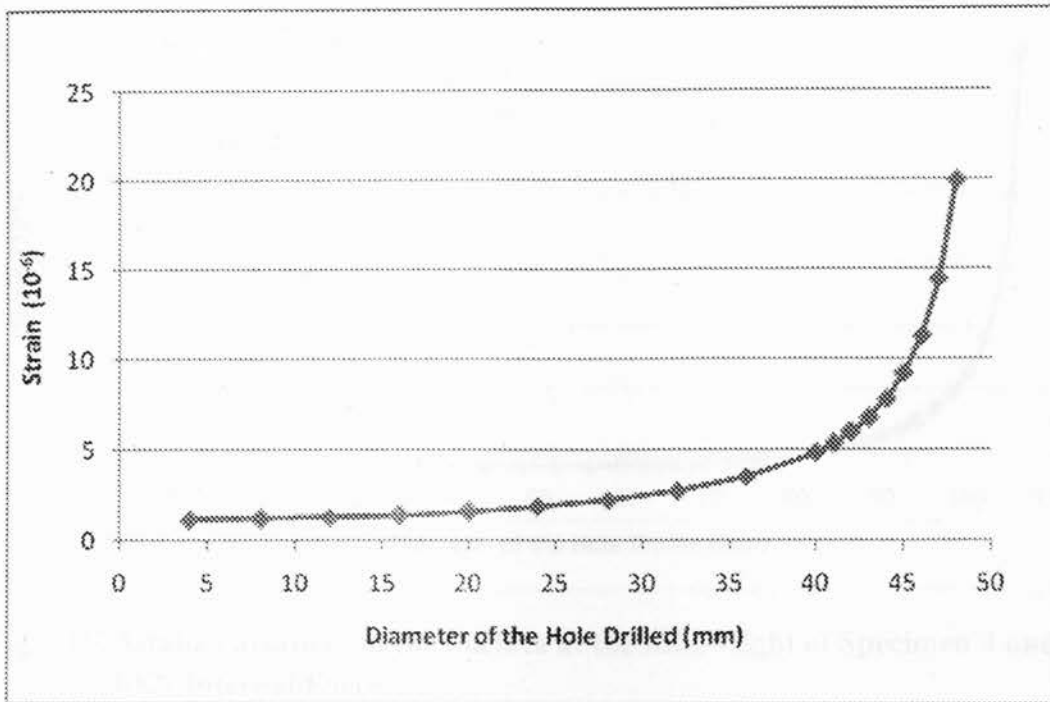


Figure 3-13: Strain Variation on the Surface at the Mid-height of Specimen 2 under 1 kN Internal Force

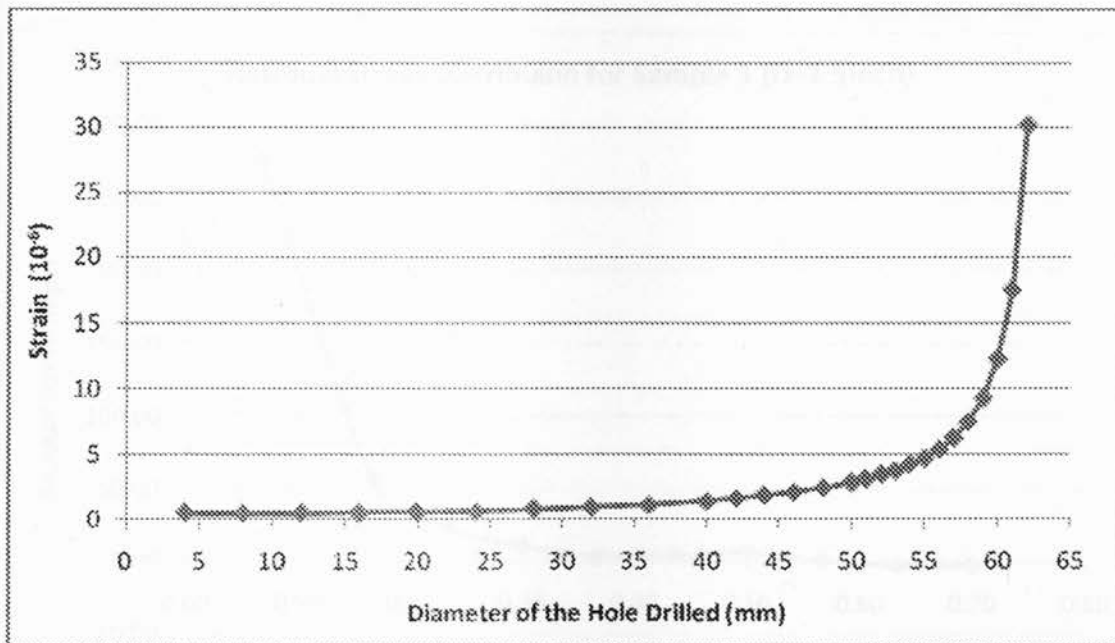


Figure 3-14: Strain Variation on the Surface at the Mid-height of Specimen 3 under 1 kN Internal Force

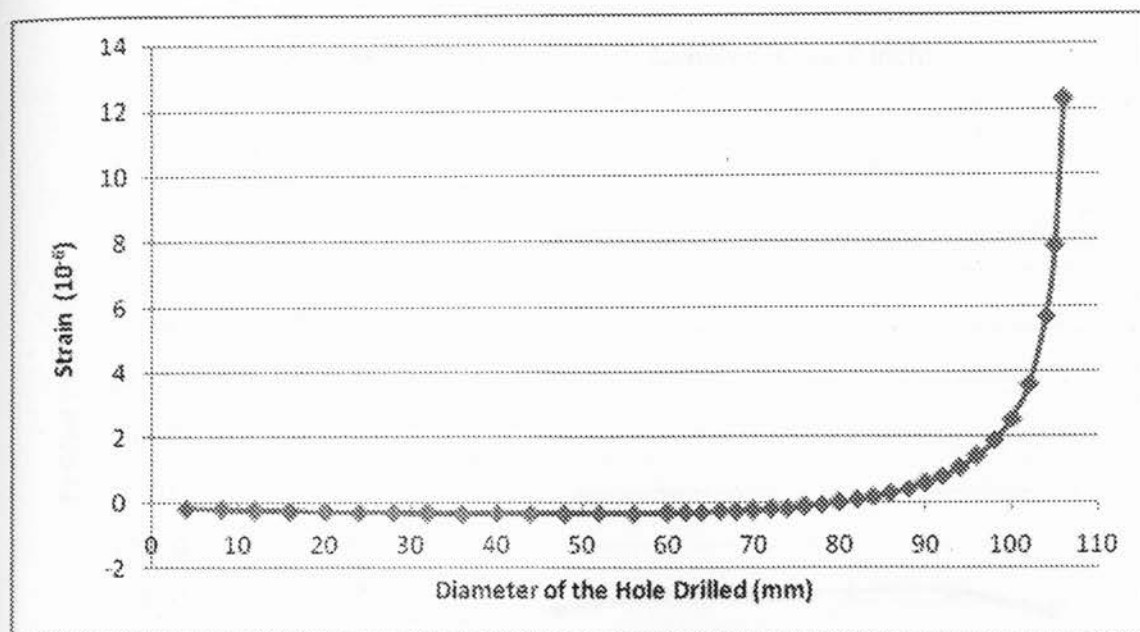


Fig 3-15: Strain Variation on the Surface at the Mid-height of Specimen 4 under 1 kN Internal Force

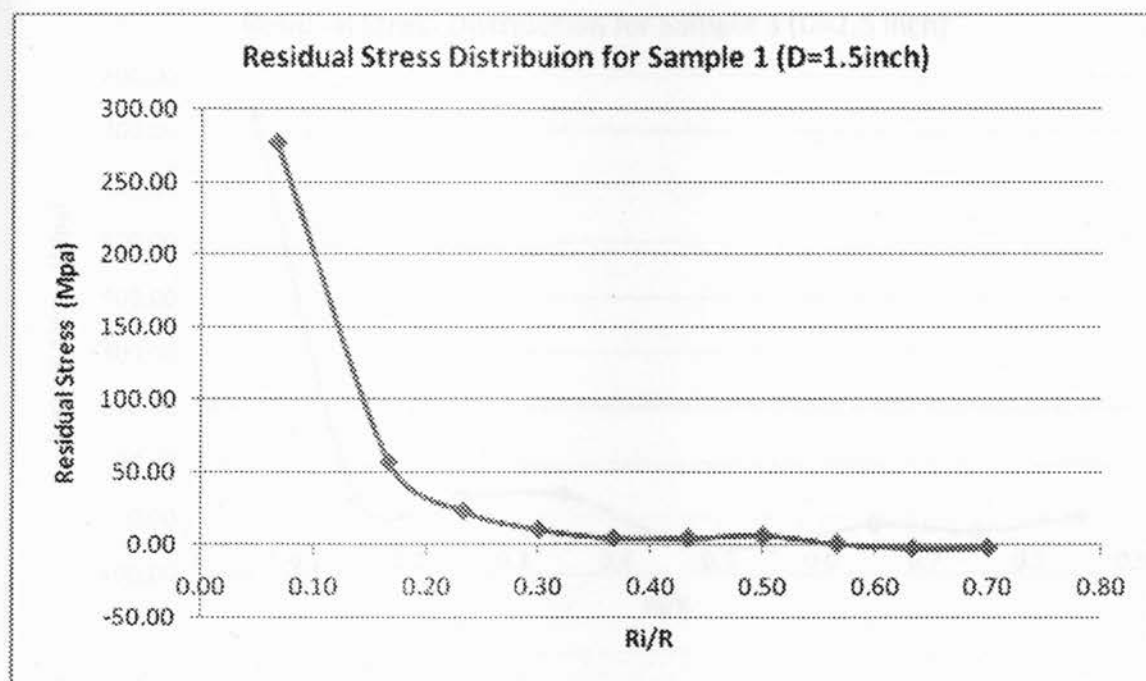


Figure 3-16: Residual Stress Distribution for Sample 1 (D=1.5 inch, H=3 inch)

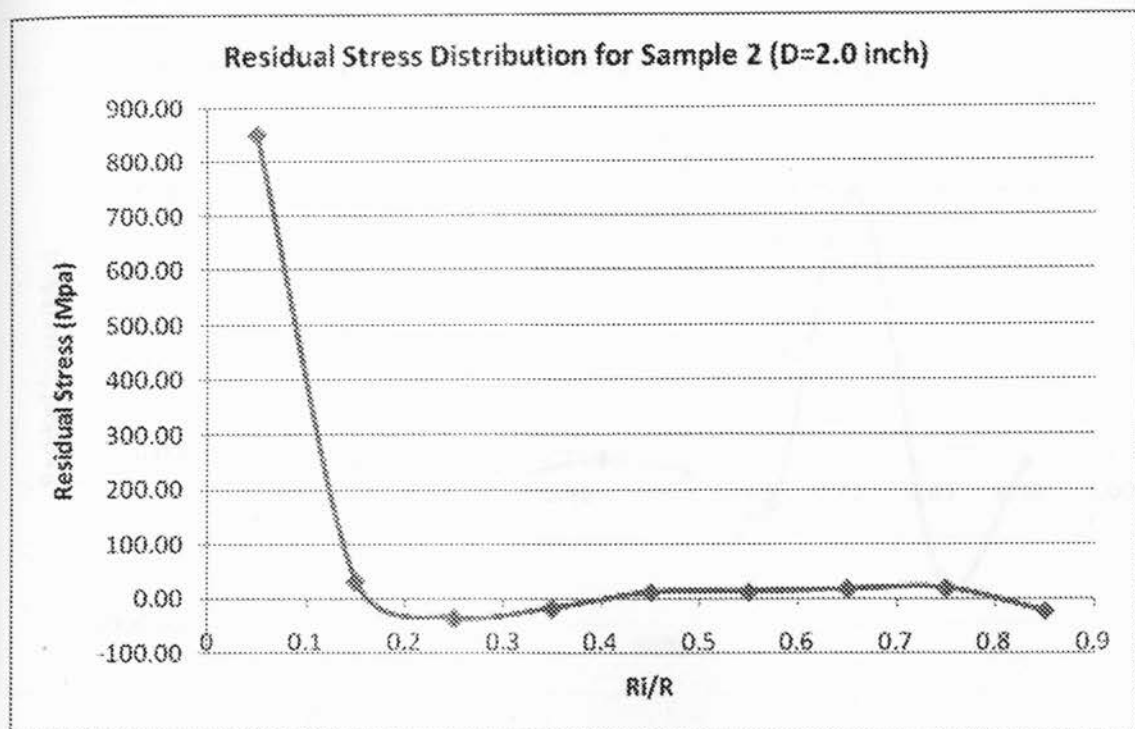


Figure 3-17: Residual Stress Distribution for Sample 2 (D=2.0 inch, H=3 inch)

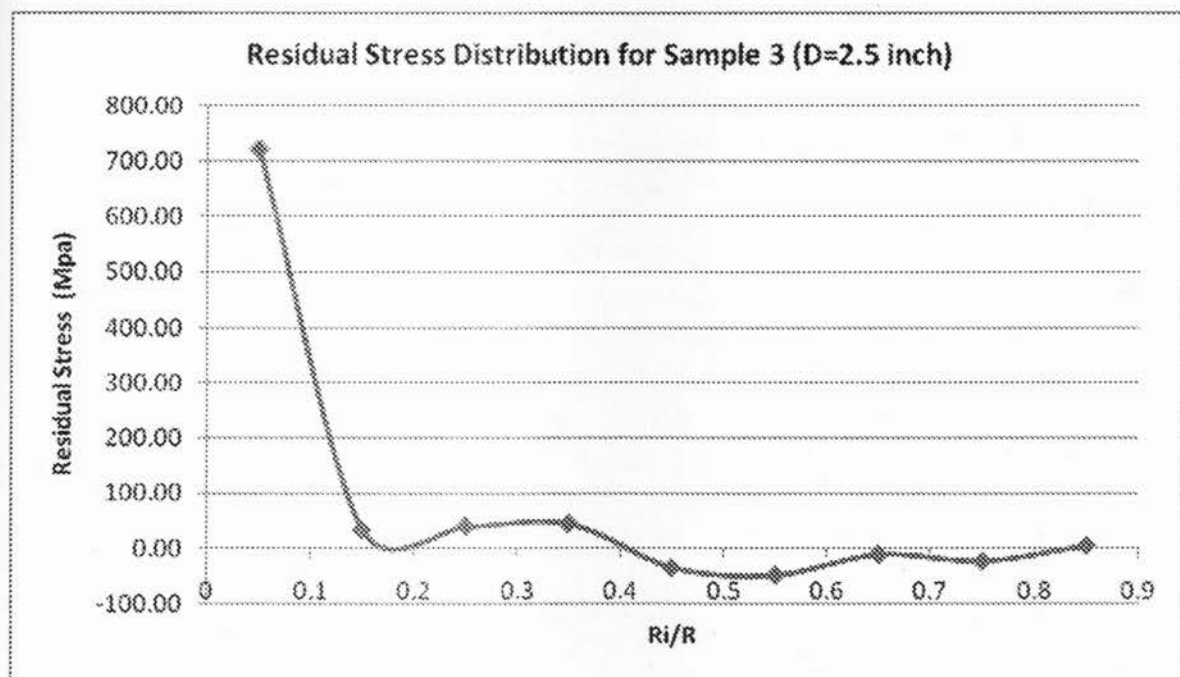


Figure 3-18: Residual Stress Distribution for Sample 3 (D=2.5 inch, H=3 inch)

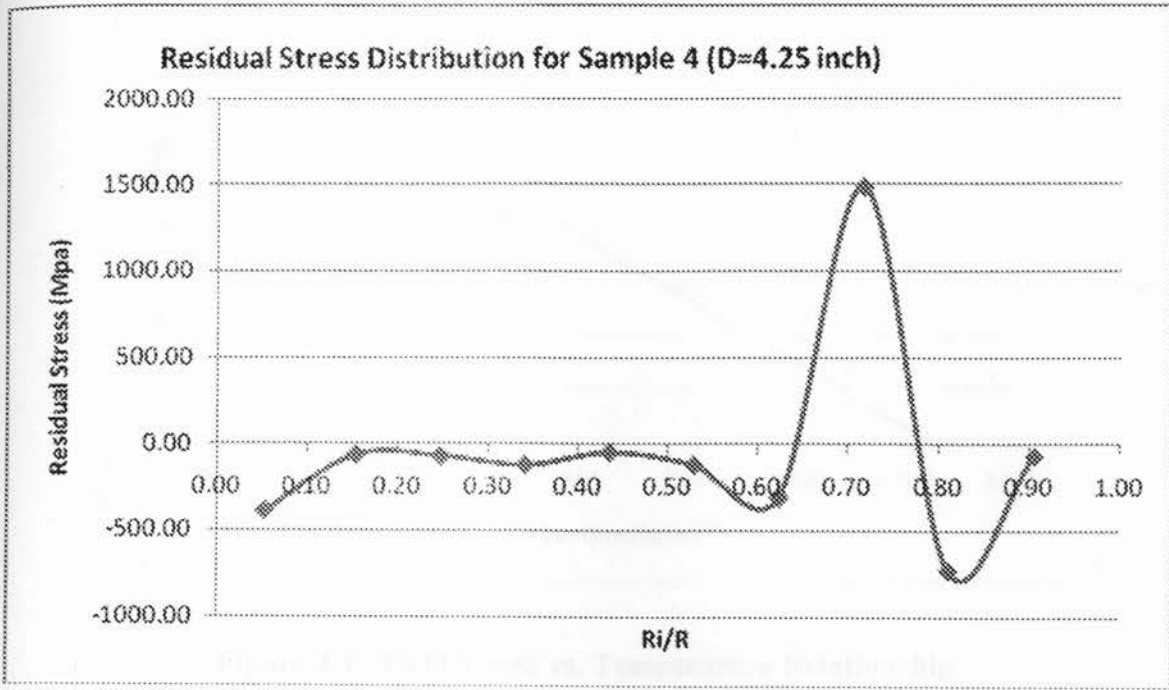


Figure 3-19: Residual Stress Distribution for Sample 4 (D=4.25 inch, H=3 inch)

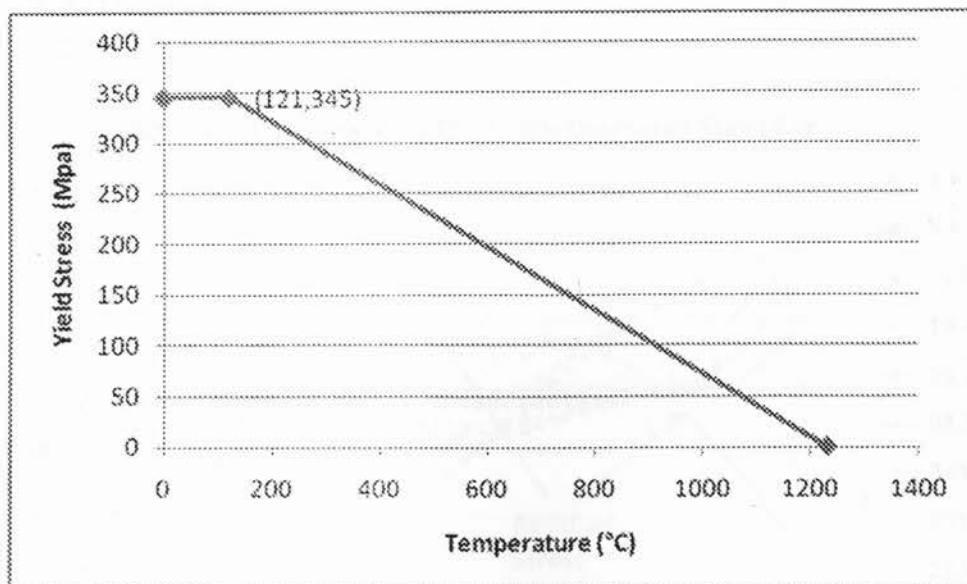
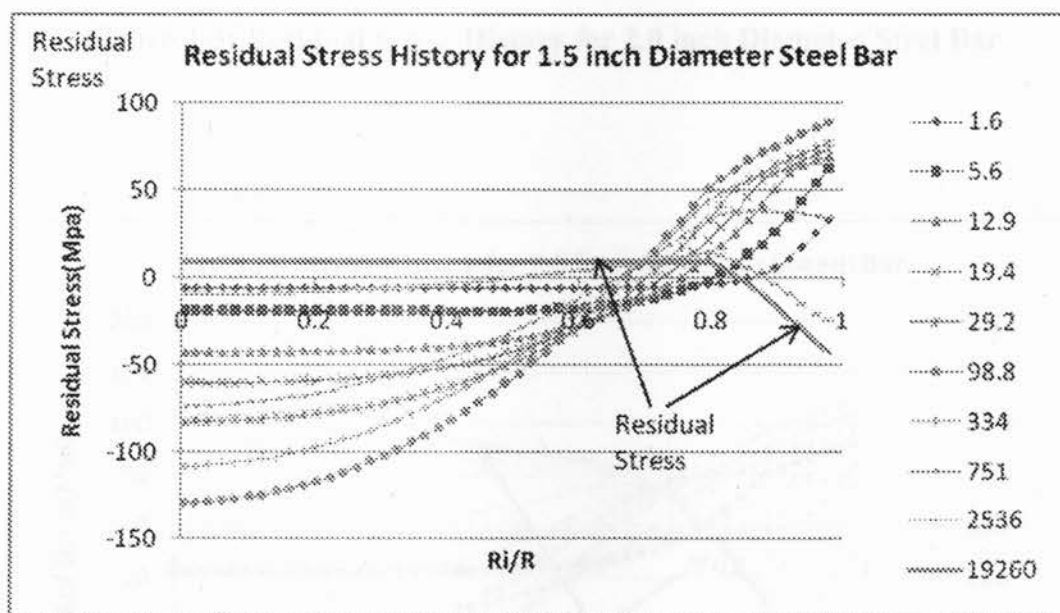


Figure 4-1: Yield Stress vs. Temperature Relationship



Note: The legend is time in seconds

Figure 4-2: Residual Stress History for 1.5 inch Diameter Steel Bar

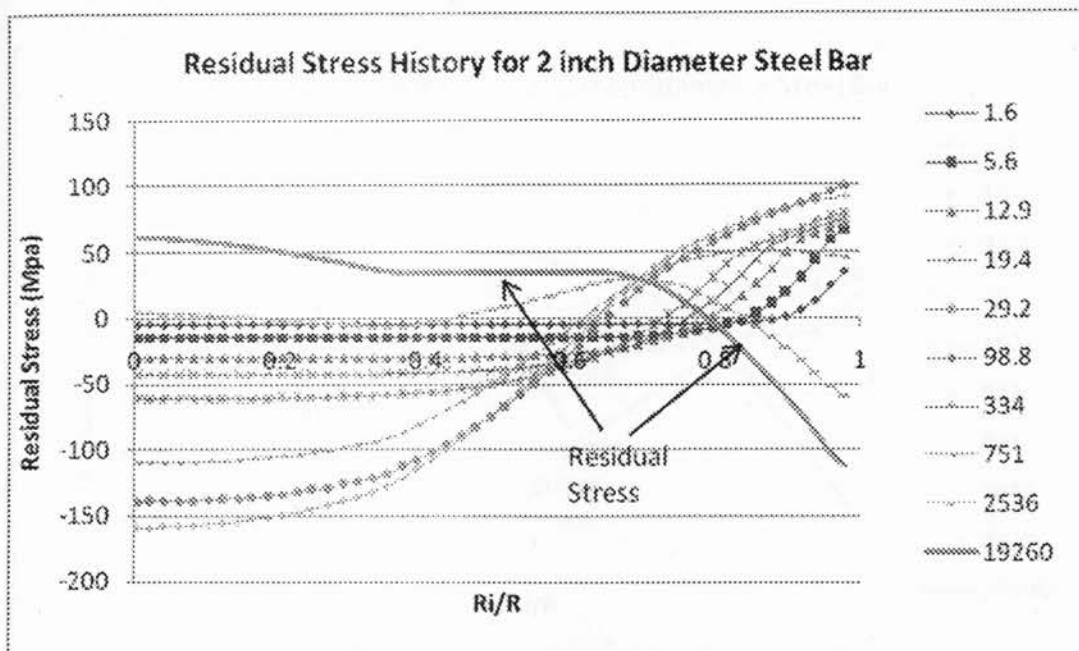


Figure 4-3: Residual Stress History for 2.0 inch Diameter Steel Bar

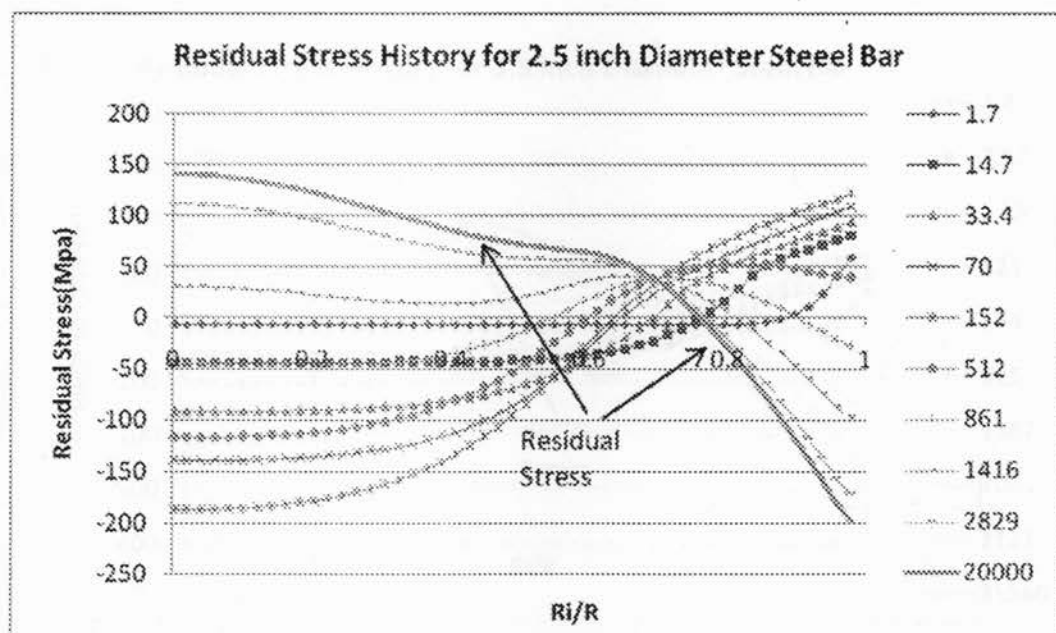


Figure 4-4: Residual Stress History for 2.5 inch Diameter Steel Bar

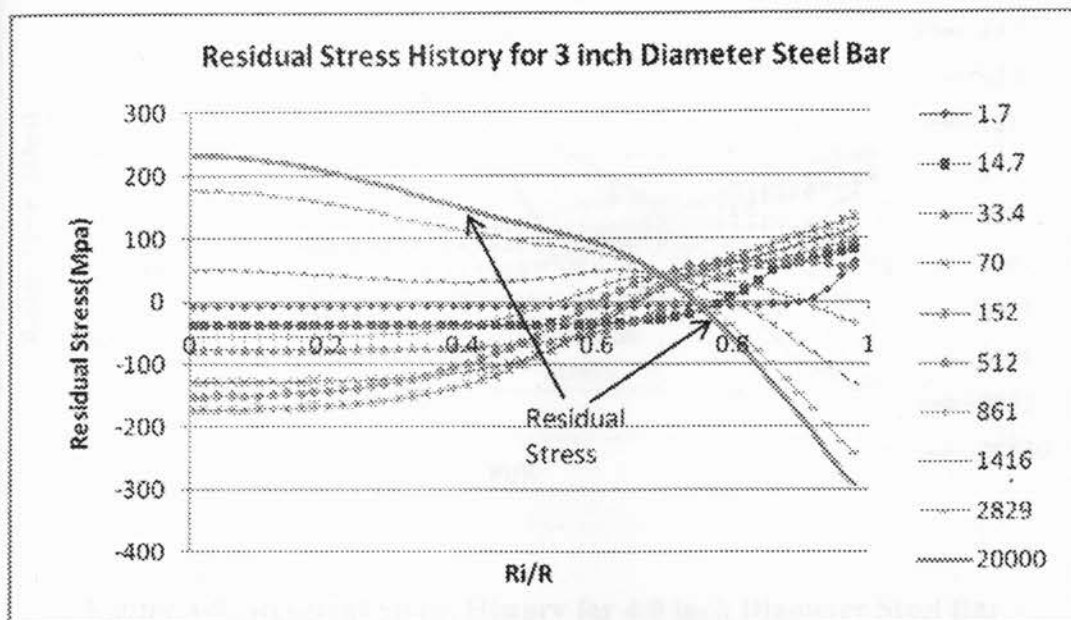


Figure 4-5: Residual Stress History for 3.0 inch Diameter Steel Bar

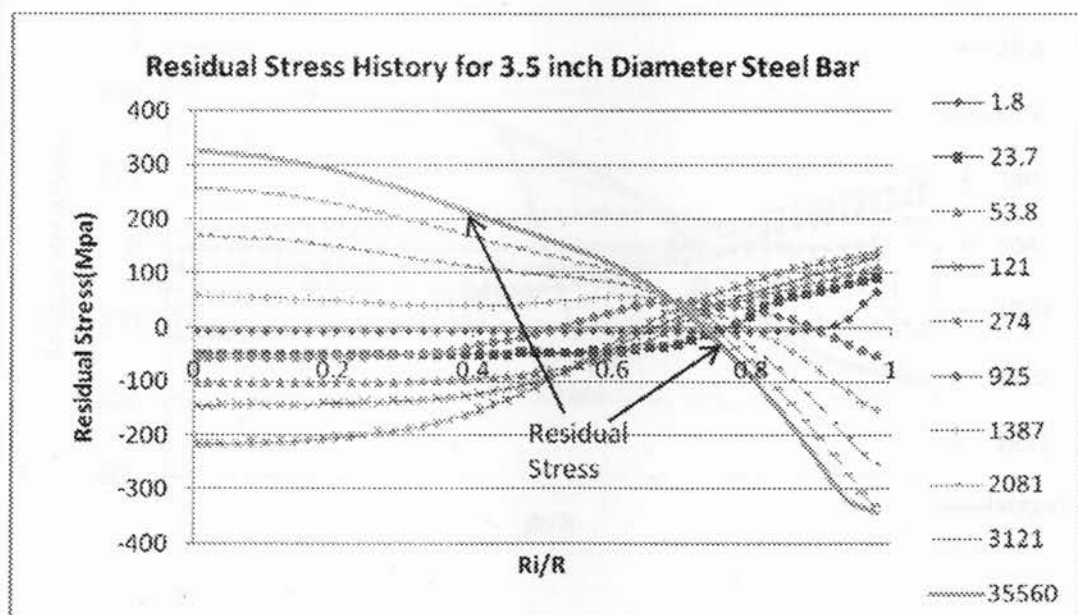


Figure 4-6: Residual Stress History for 3.5 inch Diameter Steel Bar

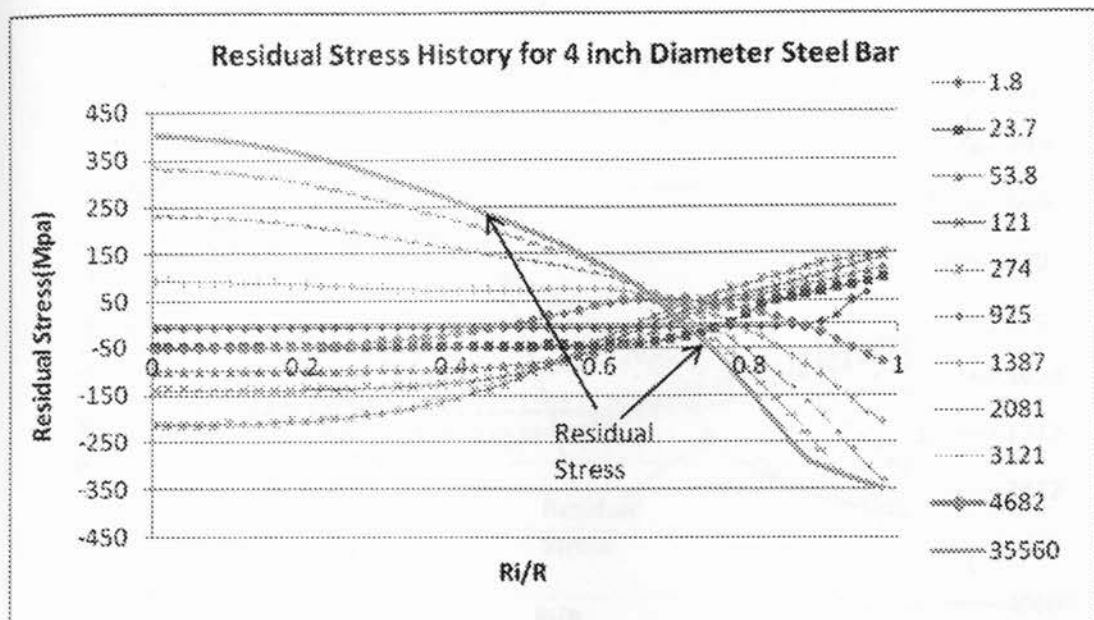


Figure 4-7: Residual Stress History for 4.0 inch Diameter Steel Bar

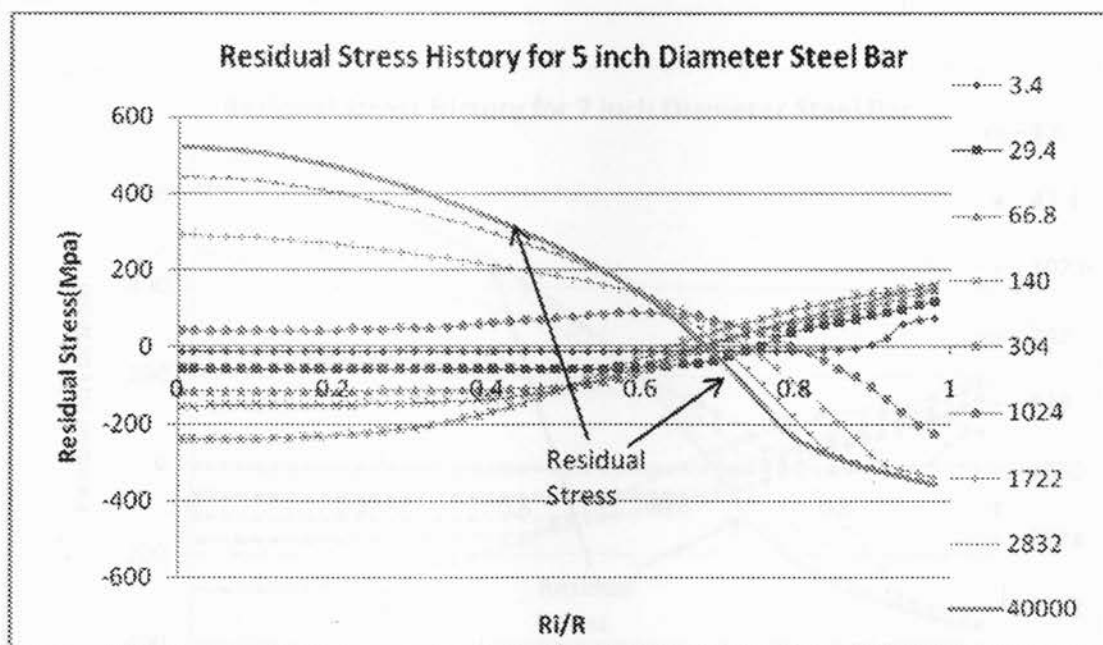


Figure 4-8: Residual Stress History for 5.0 inch Diameter Steel Bar

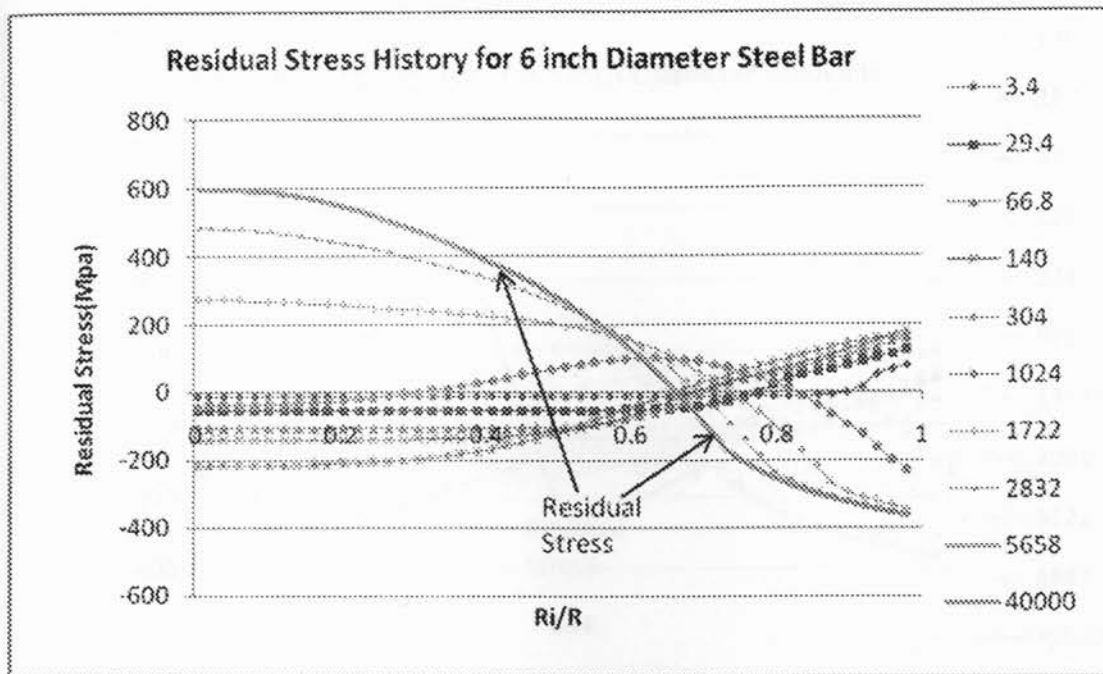


Figure 4-9: Residual Stress History for 6.0 inch Diameter Steel Bar

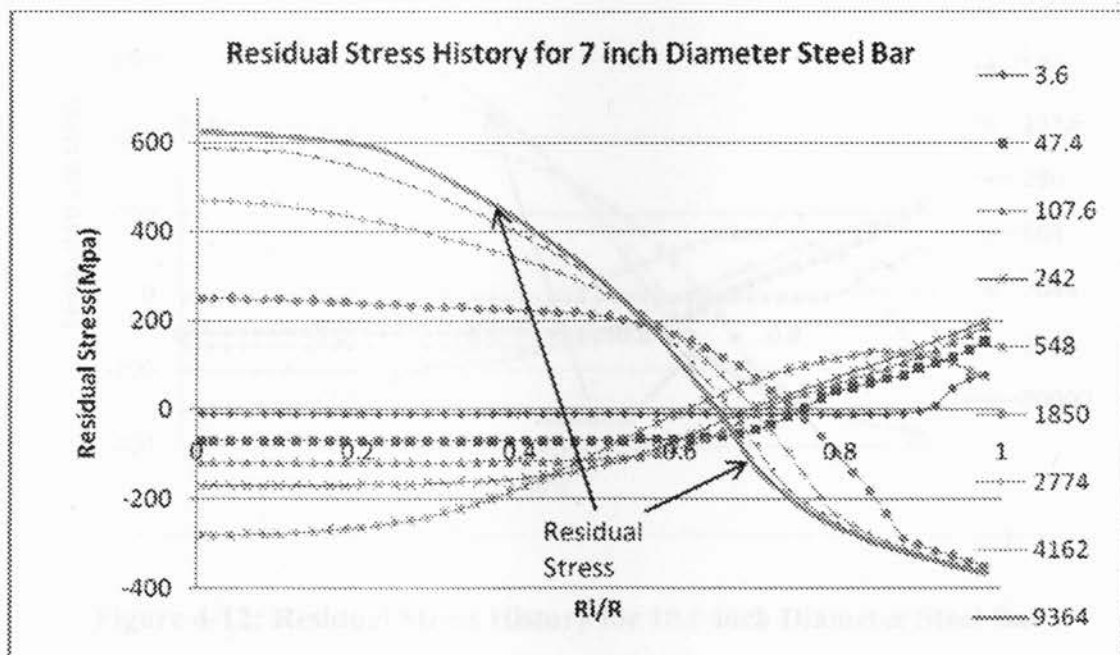


Figure 4-10: Residual Stress History for 7.0 inch Diameter Steel Bar

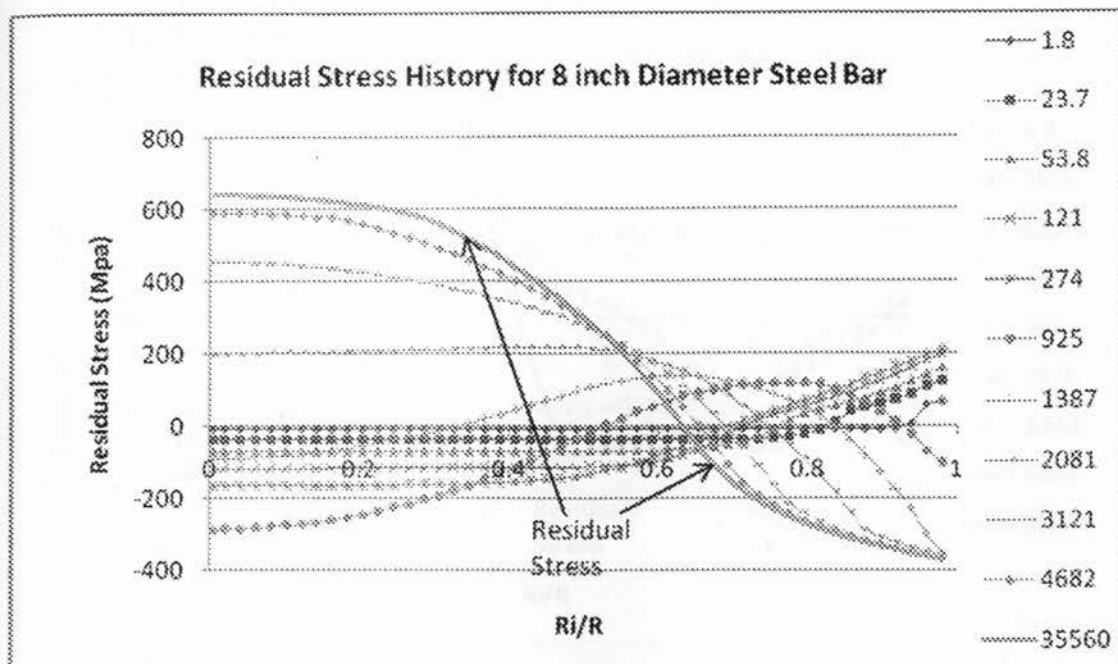


Figure 4-11: Residual Stress History for 8.0 inch Diameter Steel Bar

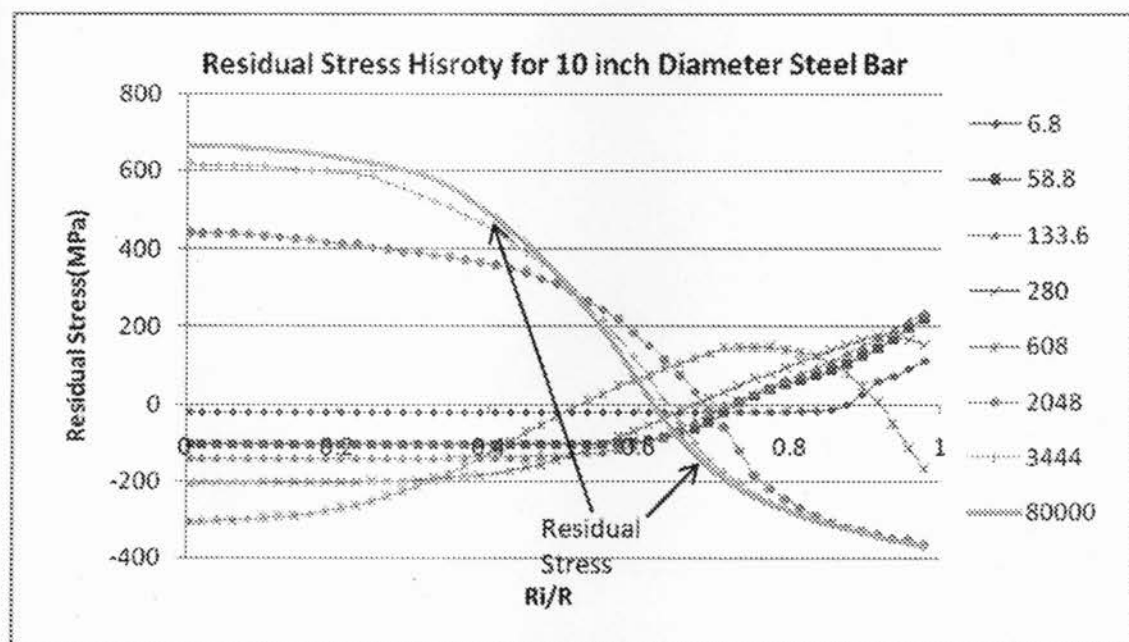


Figure 4-12: Residual Stress History for 10.0 inch Diameter Steel Bar

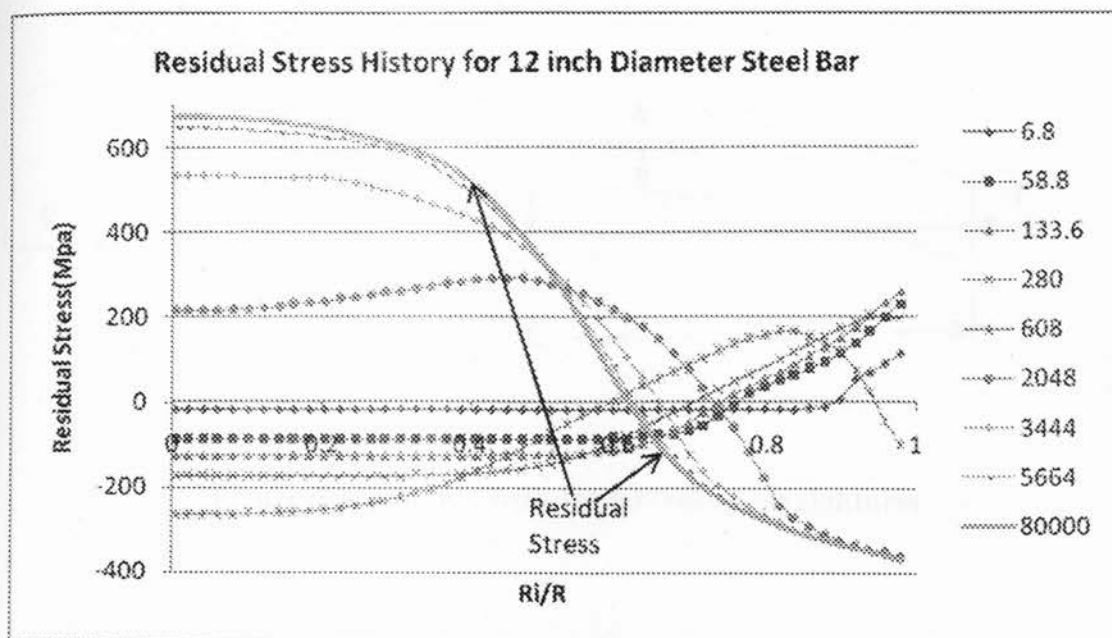


Figure 4-13: Residual Stress History for 12.0 inch Diameter Steel Bar

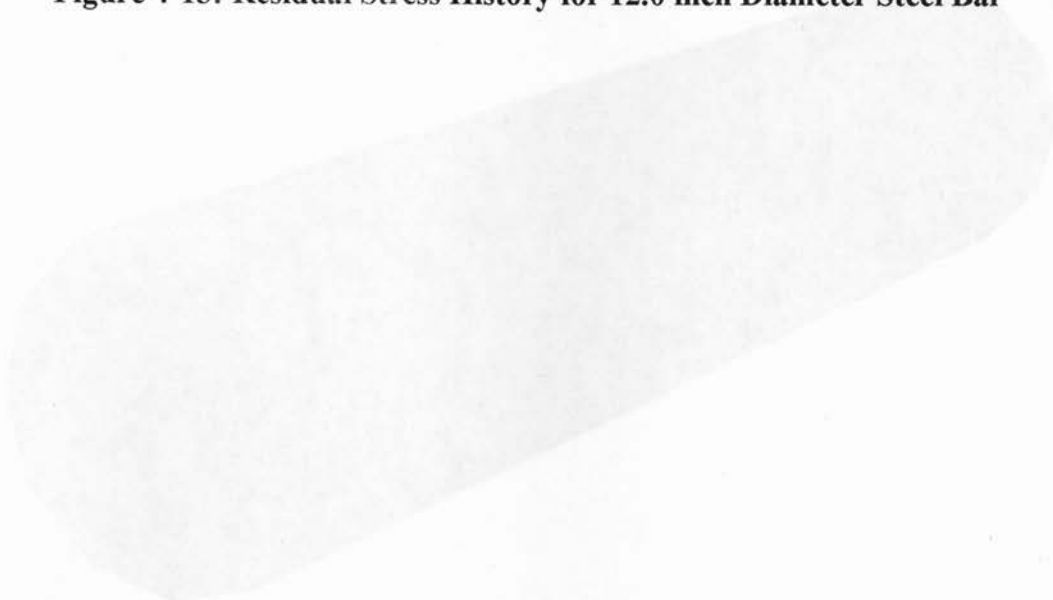


Figure 4-12: ABAQUS (shell) Modeling for Steel Columns without Residual Stress or with Symmetric or Asymmetric Residual Stress

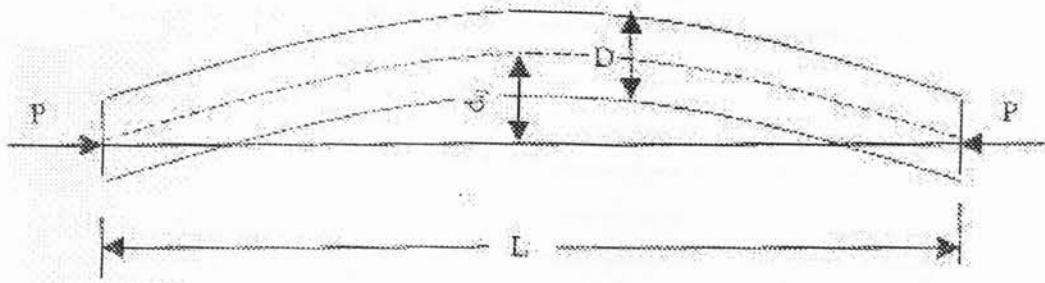


Figure 5-1: Column with Initial Out-of-Straightness

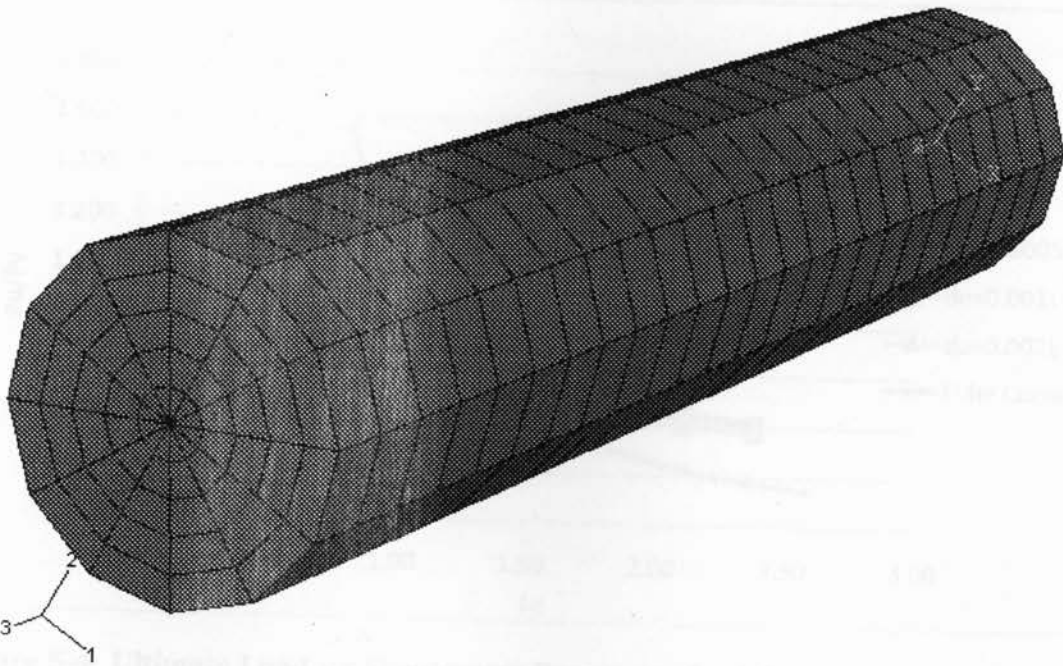


Figure 5-2: ABAQUS Model Meshing for Steel Columns without Residual Stress or with Symmetrical Residual Stress

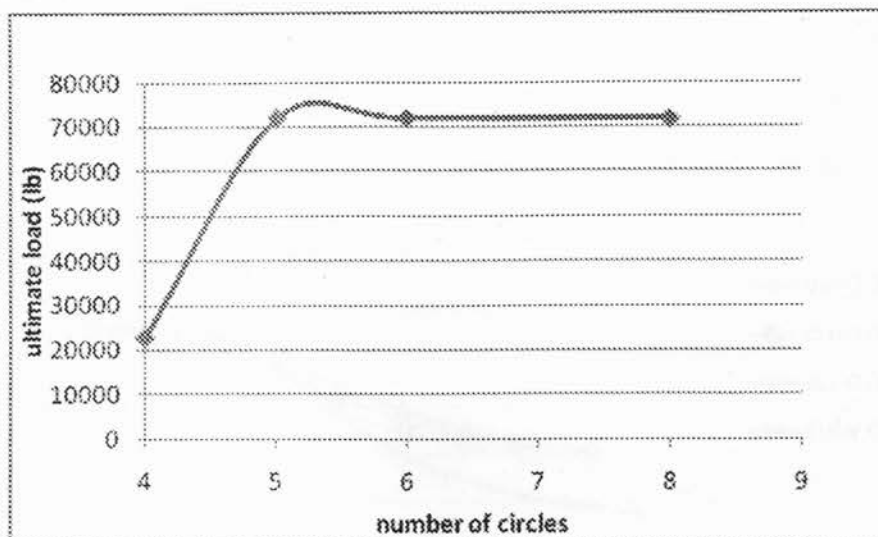


Figure 5-3: Effect of Number of Circles in the Cross Section on the Ultimate Load

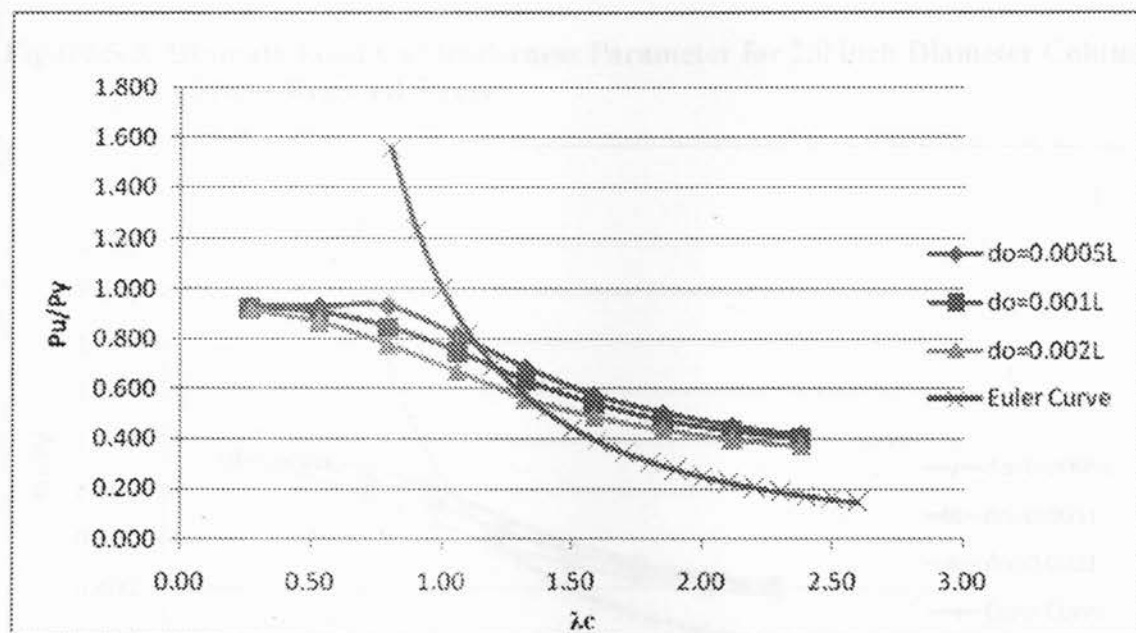


Figure 5-4: Ultimate Load v.s Slenderness Parameter for 1.5 inch Diameter Column without Residual Stress

Note: λc is slenderness parameter of the steel column

P_u is the ultimate load obtained by ABAQUS analysis

P_y is the yield strength of steel column

d_o is the initial deflection

L is the length of steel column

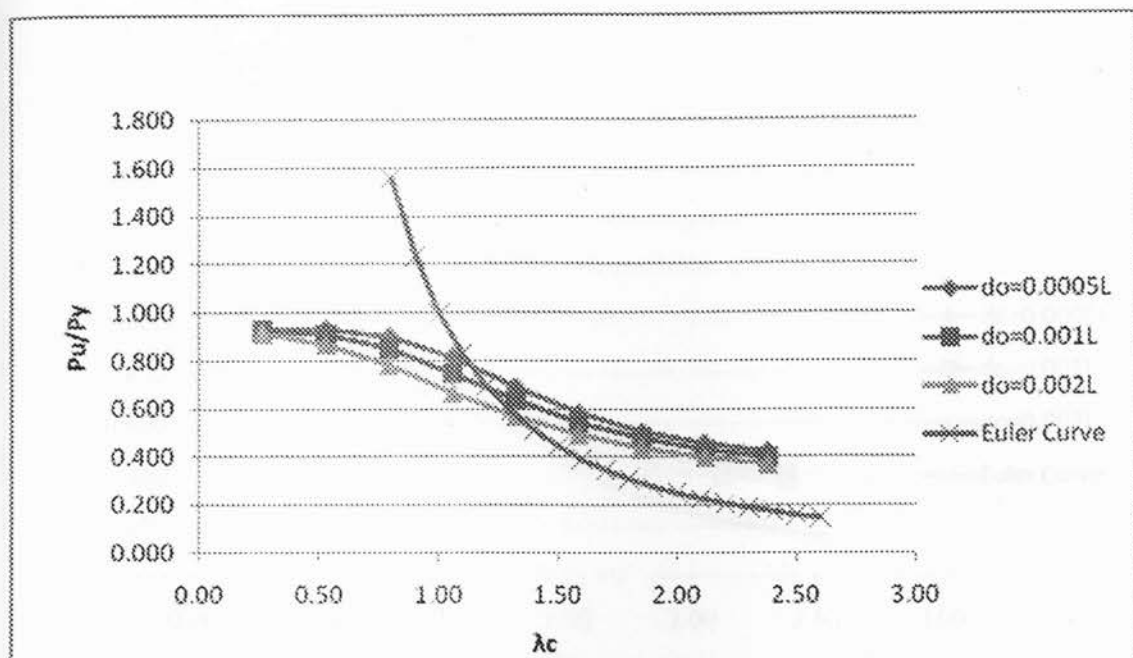


Figure 5-5: Ultimate Load v.s Slenderness Parameter for 2.0 inch Diameter Column without Residual Stress

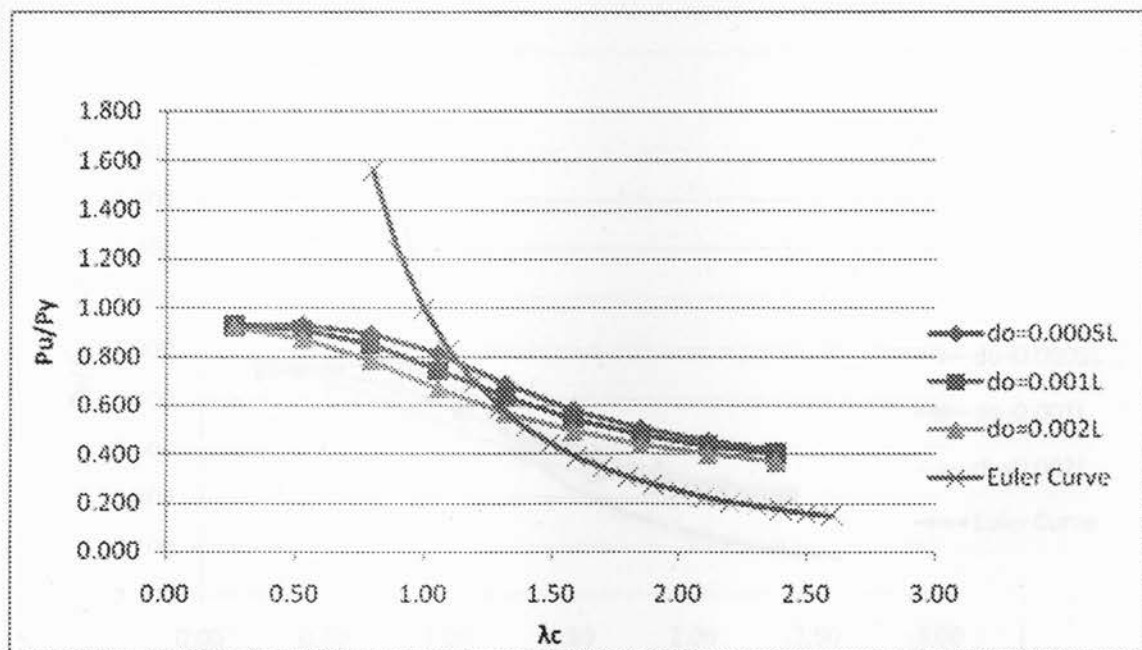


Figure 5-6: Ultimate Load v.s Slenderness Parameter for 2.5 inch Diameter Column without Residual Stress

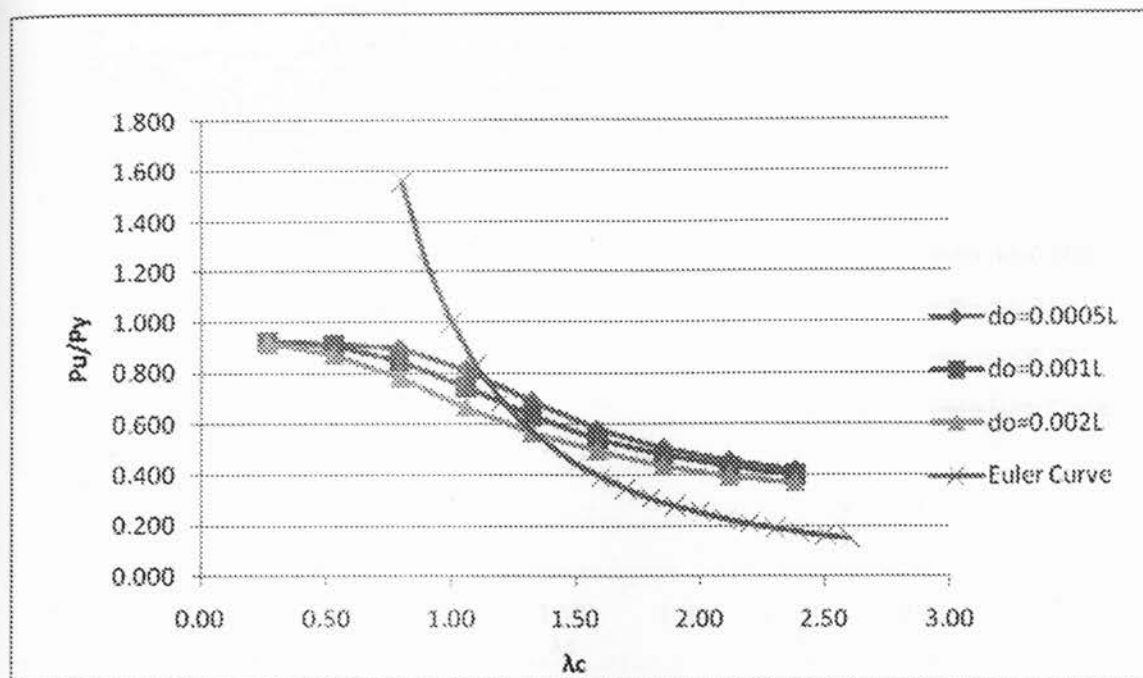


Figure 5-7: Ultimate Load v.s Slenderness Parameter for 3.0 inch Diameter Column without Residual Stress

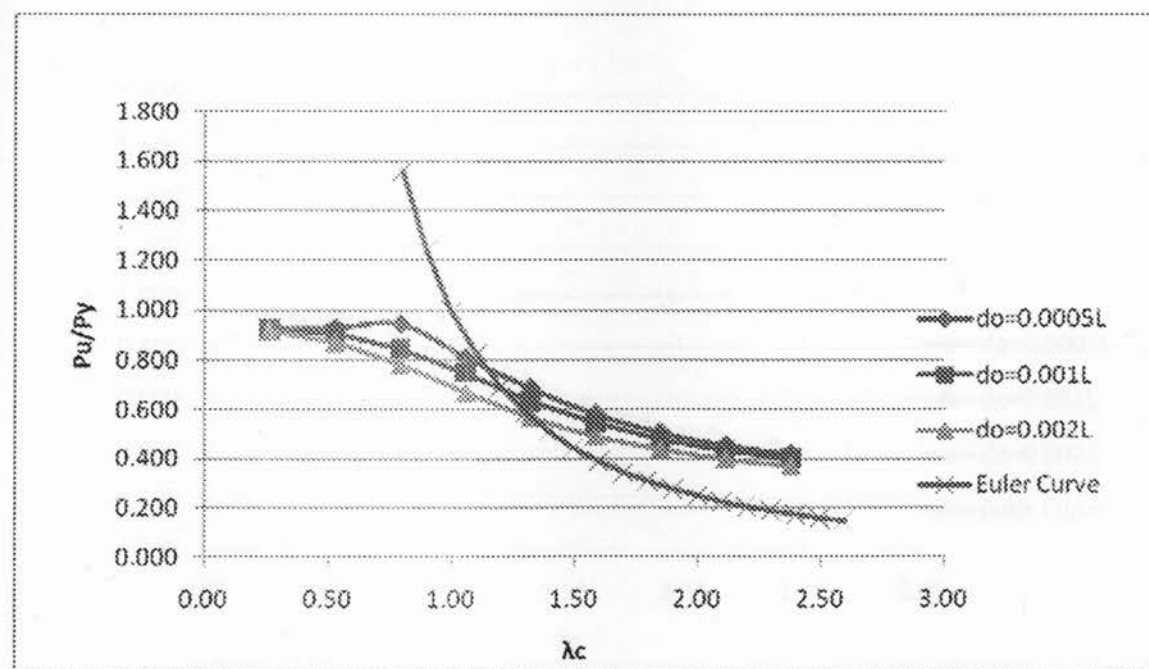


Figure 5-8: Ultimate Load v.s Slenderness Parameter for 3.5 inch Diameter Column without Residual Stress

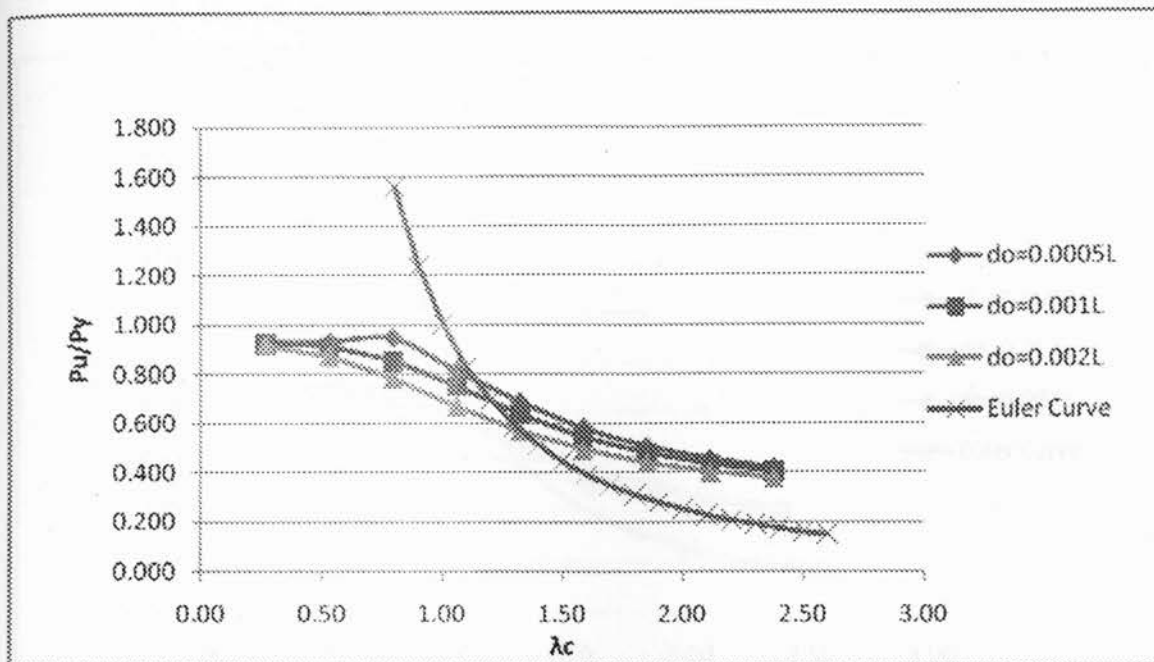


Figure 5-9: Ultimate Load v.s Slenderness Parameter for 4.0 inch Diameter Column without Residual Stress

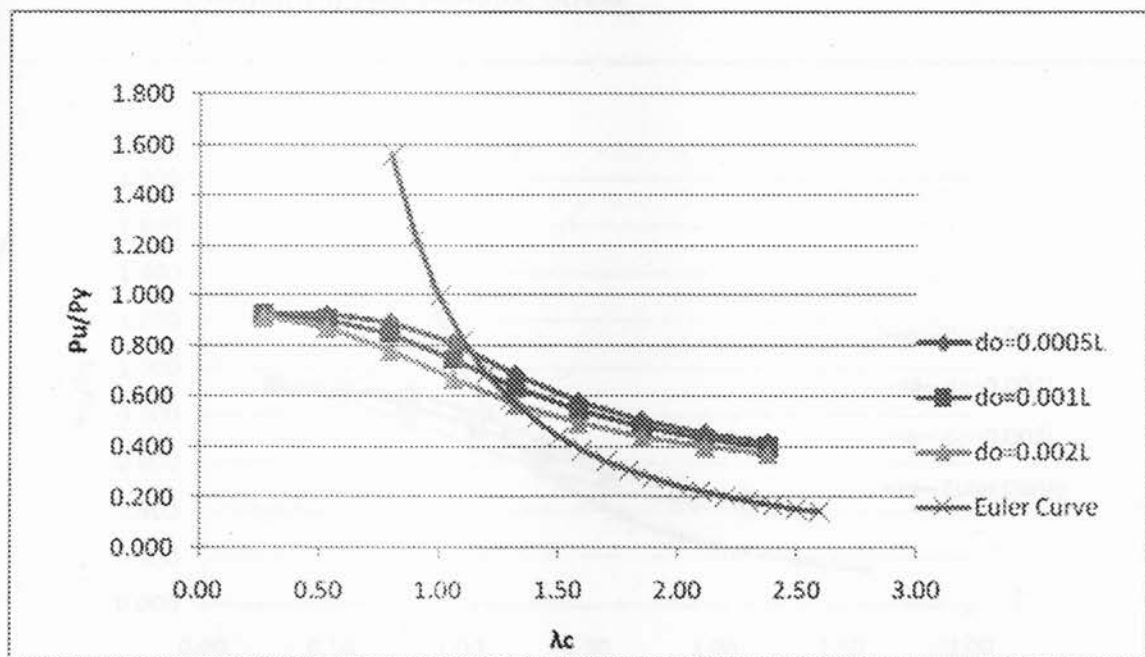


Figure 5-10: Ultimate Load v.s Slenderness Parameter for 5.0 inch Diameter Column without Residual Stress

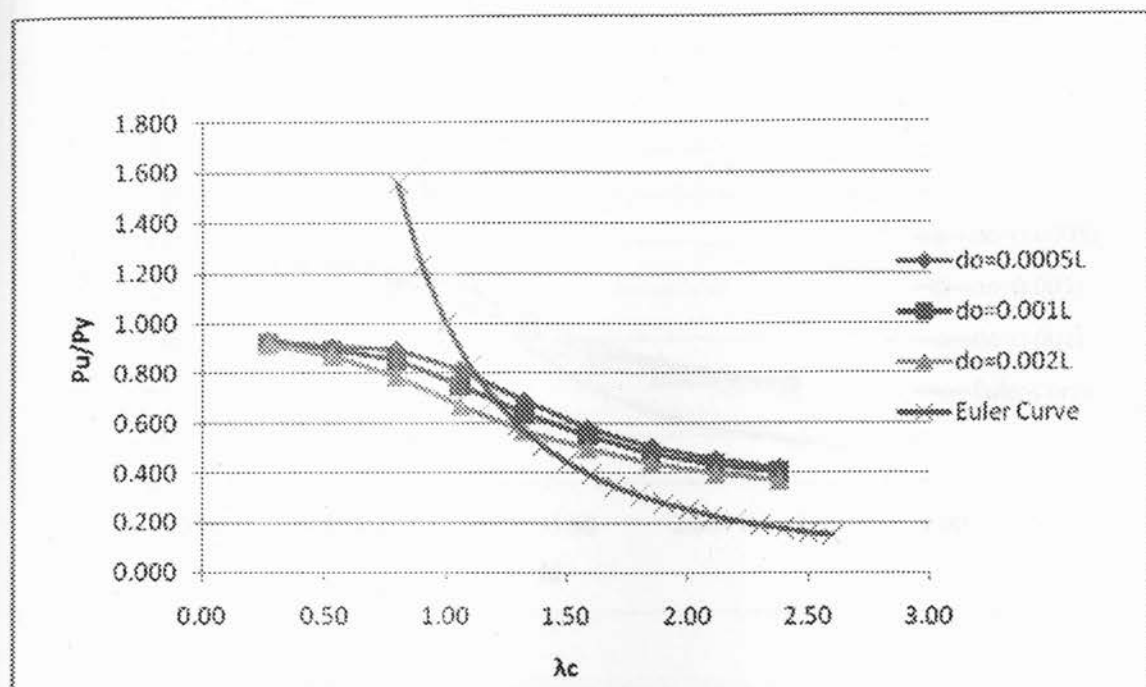


Figure 5-11: Ultimate Load v.s Slenderness Parameter for 6.0 inch Diameter Column without Residual Stress

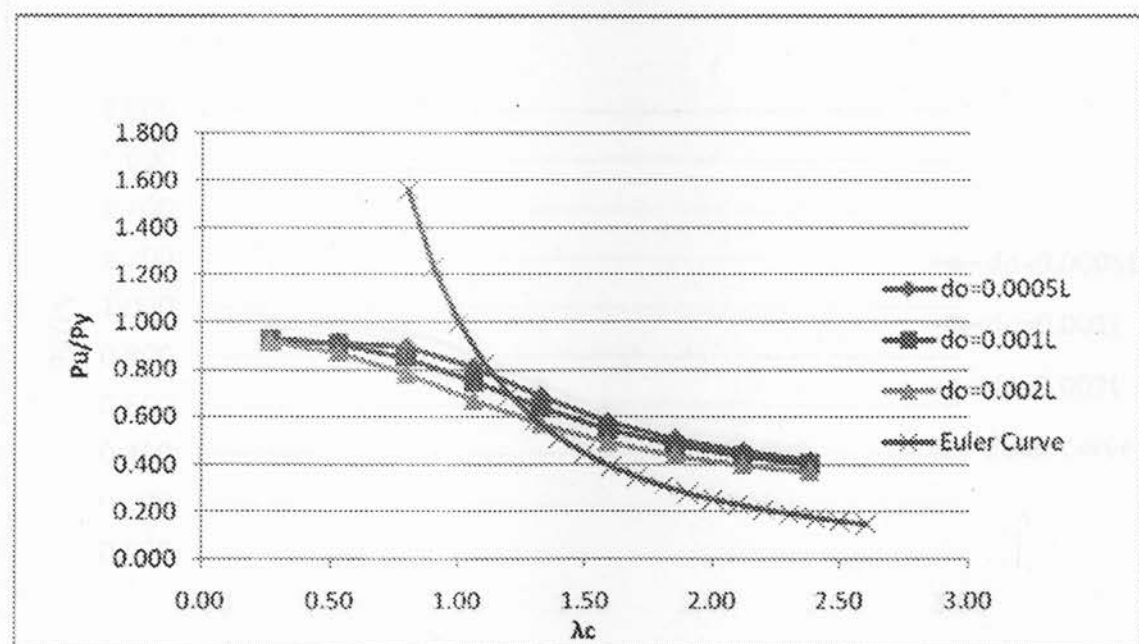


Figure 5-12: Ultimate Load v.s Slenderness Parameter for 7.0 inch Diameter Column without Residual Stress

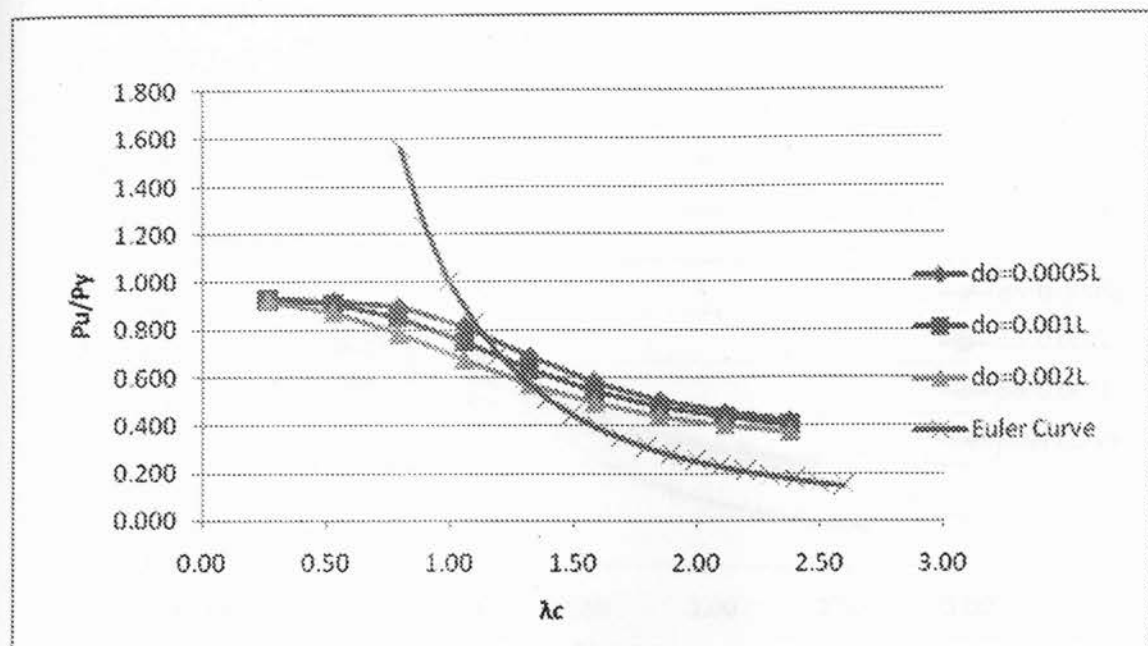


Figure 5-13: Ultimate Load v.s Slenderness Parameter for 8.0 inch Diameter Column without Residual Stress

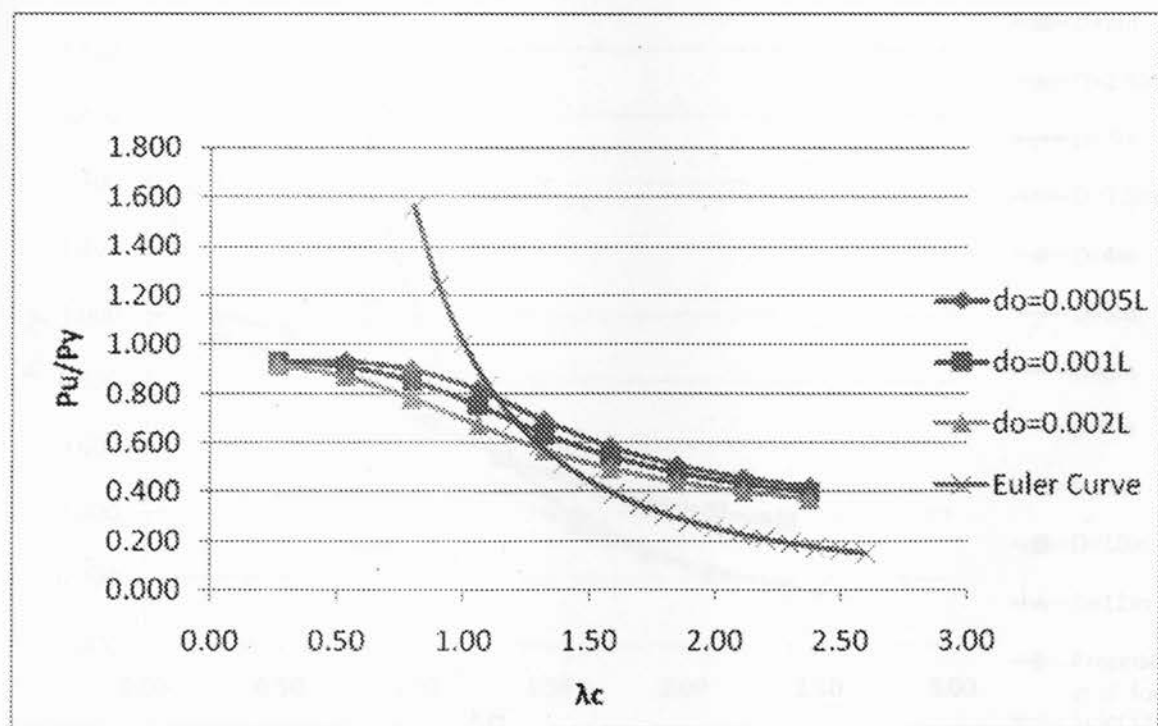


Figure 5-14: Ultimate Load v.s Slenderness Parameter for 10 inch Diameter Column without Residual Stress

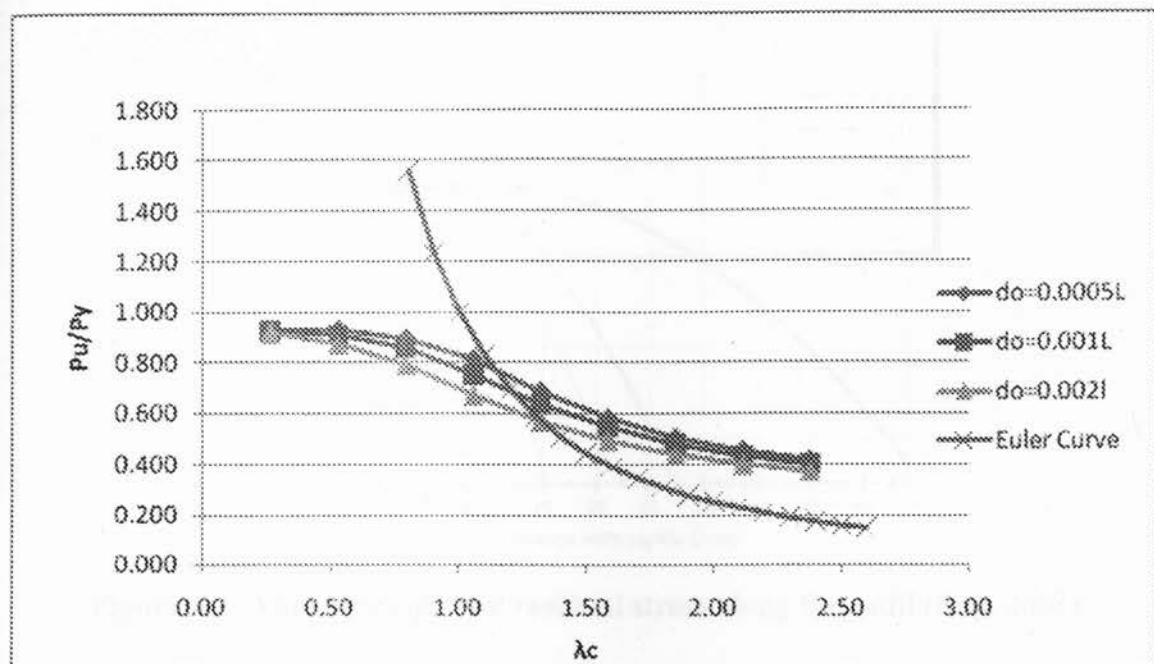


Figure 5-15: Ultimate Load v.s Slenderness Parameter for 12 inch Diameter Column without Residual Stress

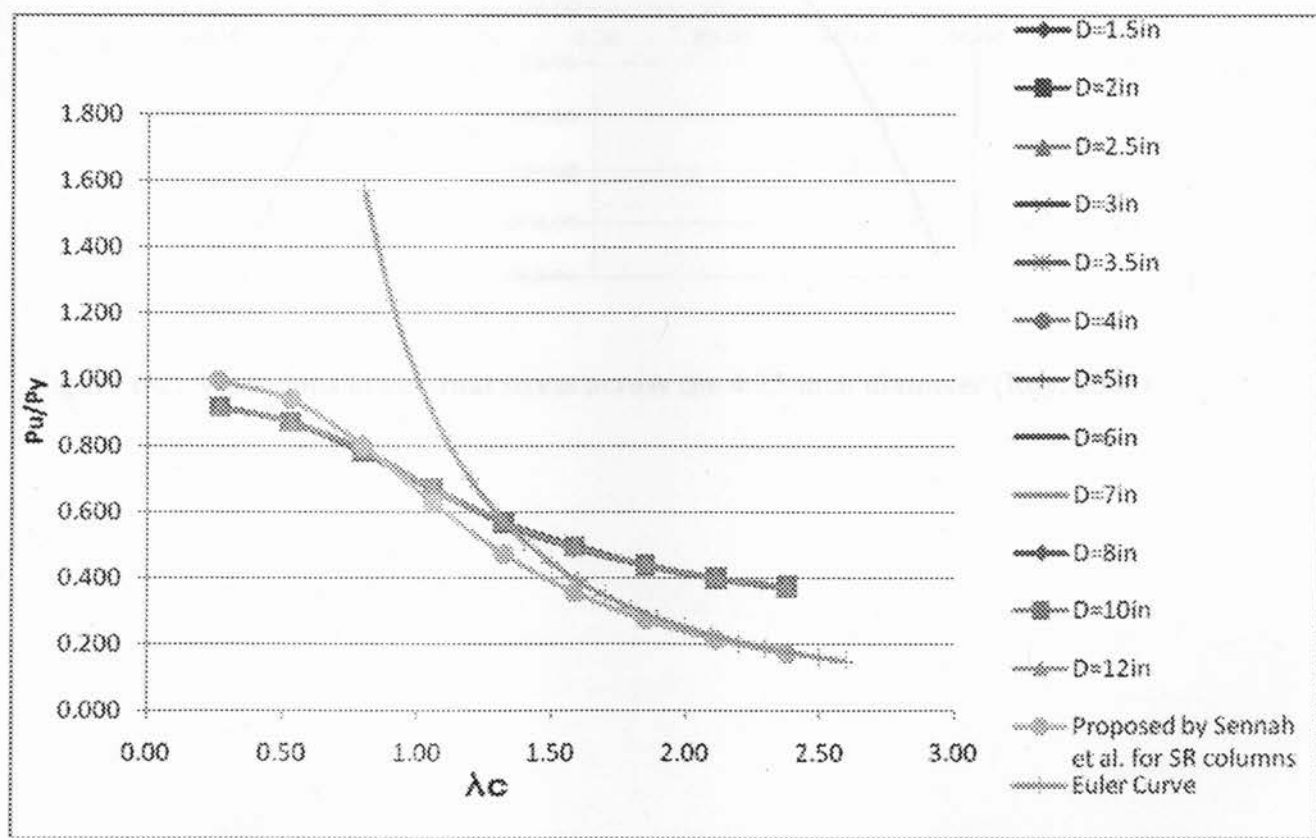


Figure 5-16: Ultimate Load v.s Slenderness Parameter curves for Columns without Residual Stress and $L/500$ Initial Out-of-Straightness

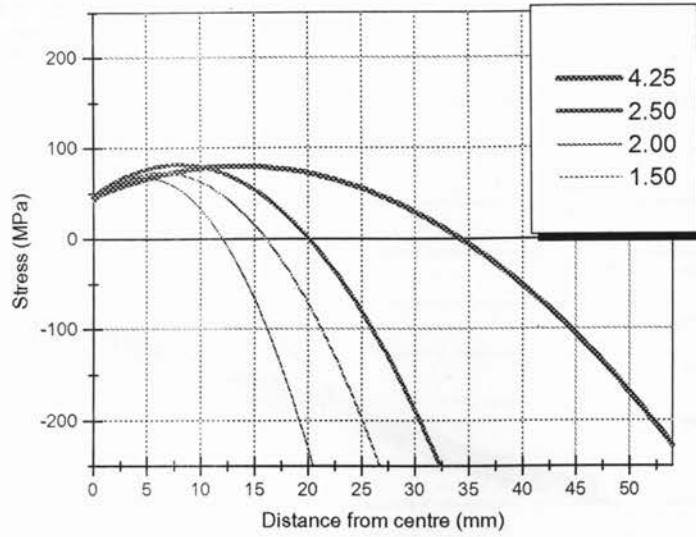


Figure 6-1: Variations of axial residual stress along the radii (Roy, 2008)

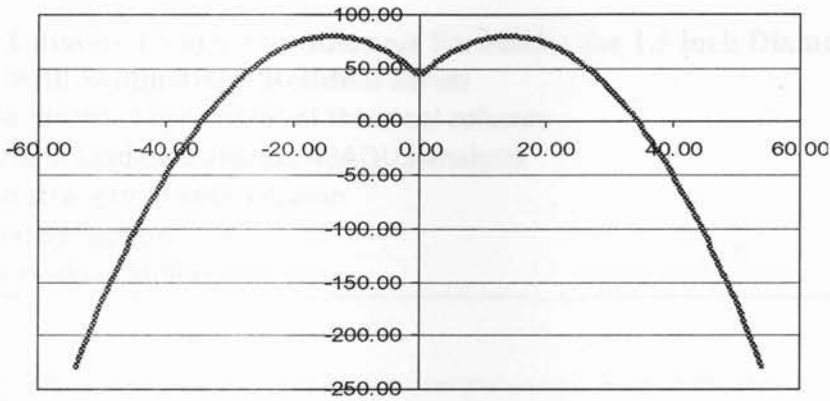


Figure 6-2: Variations of residual stress across the 4.25-inch diameter (Roy, 2008)

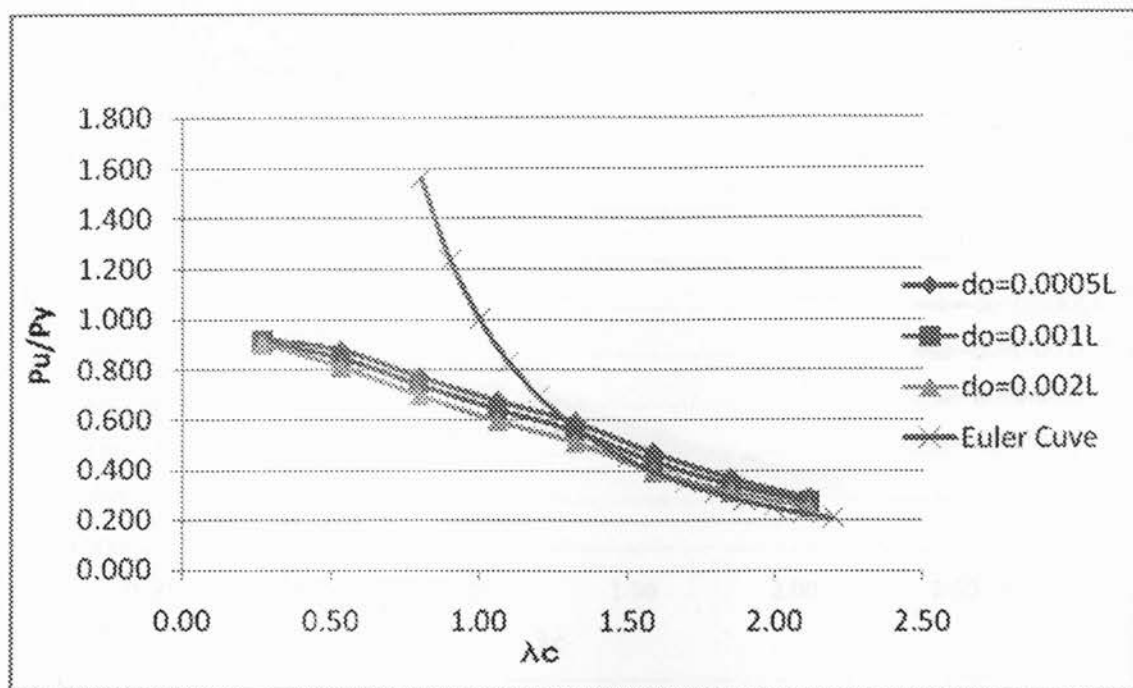


Figure 6-3: Ultimate Load v.s Slenderness Parameter for 1.5 inch Diameter Column with Symmetrical Residual Stress

Note: λ_c is slenderness parameter of the steel column

P_u is the ultimate load obtained by ABAQUS analysis

P_y is the yield strength of steel column

d_o is the initial deflection

L is the length of steel column

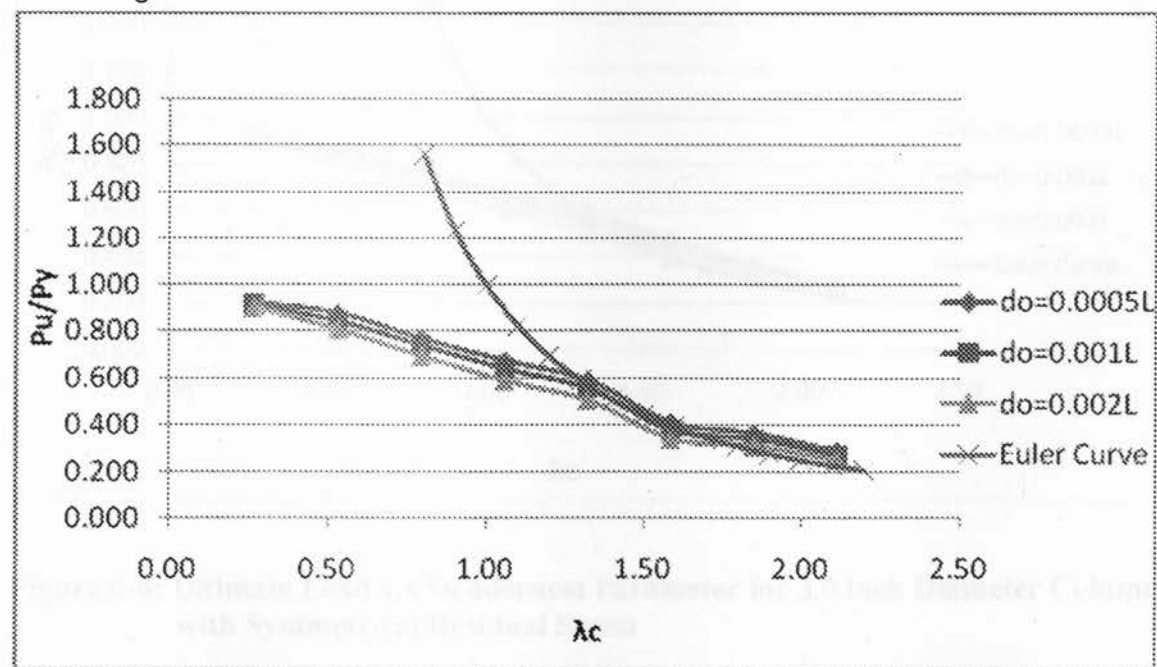


Figure 6-4: Ultimate Load v.s Slenderness Parameter for 2.0 inch Diameter Column with Symmetrical Residual Stress

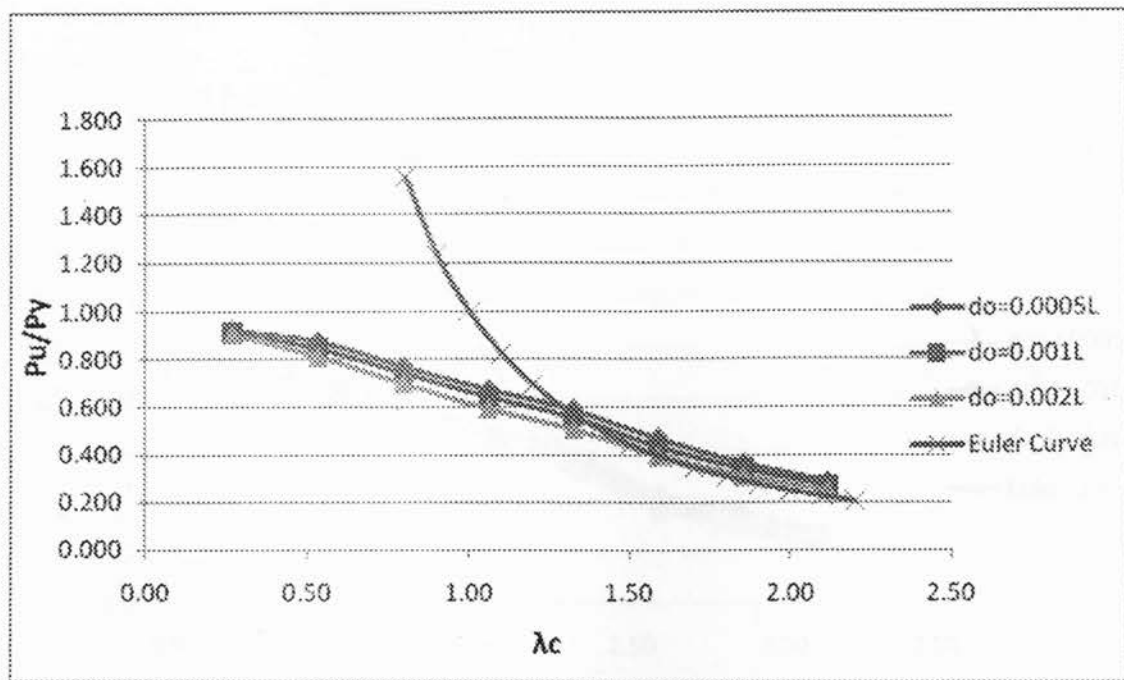


Figure 6-5: Ultimate Load v.s Slenderness Parameter for 2.5 inch Diameter Column with Symmetrical Residual Stress

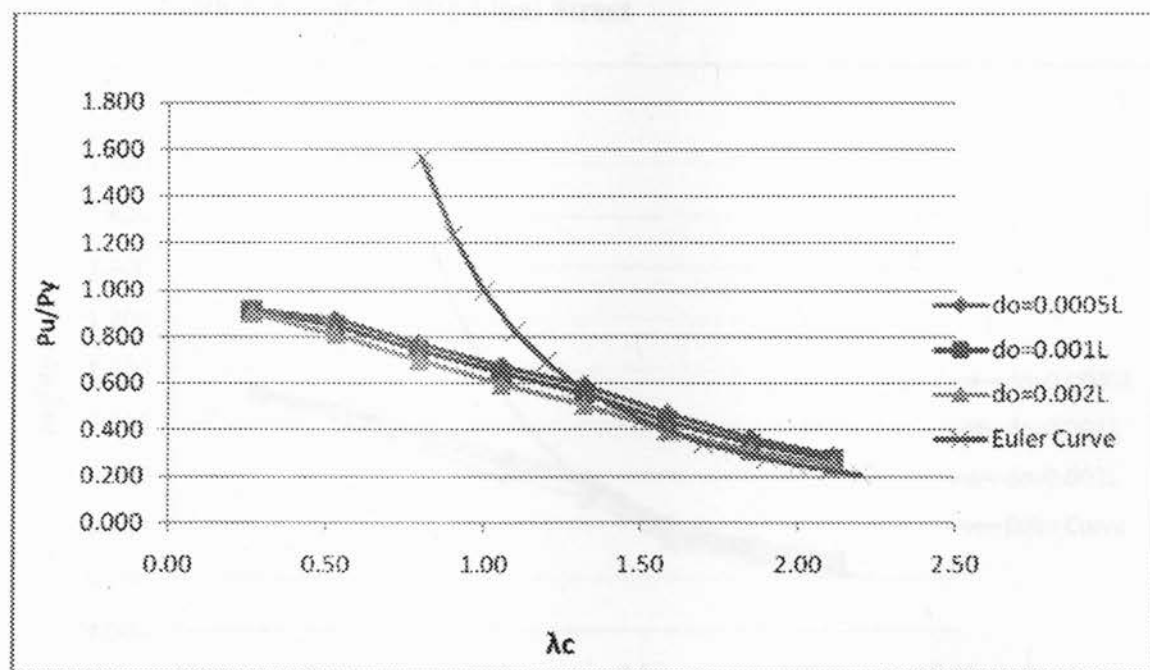


Figure 6-6: Ultimate Load v.s Slenderness Parameter for 3.0 inch Diameter Column with Symmetrical Residual Stress

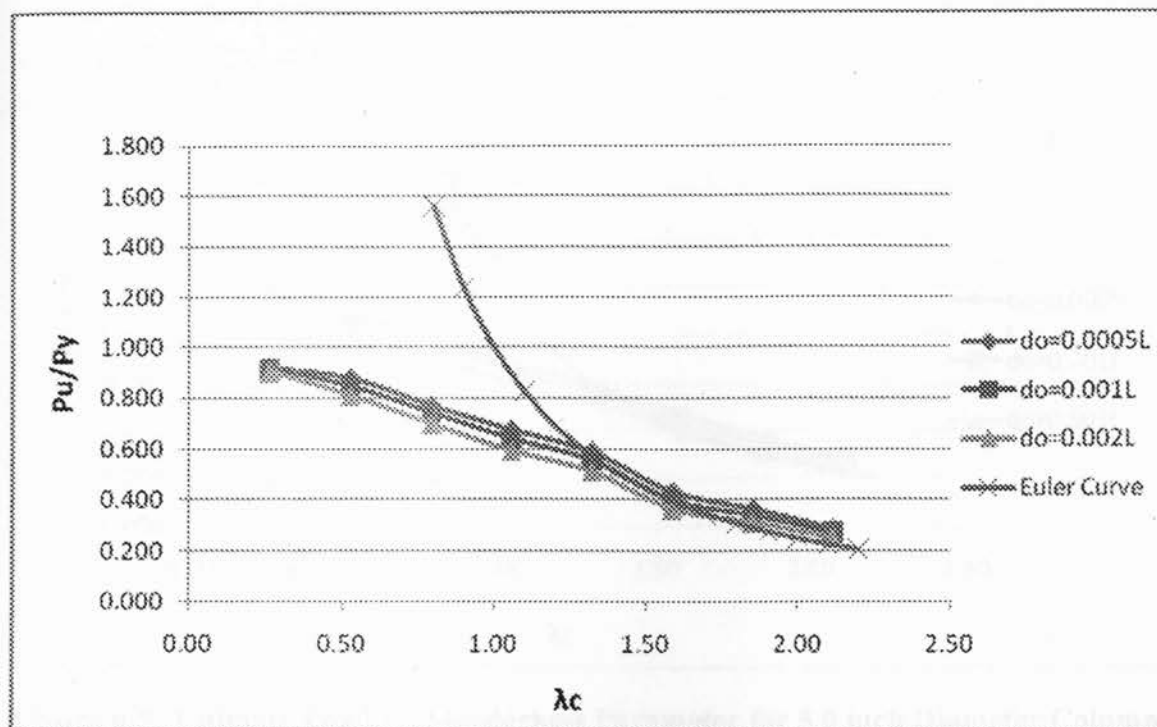


Figure 6-7: Ultimate Load v.s Slenderness Parameter for 3.5 inch Diameter Column with Symmetrical Residual Stress

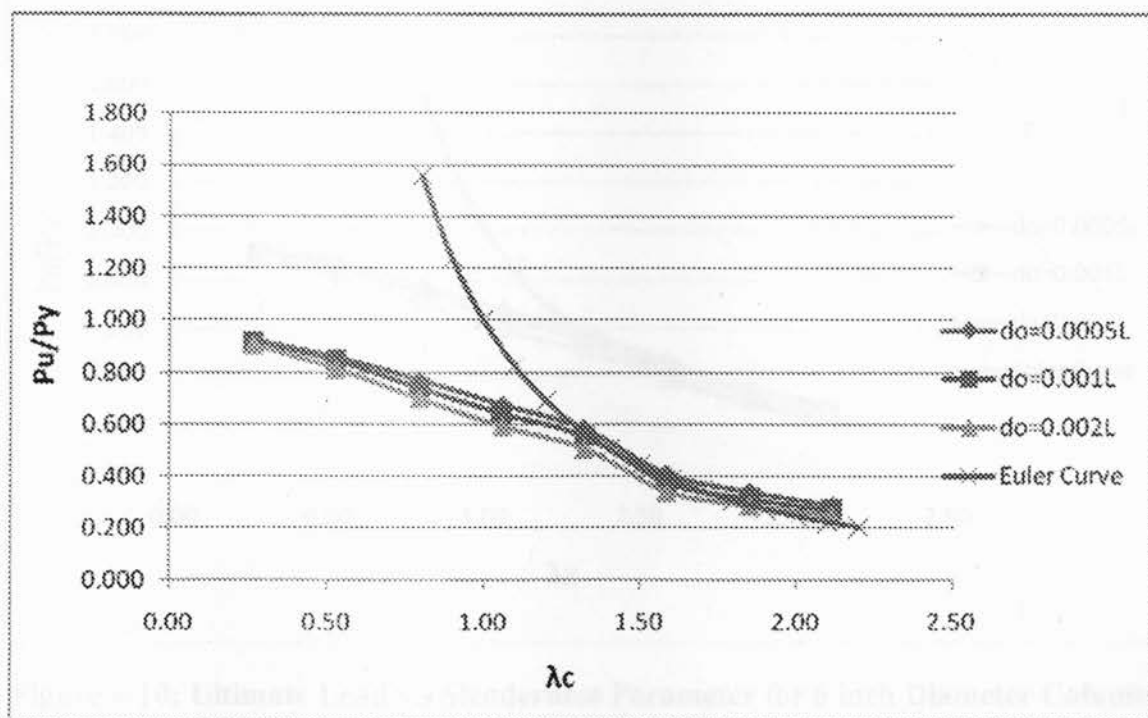


Figure 6-8: Ultimate Load v.s Slenderness Parameter for 4.0 inch Diameter Column with Symmetrical Residual Stress

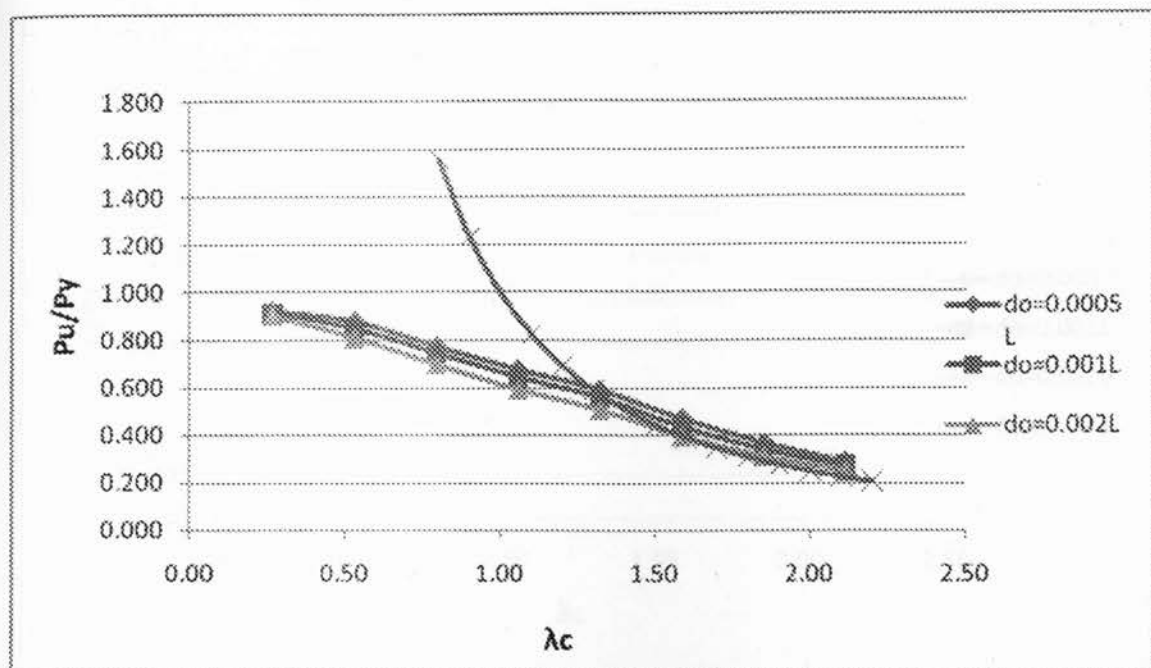


Figure 6-9: Ultimate Load v.s Slenderness Parameter for 5.0 inch Diameter Column with Symmetrical Residual Stress

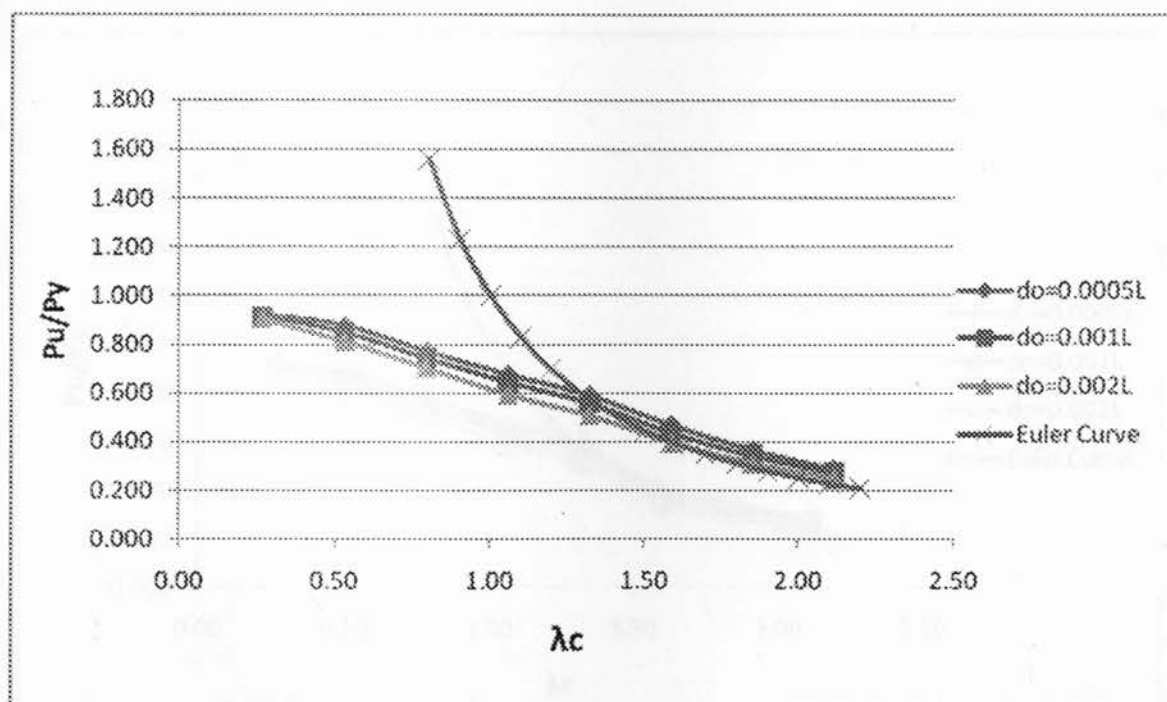


Figure 6-10: Ultimate Load v.s Slenderness Parameter for 6 inch Diameter Column with Symmetrical Residual Stress

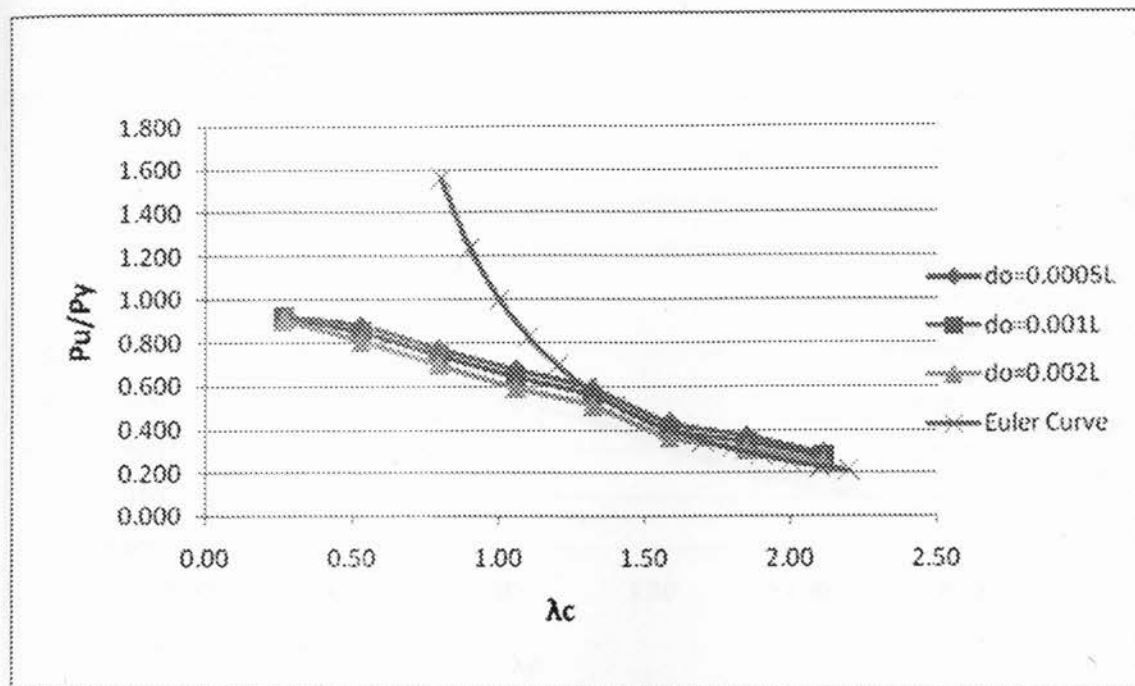


Figure 6-11: Ultimate Load v.s Slenderness Parameter for 7 inch Diameter Column with Symmetrical Residual Stress

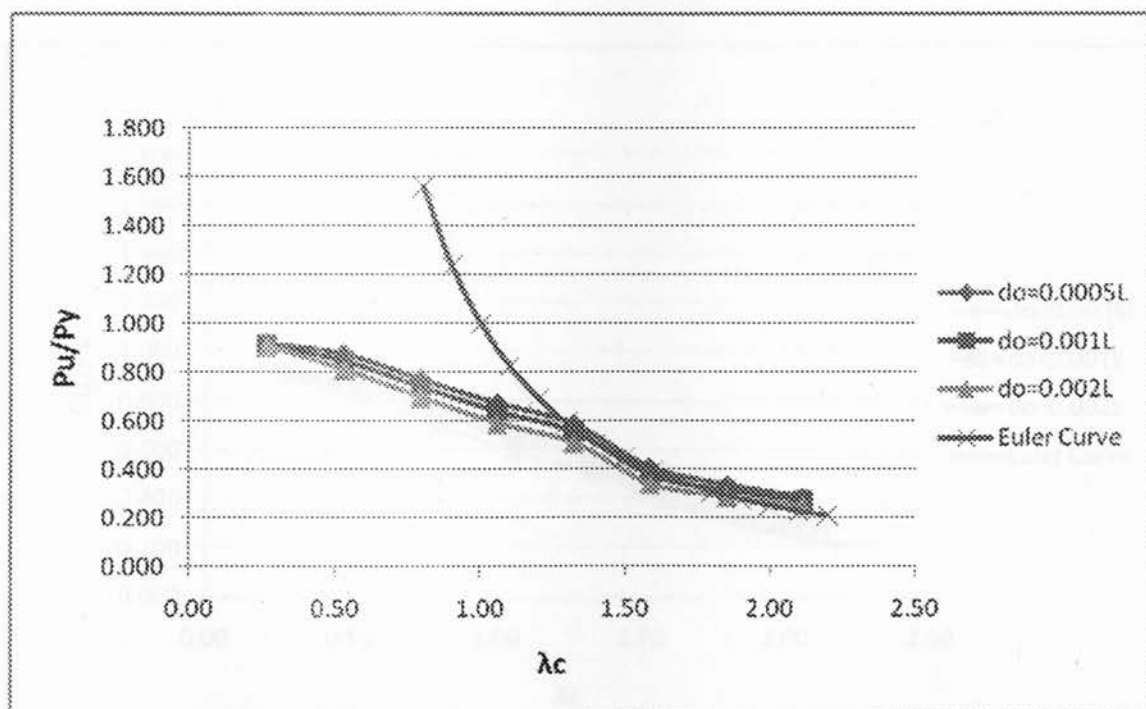


Figure 6-12: Ultimate Load v.s Slenderness Parameter for 8 inch Diameter Column with Symmetrical Residual Stress

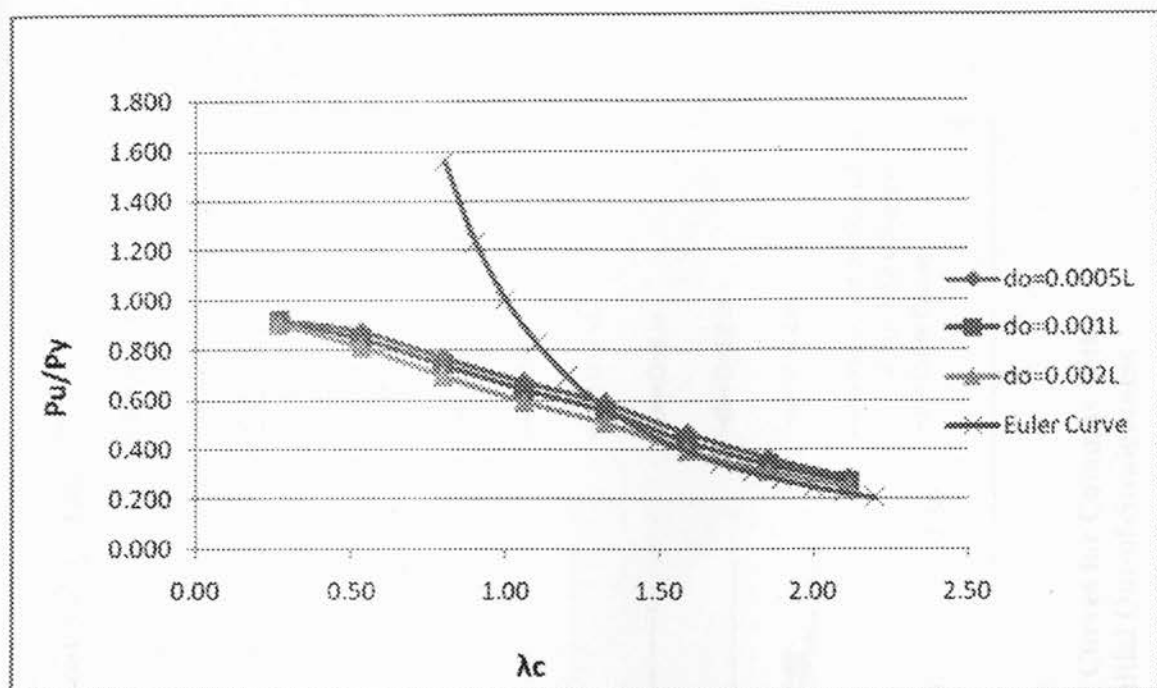


Figure 6-13: Ultimate Load v.s Slenderness Parameter for 10 inch Diameter Column with Symmetrical Residual Stress

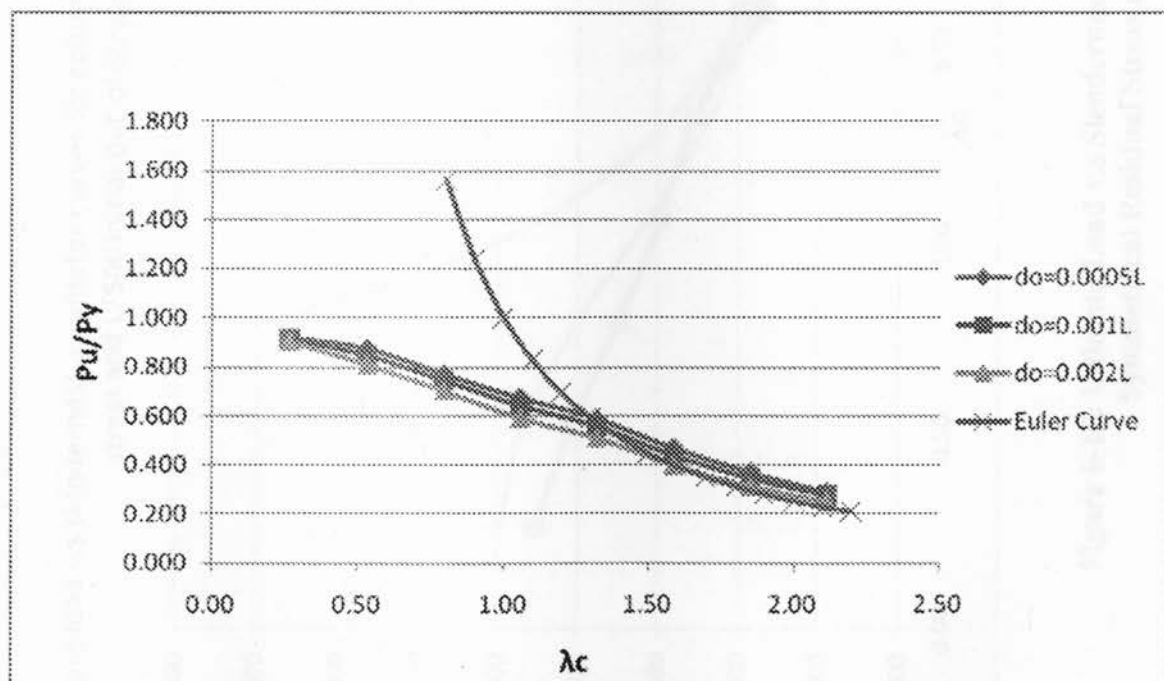


Figure 6-14: Ultimate Load v.s Slenderness Parameter for 12 inch Diameter Column with Symmetrical Residual Stress

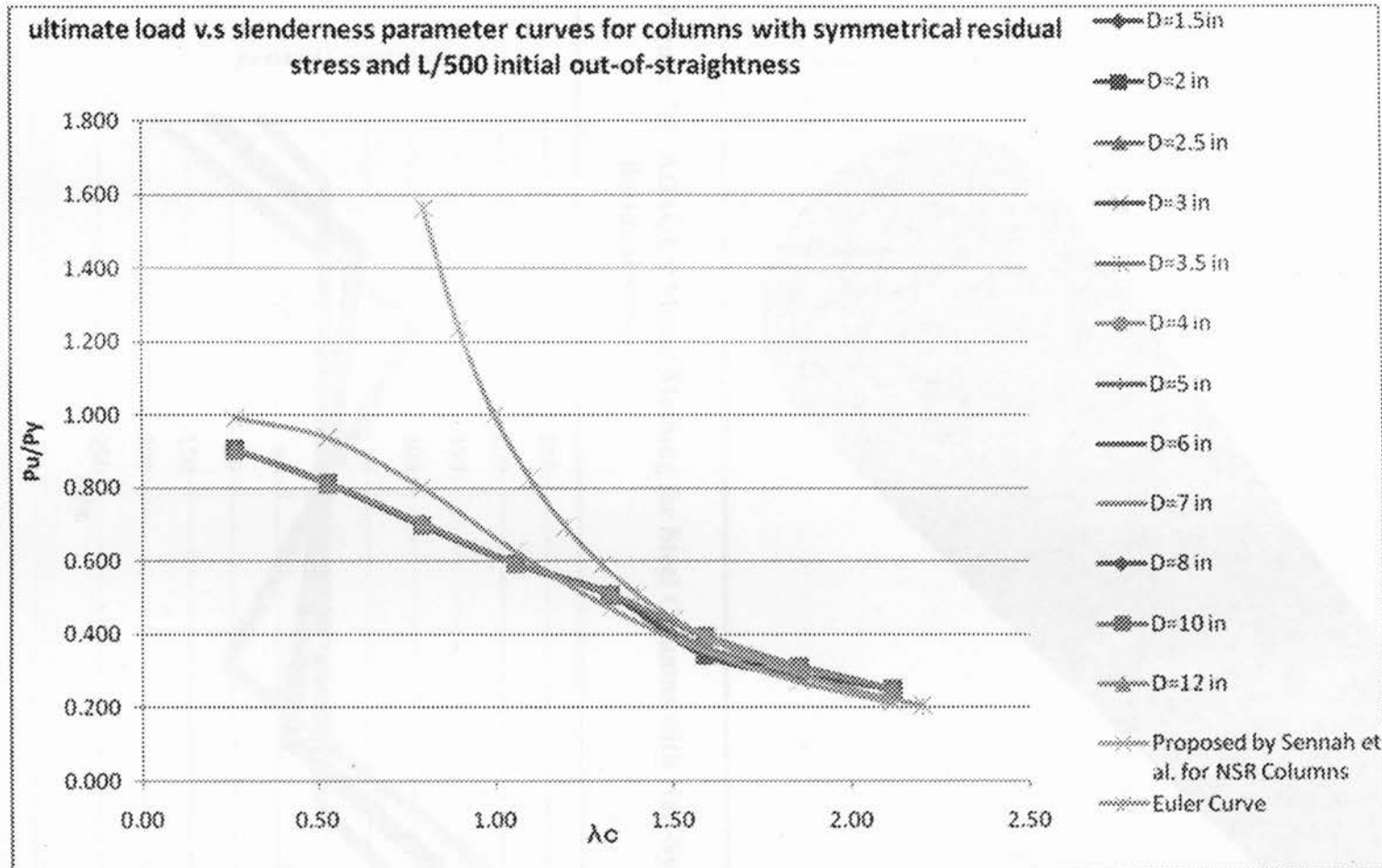


Figure 6-15: Ultimate Load v.s Slenderness Parameter Curves for Columns with Symmetrical Residual Stress and L/500 Initial Out-of-Straightness

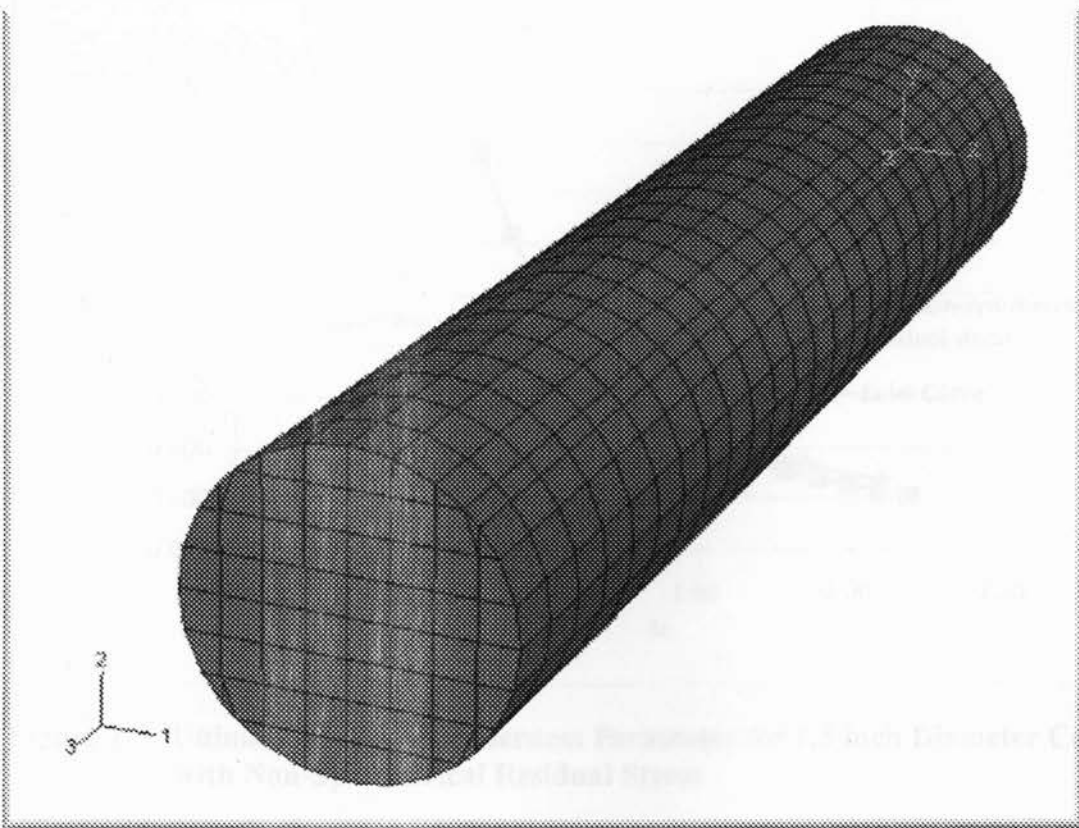


Figure 7-1: ABAQUS Model Meshing for Steel Columns with Non-Symmetrical Residual Stress

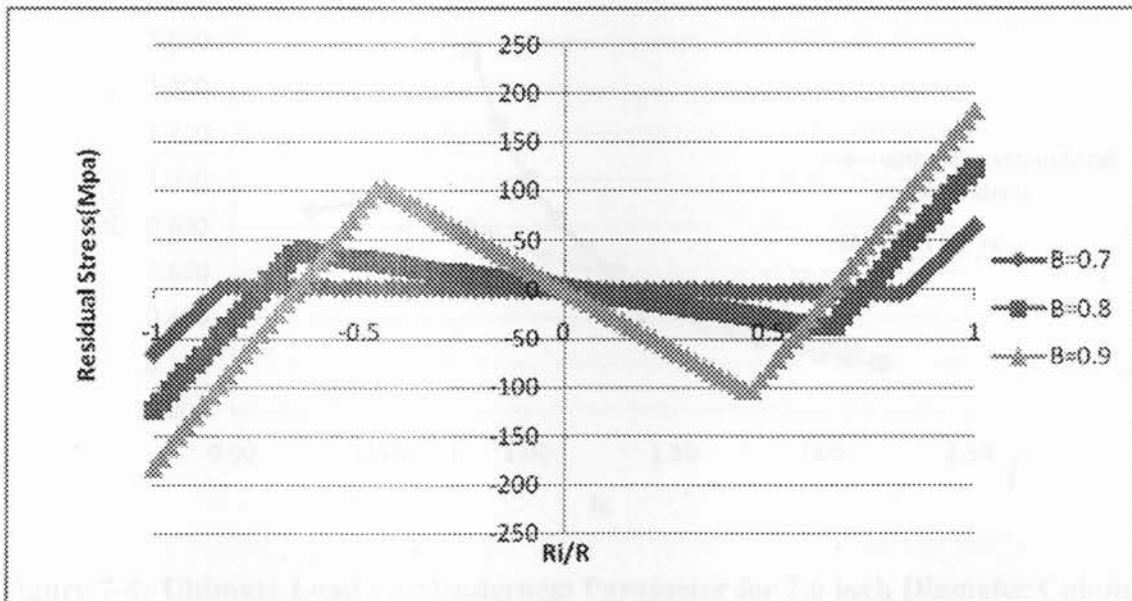


Figure 7-2: Non-symmetrical Residual Stress Distribution along the Radius of Column

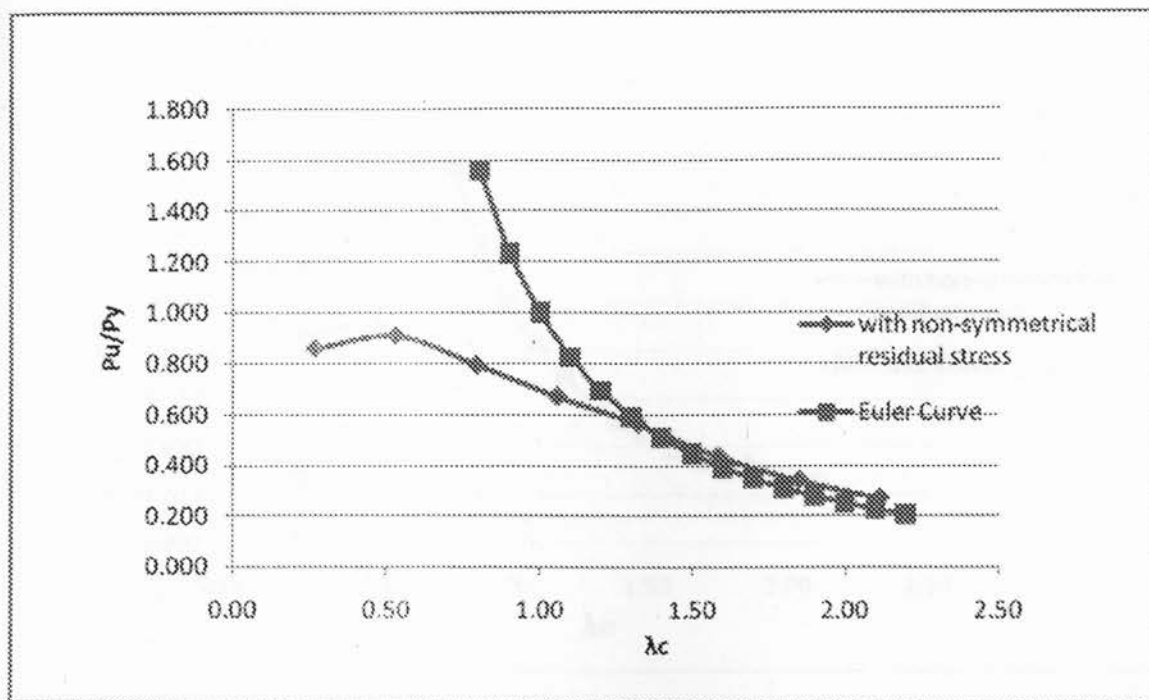


Figure 7-3: Ultimate Load v.s Slenderness Parameter for 1.5 inch Diameter Column with Non-Symmetrical Residual Stress

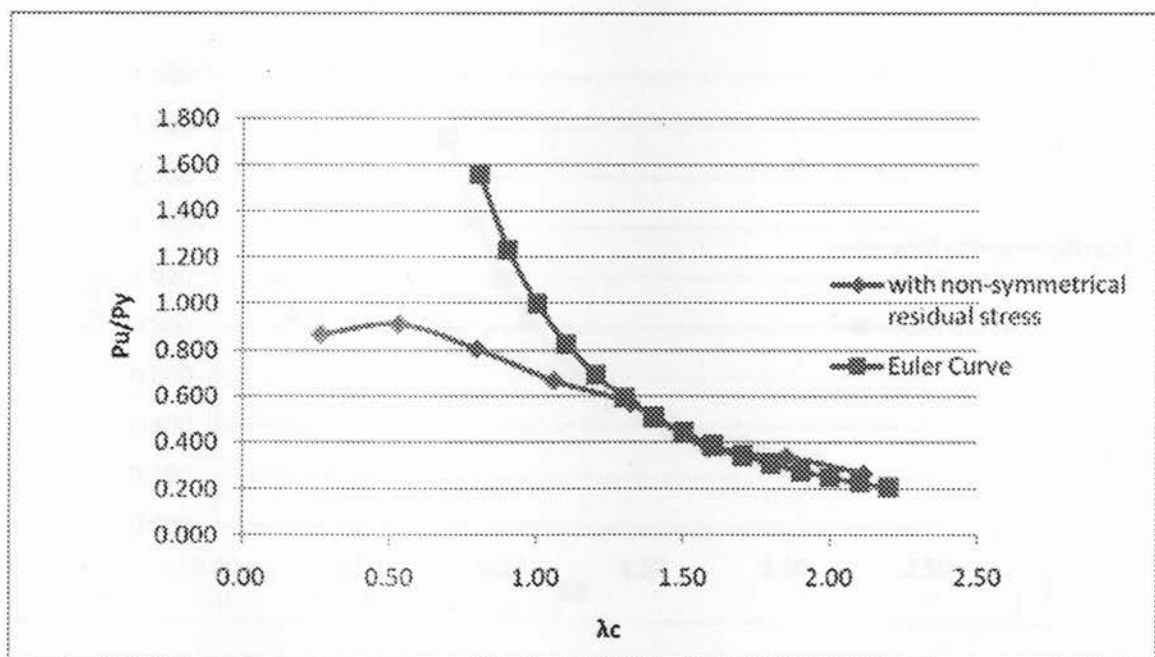


Figure 7-4: Ultimate Load v.s Slenderness Parameter for 2.0 inch Diameter Column with Non-Symmetrical Residual Stress

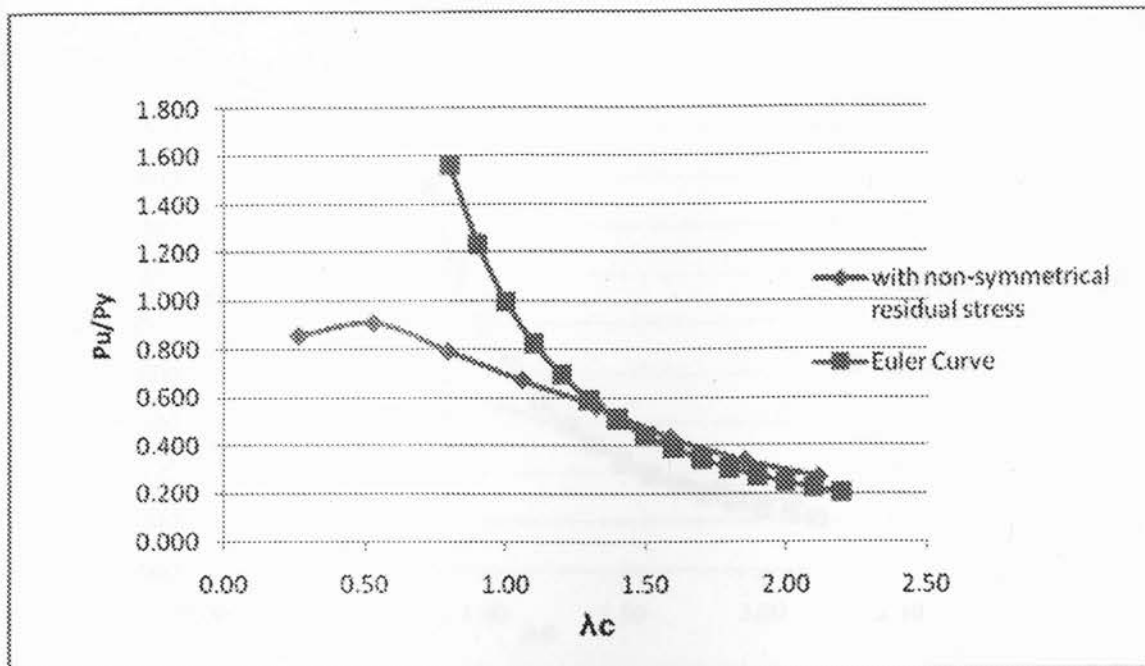


Figure 7-5: Ultimate Load v.s Slenderness Parameter for 2.5 inch Diameter Column with Non-Symmetrical Residual Stress

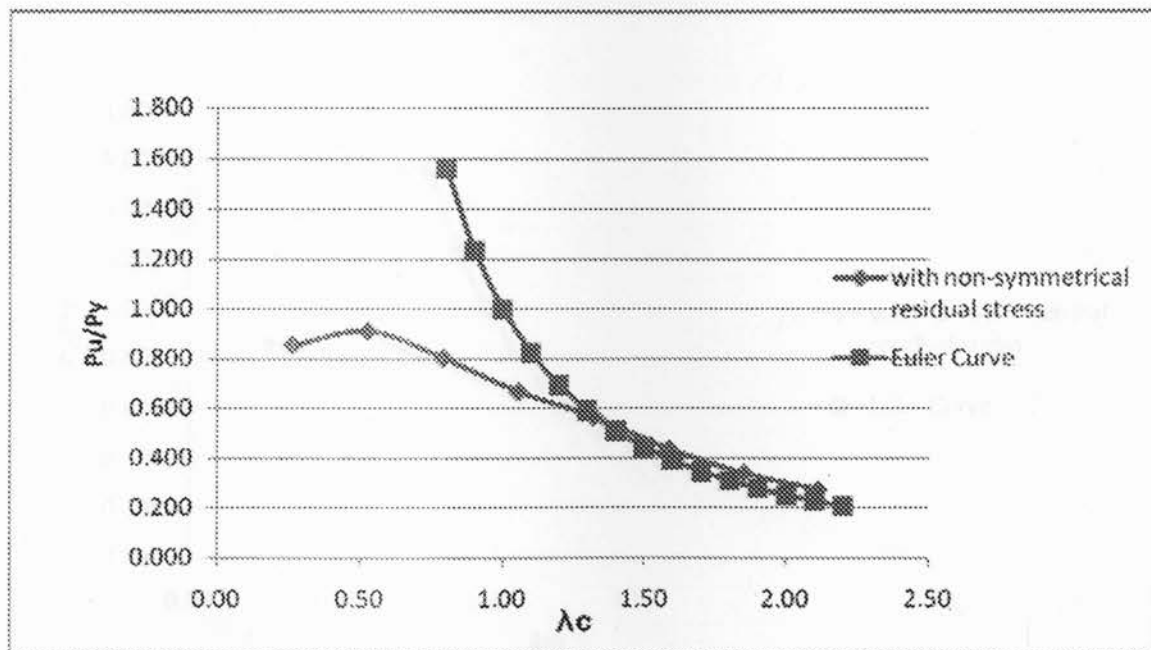


Figure 7-6: Ultimate Load v.s Slenderness Parameter for 3.0 inch Diameter Column with Non-Symmetrical Residual Stress

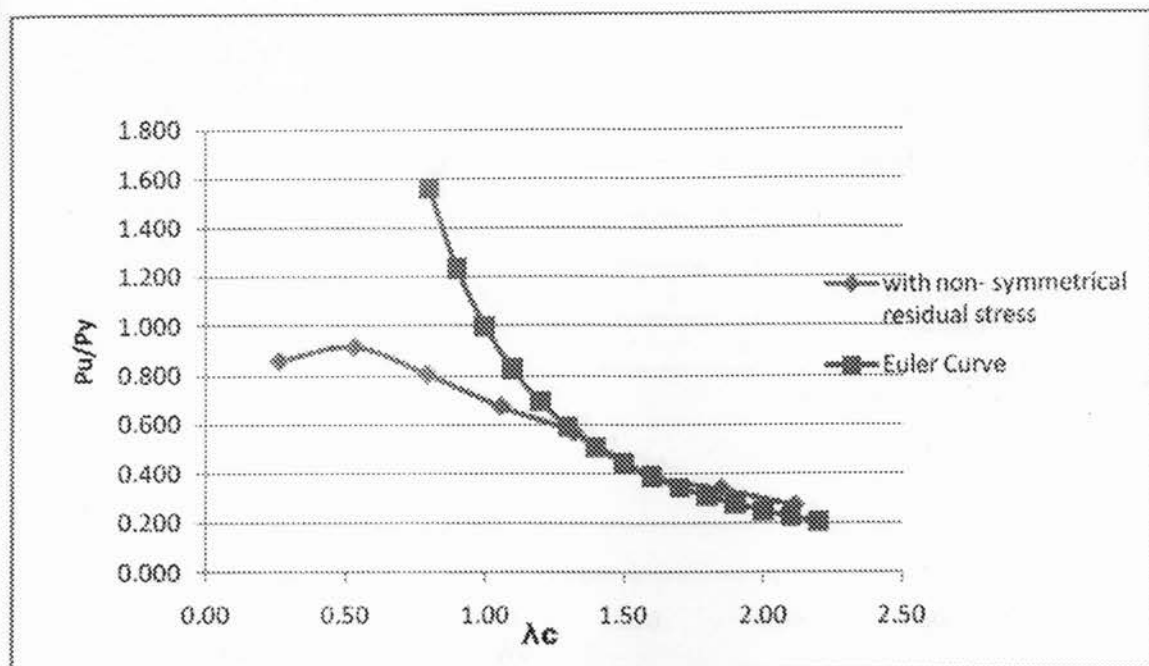


Figure 7-7: Ultimate Load v.s Slenderness Parameter for 3.5 inch Diameter Column with Non-Symmetrical Residual Stress

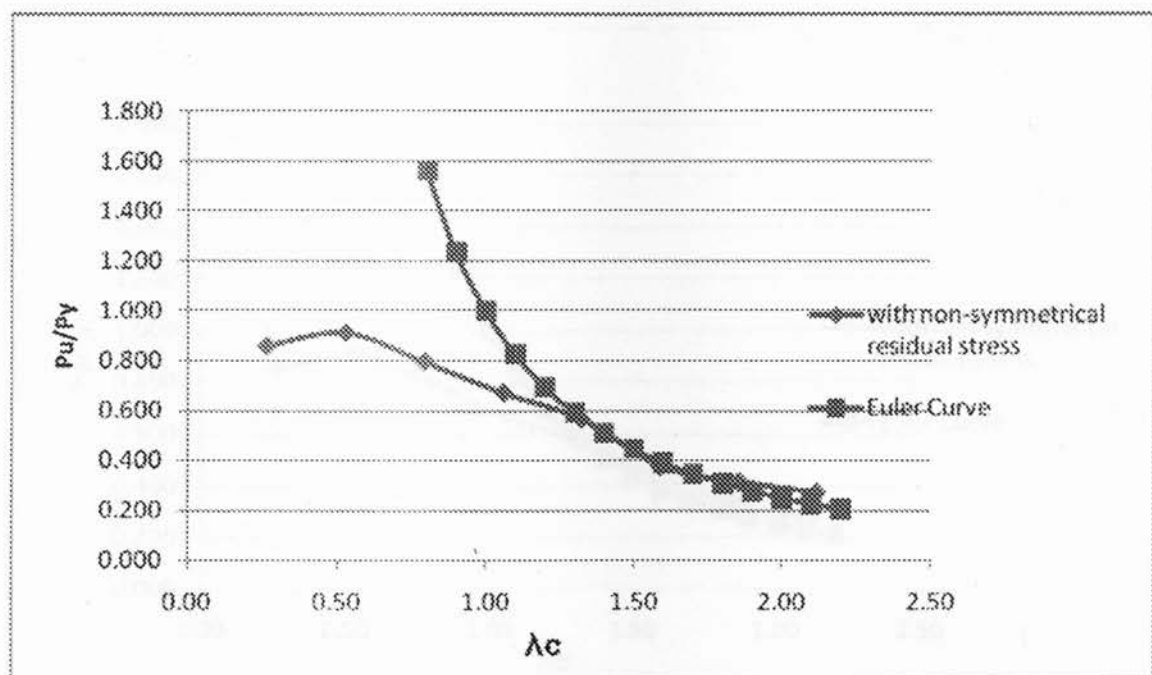


Figure 7-8: Ultimate Load v.s Slenderness Parameter for 4.0 inch Diameter Column with Non-Symmetrical Residual Stress

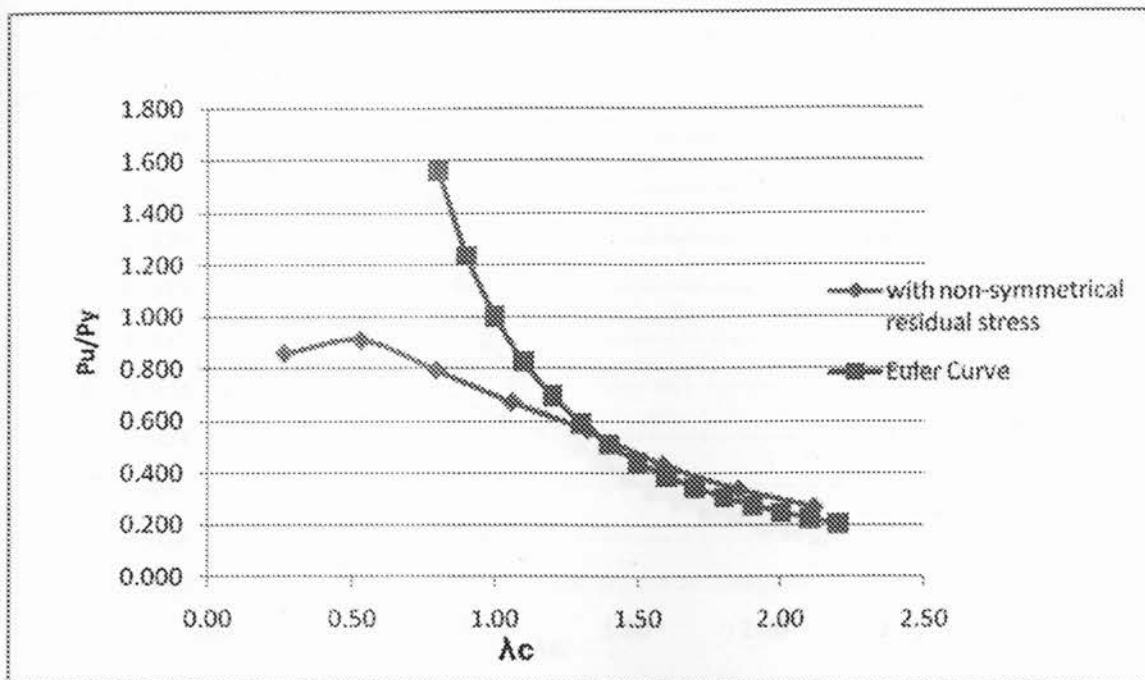


Figure 7-9: Ultimate Load v.s Slenderness Parameter for 5.0 inch Diameter Column with Non-Symmetrical Residual Stress

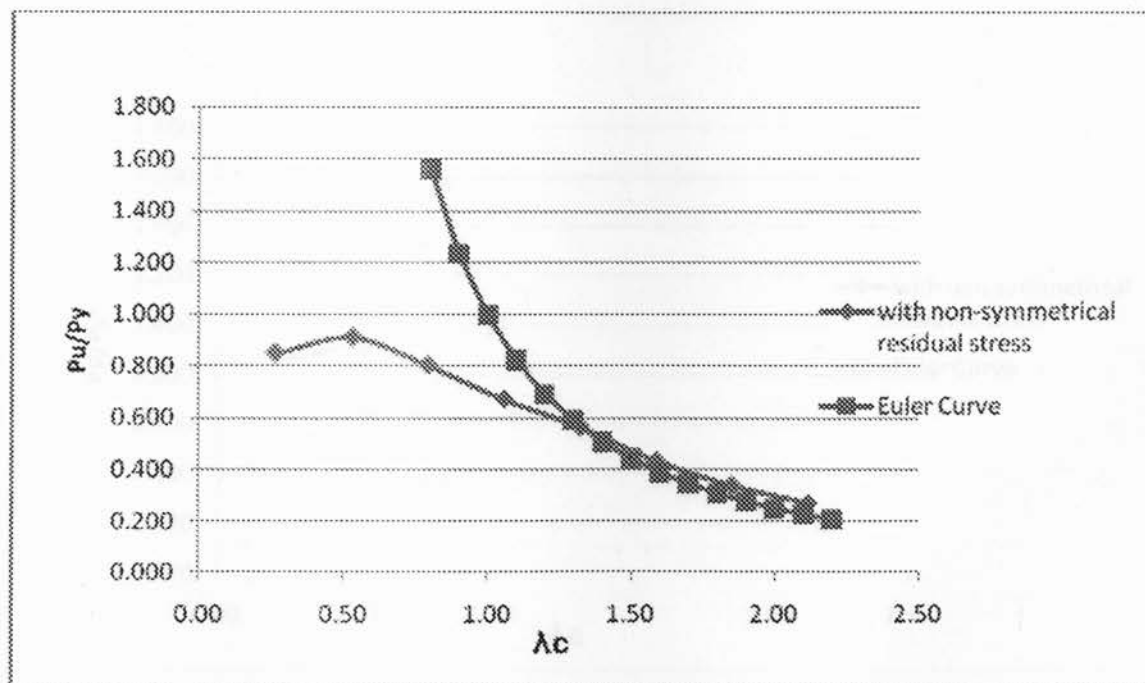


Figure 7-10: Ultimate Load v.s Slenderness Parameter for 6 inch Diameter Column with Non-Symmetrical Residual Stress

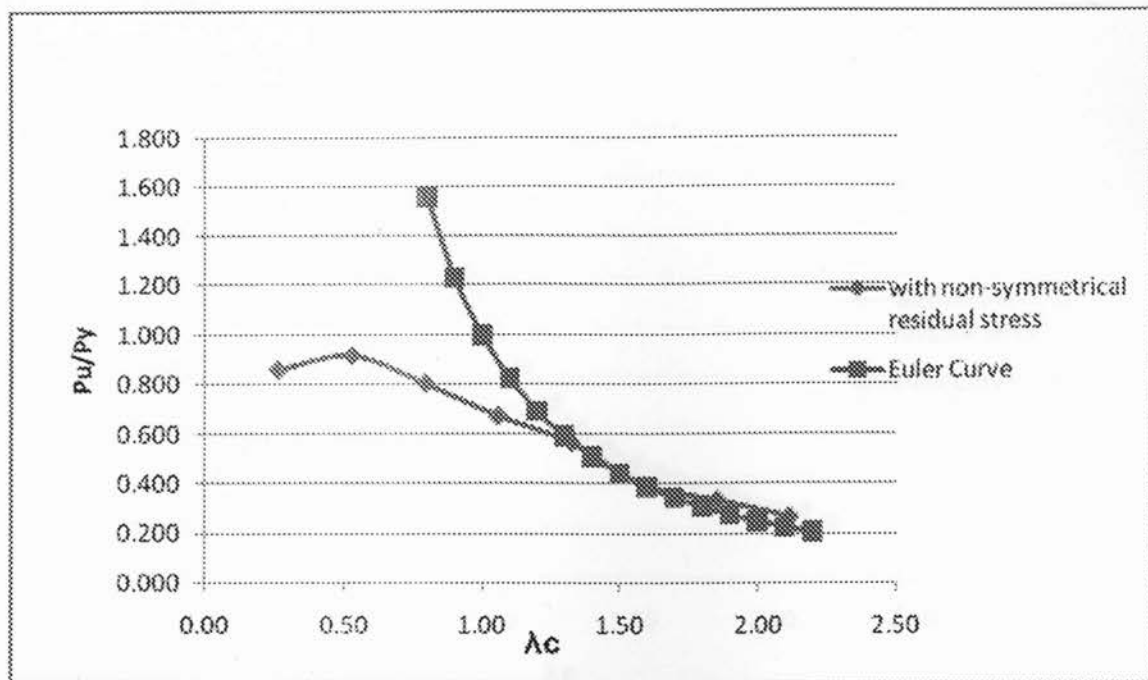


Figure 7-11: Ultimate Load v.s Slenderness Parameter for 7 inch Diameter Column with Non-Symmetrical Residual Stress

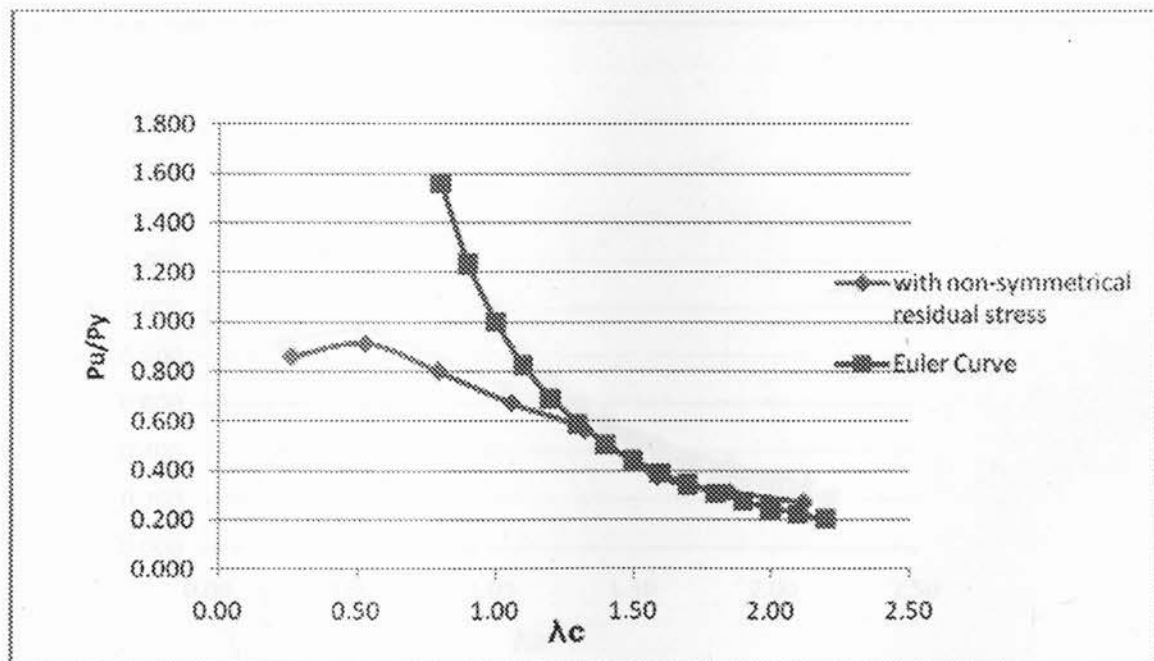


Figure 7-12: Ultimate Load v.s Slenderness Parameter for 8 inch Diameter Column with Non-Symmetrical Residual Stress

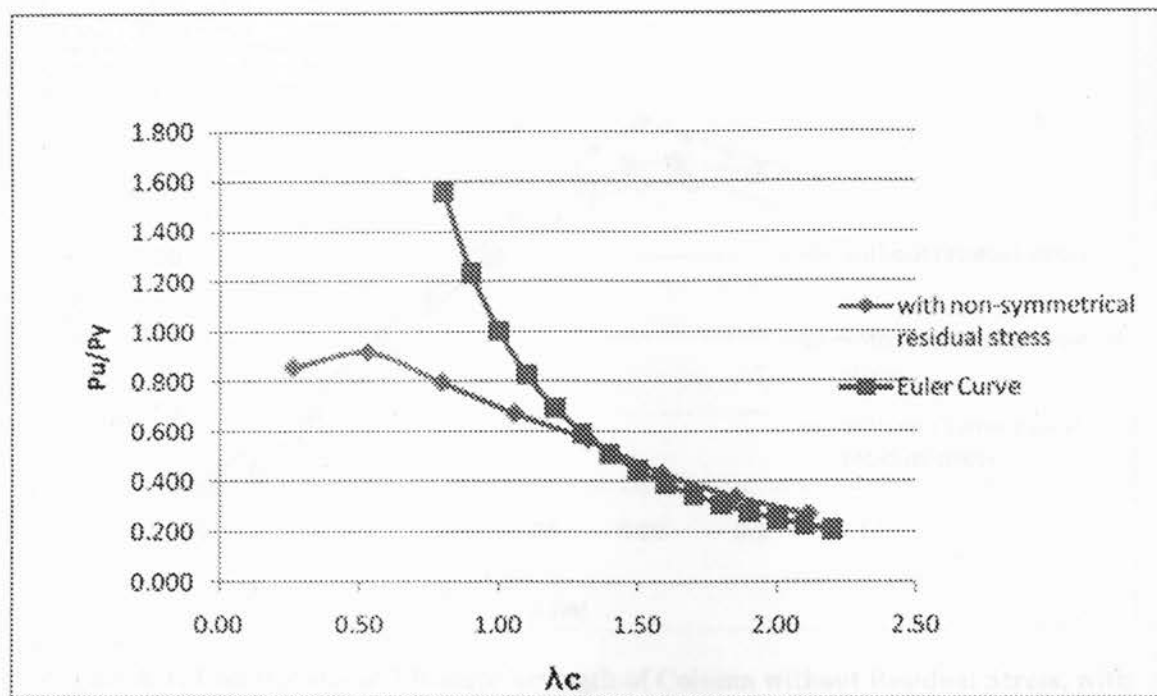


Figure 7-13: Ultimate Load v.s Slenderness Parameter for 10 inch Diameter Column with Non-Symmetrical Residual Stress

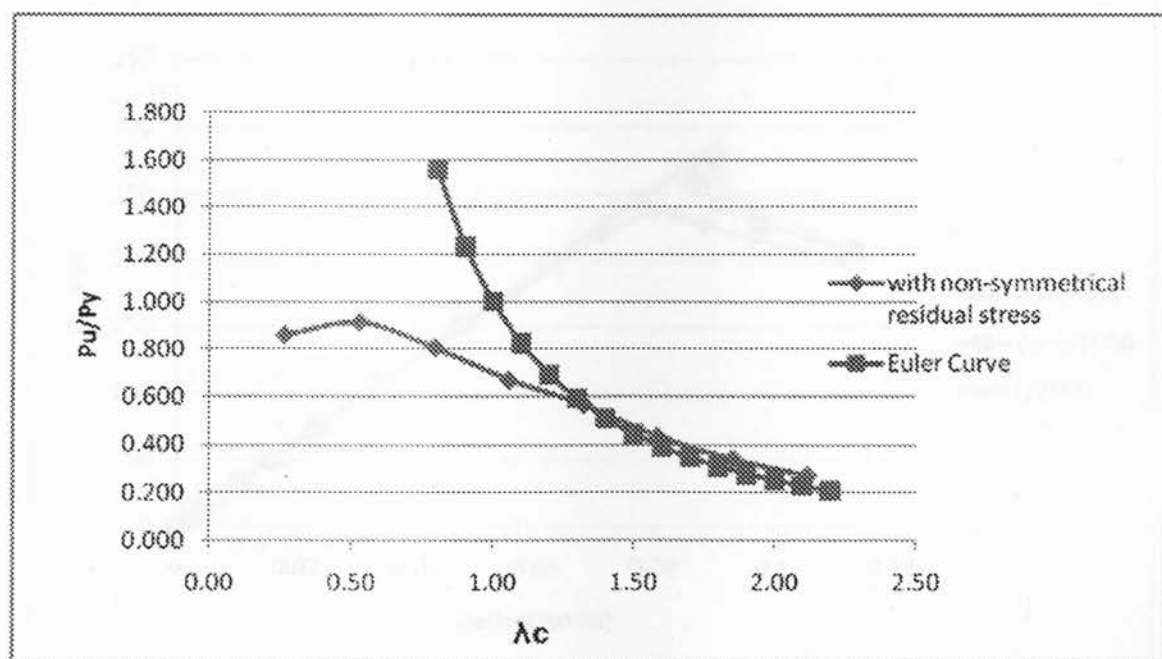


Figure 7-14: Ultimate Load v.s Slenderness Parameter for 12 inch Diameter Column with Non-Symmetrical Residual Stress

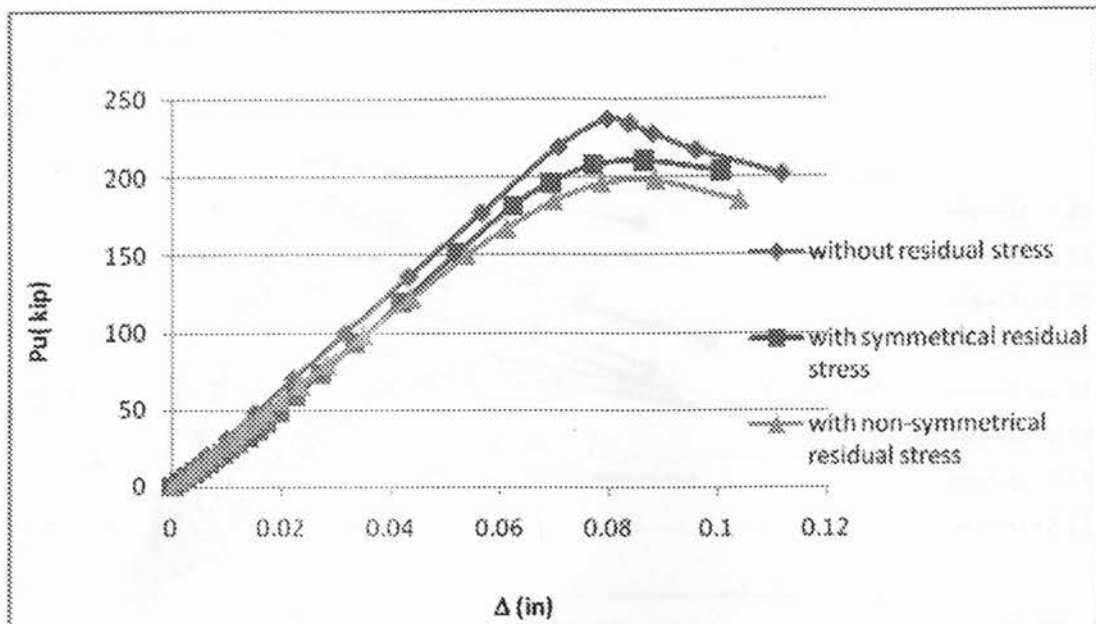


Figure 8-1: Comparison of Ultimate Strength of Column without Residual Stress, with Symmetrical Residual stress and Non-Symmetrical Residual stress for 3" Diameter, 60" Length Column

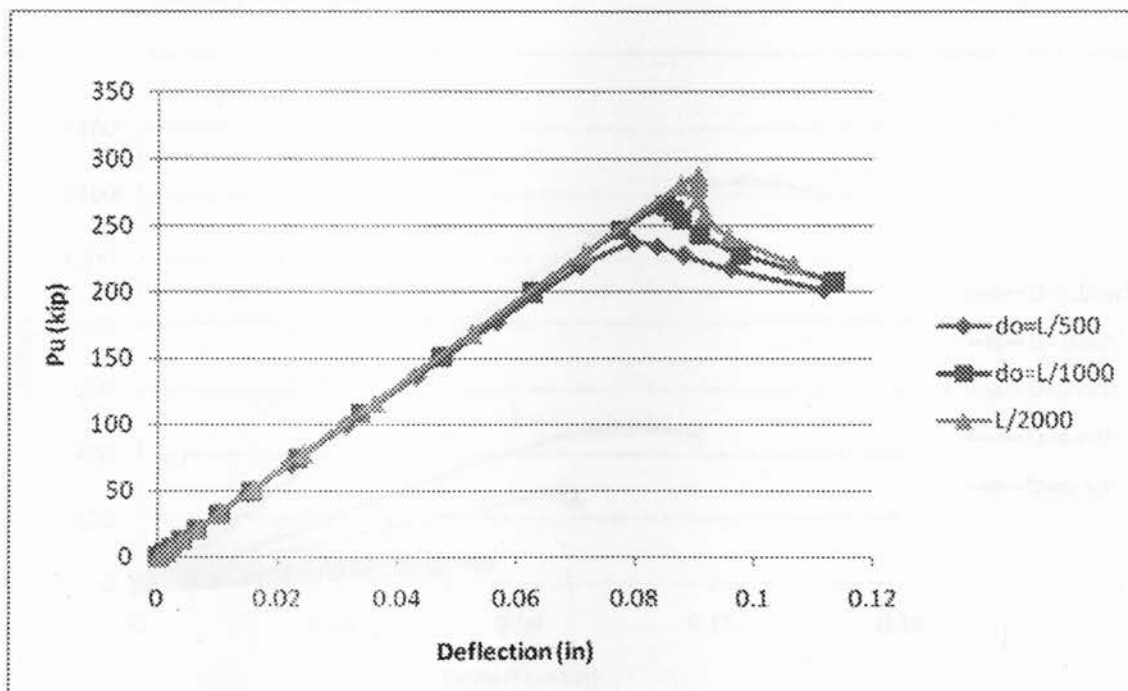


Figure 8-2: Comparison of Ultimate Strength of Column with Different Initial Deflection for 3" Diameter, 60" Length Column with Symmetrical Residual Stress

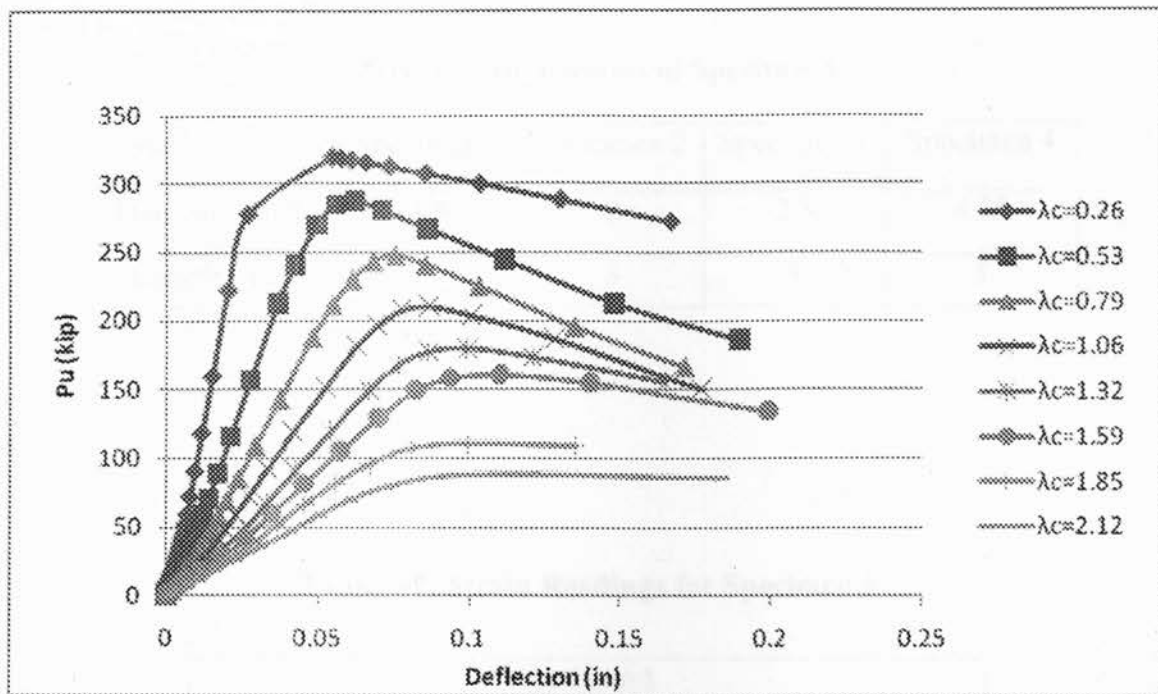


Figure 8-3: Comparison of Ultimate Strength of Column with Different Slenderness Parameter for 3" Diameter with Symmetrical Residual Stress and $L/500$ Initial Deflection

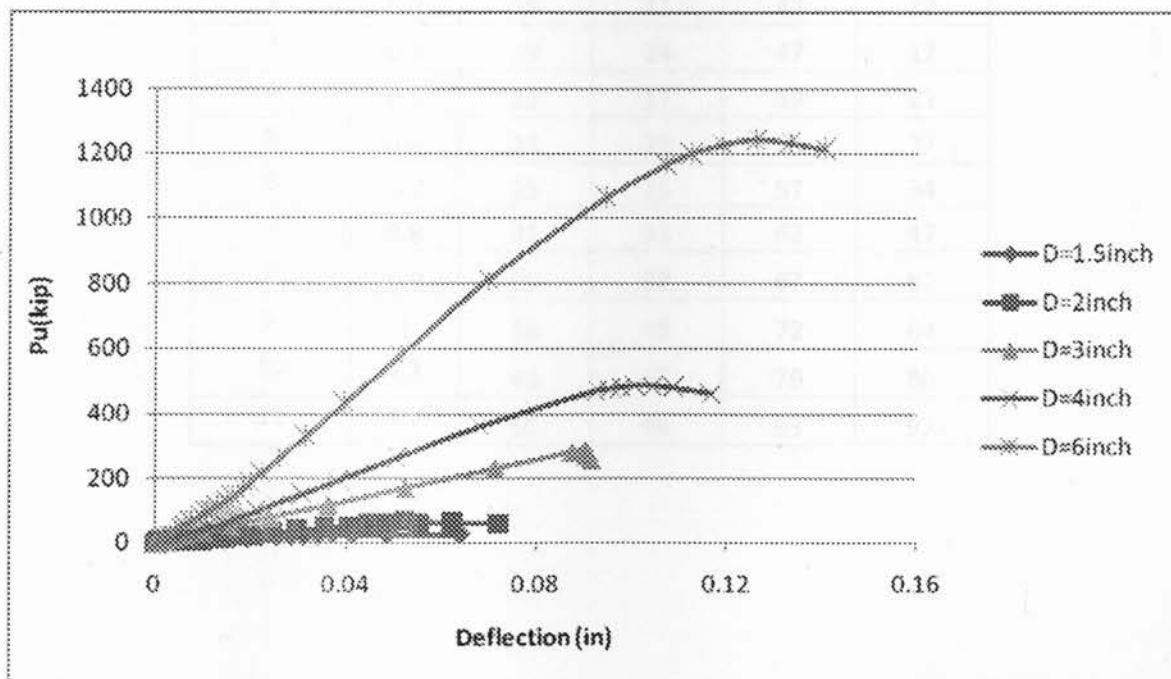


Figure 8-4: Comparison of Ultimate Strength of Column with Different Diameter for 60" Length, with Symmetrical Residual Stress and $L/2000$ Initial Deflection

Table 3-1: Dimensions of Specimens

Specimen No.	Specimen 1	Specimen 2	Specimen 3	Specimen 4
Diameter (inch)	1.5	2	2.5	4.25
Length (inch)	3	3	3	3

Table 3-2: Strain Readings for Specimen 1

Specimen 1 D=1.5" =38.1mm H=3"					
Boring #	Di (inch)	Measured Strains (micro-strain)			
		gauge 1	gauge 2	gauge 3	gauge 4
1	0.2	9	6	38	10
2	0.3	16	11	43	12
3	0.4	19	14	47	17
4	0.5	21	17	49	23
5	0.6	23	20	53	27
6	0.7	25	25	57	34
7	0.8	31	31	62	42
8	0.9	35	38	67	52
9	1	38	48	72	64
10	1.1	43	66	79	80
11	1.2	50	96	93	97

Table 3-3: Strain Readings for Specimen 2

Specimen 2					
D=2" =50.8mm H=3"					
Boring #	Di (inch)	Measured Strains (micro-strain)			
		gauge 1	gauge 2	gauge 3	gauge 4
1	0.2	22	35	7	20
2	0.4	32	22	5	20
3	0.6	44	17	-2	21
4	0.8	54	11	-5	29
5	1	68	13	-5	50
6	1.2	85	15	-1	92
7	1.4	121	26	1	173
8	1.6	220	73	10	305
9	1.8	359	98	48	417

Table 3-4: Strain Readings for Specimen 3

Specimen 3					
D=2.5" =63.5mm H=3"					
Boring #	Di (inch)	Measured Strains (micro-strain)			
		gauge 1	gauge 2	gauge 3	gauge 4
1	0.25	10	31	1	N/A
2	0.5	15	32	2	N/A
3	0.75	23	42	2	N/A
4	1	34	67	-3	N/A
5	1.25	42	65	-15	N/A
6	1.5	49	36	-43	N/A
7	1.75	79	20	-78	N/A
8	2	101	-41	-71	N/A
9	2.25	186	-12	-81	N/A

Table 3-5: Strain Readings for Specimen 4

Specimen 4					
D=4.25" =108mm H=3"					
Boring #	D _i (inch)	Measured Strains (micro-strain)			
		gauge 1	gauge 2	gauge 3	gauge 4
1	10	11	-1	5	10
2	17	14	-5	14	17
3	29	20	-22	29	29
4	55	38	-37	59	55
5	67	41	-91	77	67
6	95	54	-147	114	95
7	119	65	-234	158	119
8	127	75	-398	193	127
9	188	90	-614	266	188
10	432	307	-610	560	432

Table 3-6: Strain Variation on the Surface at the Mid-Height of Specimen 1 under 1kN Internal Force

D=1.5 in=38.1mm		H=3 in.	
D _i	Strain	D _i	Strain
(mm)	(10 ⁻⁶)	(mm)	(10 ⁻⁶)
4	2.77	28	7.40
8	2.93	30	9.19
12	3.21	32	12.23
16	3.65	33	14.70
20	4.32	34	18.41
22	4.79	35	24.57
24	5.40	36	36.73
26	6.22	37	71.34

Note: D=diameter of specimen; H=length of specimen;
D_i=diameter of the hole drilled.

Table 3-7: Strain Variation on the Surface at the Mid-height of Specimen 2 under 1kN Internal Force

D=2.0 in. =50.8mm				H=3.0 in.	
D _i	Strain	D _i	Strain	D _i	Strain
(mm)	(10 ⁻⁶)	(mm)	(10 ⁻⁶)	(mm)	(10 ⁻⁶)
4	1.21	28	2.26	43	6.79
8	1.25	32	2.76	44	7.83
12	1.33	36	3.54	45	9.25
16	1.46	40	4.87	46	11.29
20	1.65	42	5.38	47	14.46
24	1.90	42	6.00	48	19.96

Note: D=diameter of specimen; H=length of specimen;
D_i=diameter of the hole drilled.

Table 3-8: Strain Variation on the Surface at the Mid-height of Specimen 3 under 1kN Internal Force

D=2.5 in. = 63.5mm				H=3.0 in.	
D _i	Strain	D _i	Strain	D _i	Strain
(mm)	(10 ⁻⁶)	(mm)	(10 ⁻⁶)	(mm)	(10 ⁻⁶)
4	0.46	40	1.43	54	4.19
8	0.46	42	1.61	55	4.72
12	0.47	44	1.83	56	5.39
16	0.51	46	2.10	57	6.27
20	0.57	48	2.43	58	7.50
24	0.65	50	2.85	59	9.31
28	0.77	51	3.11	60	12.21
32	0.93	52	3.41	61	17.53
36	1.14	53	3.76	62	30.12

Note: D=diameter of specimen; H=length of specimen;
D_i=diameter of the hole drilled.

Table 3-9: Strain Variation on the Surface at the Mid-height of Specimen 4 under 1kN Internal Force

D=4.25 in. =108 mm				H=3 in.	
D _i	Strain	D _i	Strain	D _i	Strain
(mm)	(10 ⁻⁶)	(mm)	(10 ⁻⁶)	(mm)	(10 ⁻⁶)
4	-0.17	56	-0.32	84	0.18
8	-0.19	60	-0.31	86	0.29
12	-0.22	62	-0.30	88	0.43
16	-0.24	64	-0.28	90	0.60
20	-0.26	66	-0.27	92	0.82
24	-0.28	68	-0.25	94	1.08
28	-0.29	70	-0.22	96	1.43
32	-0.31	72	-0.19	98	1.89
36	-0.32	74	-0.16	100	2.55
40	-0.33	76	-0.11	102	3.61
44	-0.33	78	-0.06	104	5.70
48	-0.33	80	0.01	105	7.84
52	-0.33	82	0.08	106	12.29

Note: D=diameter of specimen; H=length of specimen;
D_i=diameter of the hole drilled.

Table 3-10: Residual Stress Distribution for Sample 1(D=1.5 inch, H=3 inch)

D _i	D _i	Area	Measured Strains					Unit Force Strain	Total Force Released	ΔF _i	Residual Stress	R _i /R
			1	2	3	4	Ave.					
(in.)	(mm)	(mm ²)	(10 ⁻⁶)					(10 ⁻⁶)	(kN)	(kN)	(Mpa)	
0.2	5.08	20.27	9	6	38	10	15.75	2.81	5.605	5.605	276.54	0.07
0.3	7.62	45.60	16	11	43	12	20.5	2.91	7.045	1.440	56.83	0.17
0.4	10.16	81.07	19	14	47	17	24.25	3.08	7.873	0.829	23.36	0.23
0.5	12.7	126.68	21	17	49	23	27.5	3.29	8.359	0.485	10.64	0.30
0.6	15.24	182.41	23	20	53	27	30.75	3.57	8.613	0.255	4.57	0.37
0.7	17.78	248.29	25	25	57	34	35.25	3.95	8.924	0.311	4.72	0.43
0.8	20.32	324.29	31	31	62	42	41.5	4.4	9.432	0.508	6.68	0.50
0.9	22.86	410.43	35	38	67	52	48	5.05	9.505	0.073	0.85	0.57
1	25.4	506.71	38	48	72	64	55.5	5.97	9.296	-0.208	-2.17	0.63
1.1	27.94	613.12	43	66	79	80	67	7.36	9.103	-0.193	-1.82	0.70
1.2	30.48	729.66	50	96	93	97	84	9.92	8.468			

Table 3-11: Residual Stress Distribution for Sample 2 (D=2.0 inch, H=3 inch)

D _i	D _i	Area	Measured Strains					Unit Force Strain	Total Force Released	ΔF _i	Residual Stress	R _i /R
			1	2	3	4	Ave.					
(in.)	(mm)	(mm ²)	(10 ⁻⁶)					(10 ⁻⁶)	(kN)	(kN)	(Mpa)	
0.2	5.08	20.27	22	35	7	20	21	1.22	17.20	17.20	848.57	0.05
0.4	10.16	81.07	32	42	5	20	24.75	1.29	19.14	1.94	31.95	0.15
0.6	15.24	182.41	44	27	-2	21	22.5	1.44	15.68	-3.46	-34.16	0.25
0.8	20.32	324.29	54	11	-5	29	22.25	1.67	13.32	-2.36	-16.61	0.35
1	25.4	506.71	68	13	-5	50	31.5	2.03	15.55	2.22	12.19	0.45
1.2	30.48	729.66	85	15	-1	92	47.75	2.57	18.58	3.03	13.60	0.55
1.4	35.56	993.15	121	26	1	173	80.25	3.45	23.23	4.65	17.66	0.65
1.6	40.64	1297.17	220	73	10	305	152	5.20	29.25	6.02	19.80	0.75
1.8	45.72	1641.73	359	98	48	417	230.5	10.72	21.50	-7.75	-22.49	0.85

Table 3-12: Residual Stress Distribution for Sample 3 (D=2.5 inch, H=3 inch)

D _i	D _i	Area	Measured Strains					Unit Force Strain	Total Force Released	ΔF _i	Residual Stress	R _i /R
			1	2	3	4	Ave.					
(in.)	(mm)	(mm ²)	(10 ⁻⁶)					(10 ⁻⁶)	(kN)	(kN)	(Mpa)	
0.25	6.35	31.67	10	31	1	N/A	13.67	0.46	29.71	22.83	720.77	0.05
0.5	12.7	126.68	15	32	2	N/A	15.67	0.48	32.84	3.13	32.99	0.15
0.75	19.05	285.02	23	42	2	N/A	21.67	0.56	38.97	6.12	38.68	0.25
1	25.4	506.71	34	67	-3	N/A	33.67	0.69	48.65	9.68	43.68	0.35
1.25	31.75	791.73	42	65	-15	N/A	35.67	0.92	38.77	-9.88	-34.67	0.45
1.5	38.1	1140.09	49	36	-43	N/A	28.33	1.29	21.93	-16.84	-48.34	0.55
1.75	44.45	1551.79	79	20	-78	N/A	33.00	1.89	17.45	-4.48	-10.88	0.65
2	50.8	2026.83	101	-41	-71	N/A	20.00	3.06	6.54	-10.91	-22.97	0.75
2.25	57.15	2565.21	186	-12	-81	N/A	58.00	6.46	8.99	2.45	4.54	0.85

Table 3-13: Residual Stress Distribution for Sample 4 (D=4.25 inch, H=3 inch)

D _i	D _i	Area	Measured Strains					Unit Force Strain	Total Force Released	ΔF _i	Residual Stress	R _i /R
			1	2	3	4	Ave.					
(in.)	(mm)	(mm ²)	(10 ⁻⁶)					(10 ⁻⁶)	(kN)	(kN)	(Mpa)	
0.45	11.43	102.61	10	11	-1	5	8.67	-0.22	-40.12	-39.39	-383.93	0.05
0.85	21.59	366.10	17	14	-5	14	15.00	-0.27	-55.97	-15.85	-60.14	0.15
1.25	31.75	791.73	29	20	-22	29	26.00	-0.31	-84.14	-28.17	-66.19	0.25
1.65	41.91	1379.51	55	38	-37	59	50.67	-0.33	-153.54	-69.39	-118.06	0.34
2.05	52.07	2129.44	67	41	-91	77	61.67	-0.33	-186.87	-33.33	-44.45	0.44
2.45	62.23	3041.51	95	54	-147	114	87.67	-0.30	-294.18	-107.31	-117.66	0.53
2.85	72.39	4115.73	119	65	-234	158	114.00	-0.18	-619.57	-325.38	-302.90	0.62
3.25	82.55	5352.10	127	75	-398	193	131.67	0.11	1219.14	1838.70	1487.18	0.72
3.65	92.71	6750.61	188	90	-614	266	181.33	0.91	198.83	-1020.31	-729.56	0.81
4.05	102.87	8311.27	432	307	-610	560	433.00	4.52	95.82	-103.01	-66.01	0.91

Table 5-1: Number of Circles on the Cross Section vs. Ultimate Load for Columns without Residual Stress

Number of Circles	Ultimate load/node (lb)	Totally Node Numbers	Ultimate load of the Column (lb)
4	466.545	49	22860.71
5	1178.67	61	71898.67
6	986.318	73	72001.21
8	739.44	97	71725.68

Table 5-2: Number of Elements in Longitudinal Direction vs. Ultimate Load for Columns without Residual Stress

Number of Elements	Ultimate load/node (lb)	Totally Node Numbers	Ultimate load of the Column (lb)
20	1241.68	61	75742.8
25	1178.67	61	71898.87
30	1127.89	61	68801.29

Table 6-1: Number of Circles in the Cross Section vs. Ultimate Load for Columns with Symmetrical Residual Stress

Number of Circles	Ultimate load/node (lb)	Totally Node Numbers	Ultimate load of the Column (lb)
4	428.637	49	21003.21
5	980.452	61	59807.57
6	813.658	73	59397.03
8	611.627	97	59327.82

Table 6-2: Number of Elements in Longitudinal Direction vs. Ultimate Load for Columns with Symmetrical Residual Stress

Number of Elements	Ultimate load/node (lb)	Totally Node Numbers	Ultimate load of the Column (lb)
20	1060.49	61	64689.89
25	980.452	61	59807.57
30	932.684	61	56893.72

Table 7-1: Ultimate Strength to Yield Strength Ratio for 3 inch Diameter Columns

L (inch)	Slenderness ratio	Slenderness Parameter	do=0.0005L			do=0.001L			do=0.002L		
			$\beta=0.7$	$\beta=0.8$	$\beta=0.9$	$\beta=0.7$	$\beta=0.8$	$\beta=0.9$	$\beta=0.7$	$\beta=0.8$	$\beta=0.9$
15	20	0.264	0.862	0.858	0.852	0.861	0.862	0.853	0.856	0.859	0.854
30	40	0.529	0.966	0.962	0.963	0.946	0.947	0.945	0.908	0.910	0.911
45	60	0.793	0.937	0.913	0.898	0.892	0.875	0.860	0.822	0.812	0.803
60	80	1.058	0.861	0.808	0.772	0.793	0.759	0.728	0.708	0.690	0.667
75	100	1.322	0.734	0.680	0.657	0.675	0.638	0.618	0.601	0.584	0.565
90	120	1.586	0.545	0.537	0.535	0.530	0.484	0.472	0.459	0.447	0.435
105	140	1.851	0.413	0.394	0.394	0.389	0.372	0.367	0.357	0.346	0.338
120	160	2.115	0.319	0.309	0.311	0.304	0.294	0.291	0.285	0.273	0.271

Note: Column 1 is the length of steel members in inch.

Column 2 is the slenderness ratio calculated by Equation 5-1.

Column 3 is the slenderness parameter calculated by Equation 5-2.

Column 4 -12 is the P_u/P_y value for column with initial deflection of 0.0005L/0.001L/ 0.002L and non-symmetrical residual stress calculated based on $\beta=0.7/0.8/0.9$.

where P_u is the ultimate strength , P_y is the yield strength and L is the length of steel member

Table 7-2: Number of Slices in the Cross Section vs. the Ultimate Load for Columns with Non-Symmetrical Residual Stress

Number of Slices	Ultimate load/node (lb)	Totally Node Numbers	Ultimate load of the Column (lb)
6	1442.41	45	64908.45
8	931.341	73	67987.89
10	781.66	87	68004.42

Table 7-3: Number of Elements in Longitudinal Direction vs. the Ultimate Load for Columns with Non-Symmetrical Residual Stress

Number of Elements	Ultimate load/node (lb)	Totally Node Numbers	Ultimate load of the Column (lb)
20	1013.97	73	74019.81
25	931.341	73	67987.89
30	929.416	73	67847.37

Table 7-4: Ultimate Strength to Yield Strength Ratio for Different Diameter Column

Slenderness Ratio	Slenderness Parameter (λ_c)	Ultimate Strength to Yield Strength Ratio (P_u/P_y)											
		1.5in	2in	2.5in	3in	3.5in	4in	5in	6in	7in	8in	10in	12in
20	0.264	0.860	0.866	0.858	0.854	0.857	0.859	0.858	0.850	0.858	0.860	0.855	0.860
40	0.529	0.910	0.911	0.912	0.911	0.913	0.912	0.912	0.912	0.913	0.912	0.915	0.913
60	0.793	0.795	0.804	0.794	0.803	0.802	0.795	0.794	0.803	0.802	0.799	0.795	0.806
80	1.058	0.670	0.667	0.671	0.667	0.671	0.671	0.671	0.671	0.671	0.671	0.671	0.671
100	1.322	0.565	0.566	0.565	0.565	0.566	0.566	0.565	0.566	0.566	0.567	0.566	0.566
120	1.586	0.435	0.377	0.434	0.435	0.398	0.376	0.434	0.433	0.398	0.375	0.434	0.434
140	1.851	0.340	0.340	0.340	0.338	0.337	0.314	0.340	0.338	0.337	0.313	0.340	0.339
160	2.115	0.271	0.268	0.271	0.271	0.270	0.270	0.271	0.270	0.270	0.270	0.271	0.272

Appendix A:

An example of ABAQUS input file for calculation of strains at the middle surface when the specimen ($D=50.8$ mm, $D_i=10$ mm) is subject to 1 kN internal force

```
*HEADING
STRAIN ANALYSIS OF A CYLINDER UNDER INNER AXIAL DRAG OF 1000N.
INTERNATIONAL UNIT SYSTEM
*PREPRINT,ECHO=YES,MODEL=NO,HISTORY=NO
*NODE
1,10.,0.00,0.
39,10.,38.1,0.
961,25.4,0.00,0.
999,25.4,38.1,0.
*NGEN,NSET=IN-NODE
1,39,1
*NGEN,NSET=OUT-NODE
961,999,1
*NFILL
IN-NODE,OUT-NODE,24,40
*ELEMENT,TYPE=CAX8R
1,1,81,83,3,41,82,43,2
*ELGEN,ELSET=SS
1,19,2,1,12,80,19
*NSET,NSET=BC,GENERATE
1,961,40
*ELSET,ELSET=OUTPUT
210
*SOLID SECTION,ELSET=SS,MATERIAL=M1
*MATERIAL,NAME=M1
*ELASTIC
2.0e5,0.3
*STEP,PERTURBATION
*STATIC
*CLOAD
IN-NODE,2,25.65
*BOUNDARY
BC,2,2,0.0
*RESTART,WRITE
*EL PRINT,ELSET=OUTPUT
S22
E22
*NODE PRINT,NSET=IN-NODE
U2
*END STEP
```

Appendix B:

Sample Calculation of residual stress from strain data:

Sample 1 is chosen for demonstrating the calculation of residual stresses from the original data.

As shown in the included table, the first and second column “ D_i ” is the diameter of the successive holes drilled in inch and millimeter respectively, and the column “Area” are the corresponding areas to the second column.

$$\text{Area} = \pi D_i^2 / 4$$

Four columns “1”, “2”, “3”, “4” are the measured strains in the middle of specimen.

“Ave” is the column for the average of these four strains.

“Unit Force Strain” was obtained from finite element analysis described in Section 3.7.

These are the strains at the measured location when the diameter of the hole drilled is D_i and the released force by the bored area is 1 kN. Dividing the corrected strains by the unit strains, the total force released by the bored area is therefore calculated (listed in column “Total Force Released”).

For example, when D_i is 0.5 inch, which is equal to 12.7 mm, the averaged strain is 27.5×10^{-6} , the unit force strain obtained from Figure 3-12 is 3.29×10^{-6} . Therefore, the total force released is

$$27.5 \times 10^{-6} / 3.29 \times 10^{-6} = 8.359 \text{ kN}$$

In the same way, when D_i is 0.6 inch, which is 15.24 mm, the total force released is 8.613 kN.

The difference between two forces is the force released by the area between two diameters. That is to say, 0.255 kN (difference between 8.613 kN and 8.359 kN) is the force released by area between diameters 0.5 inch and 0.6 inch. So the residual stress in this area could be obtained simply by dividing the force by the area. In this case the residual stress is:

$$\frac{0.255}{(182.41 - 126.68) \text{mm}^2} = 4.57 \text{ MPa}$$

The normalized radius is averaged radius of two successive drilling over the radius of the specimen.

$$\frac{(12.7/2 + 15.24/2)/2}{38.1/2} = 0.37$$

With the same procedure, the residual stresses are calculated over the radius, as shown in Figure 3-16.

Appendix C:

An example of ABAQUS input file for heat transfer problem (D=1.5 inch)

```
*HEADING
HEAT TRANSFER FOR THESIS
*PREPRINT, ECHO=YES, MODEL=NO, HISTORY=NO
*NODE
1, 0.0, 0.0
50, 0.75, 0.0
2451, 0.0, 3.0
2500, 0.75, 3.0
*NGEN, NSET=BOT
1,50
*NGEN, NSET=TOP
2451, 2500
*NFill, NSET=ALL
BOT, TOP, 49,50
*ELEMENT, TYPE=DCAx4
1,1,2,52,51
*ELGEN, ELSET=ELALL
1,49,1,1,49,50,50
*ELSET, ELSET=SIDE, GENERATE
49,2499,50
*NSET, NSET=PR1, GENERATE
1201, 1250,1
*SOLID SECTION, ELSET=ELALL, MATERIAL=STEEL
*MATERIAL, NAME=STEEL
*SPECIFIC HEAT
0.1431
*DENSITY
0.2829
*CONDUCTIVITY
7.872E-4
*INITIAL CONDITIONS, TYPE=TEMPERATURE
ALL,1900.
*STEP, INC=500
*HEAT TRANSFER, DELTMX=10., END=SS
20.,4.0E6,0.005,,1.E-6
*FILM
SIDE,F3,70.,6.559E-4
*NODE PRINT, NSET=PR1, FREQUENCY=5
NT
*PRINT, FREQUENCY=10
*NODE FILE
NT
*END STEP
```

Appendix D:

An example of ABAQUS input file for thermal stress calculation (D=1.5 inch)

```
*HEADING
THERMAL STRESS FOR THESIS
*PREPRINT, ECHO=YES, MODEL=NO, HISTORY=NO
*NODE
1, 0.0, 0.0
50, 0.75, 0.0
2451, 0.0, 3.0
2500, 0.75, 3.0
*NGEN, NSET=BOT
1,50
*NGEN, NSET=TOP
2451,2500
*NFILL, NSET=ALL
BOT, TOP, 49,50
*ELEMENT, TYPE=CAX4
1,1,2,52,51
*ELGEN, ELSET=ELALL
1,49,1,1,49,50,50
*ELSET, ELSET=SIDE, GENERATE
49,2499,50
*ELSET, ELSET=ELPR, GENERATE
1201,1249,1
*NSET, NSET=NPR, GENERATE
1201, 1250, 1
*NSET, NSET=TOP1, GENERATE
2451, 2499, 1
*SOLID SECTION, ELSET=ELALL, MATERIAL=STEEL
*MATERIAL, NAME=STEEL
*ELASTIC
3.E7,.3
*PLASTIC
50038,.0
50038,.0,250
6247,.0,2000.
*EXPANSION,ZERO=70.
7.5E-6
*EQUATION
2
TOP1,2,1.0,2500,2,-1.0
*INITIAL CONDITIONS,TYPE=TEMPERATURE
ALL,1900.
*STEP,INC=100
*STATIC
10.,9.616E4
```

*BOUNDARY

BOT,2,2,0

*TEMPERATURE,FILE=heat1,BSTEP=1,BINC=1,ESTEP=1,EINC=368

*EL PRINT, ELSET=ELPR, POSITION=AVERAGED AT NODES, FREQUENCY=1

S

*NODE PRINT, NSET=TOP, FREQUENCY=999

U

*END STEP

Appendix E:

*HEADING

ULTIMATE STRENGTH OF A COLUMN without RESIDUAL STRESSES

*PREPRINT, ECHO=YES, MODEL=NO, HISTORY=NO

*NODE, SYSTEM=C, NSET=BOT

101,0.15,0.0,0.0

112,0.15,330,0.0

113,0.0,0.0,0.0

301,0.3,0.0,0.0

312,0.3,330,0.0

501,0.45,0.0,0.0

512,0.45,330,0.0

701,0.6,0.0,0.0

712,0.6,330,0.0

901,0.75,0.0,0.0

912,0.75,330,0.0

*NGEN, NSET=BOT, LINE=C

101,112,1,113,0,0,0,0,0,1.0

301,312,1,113,0,0,0,0,0,1.0

501,512,1,113,0,0,0,0,0,1.0

701,712,1,113,0,0,0,0,0,1.0

901,912,1,113,0,0,0,0,0,1.0

*NCOPY, OLD SET=BOT, CHANGENU=2000, NEW SET=NALL, SHIFT

0.00047,0,0.300000

0,0,0,0,0,0

*NCOPY, OLD SET=BOT, CHANGENU=4000, NEW SET=NALL,SHIFT

0.000933,0,0.600000

0,0,0,0,0,0

*NCOPY, OLD SET=BOT, CHANGENU=6000, NEW SET=NALL,SHIFT

0.00138,0,0.900000

0,0,0,0,0,0

*NCOPY, OLD SET=BOT, CHANGENU=8000, NEW SET=NALL,SHIFT

0.001807,0,1.200000

0,0,0,0,0,0

*NCOPY, OLD SET=BOT, CHANGENU=10000, NEW SET=NALL,SHIFT

0.002204,0,1.500000

0,0,0,0,0,0

*NCOPY, OLD SET=BOT, CHANGENU=12000, NEW SET=NALL,SHIFT

0.002567,0,1.800000

0,0,0,0,0,0

*NCOPY, OLD SET=BOT, CHANGENU=14000, NEW SET=NALL,SHIFT

0.002889,0,2.100000

0,0,0,0,0,0

*NCOPY, OLD SET=BOT, CHANGENU=16000, NEW SET=NALL,SHIFT

0.003166,0,2.400000

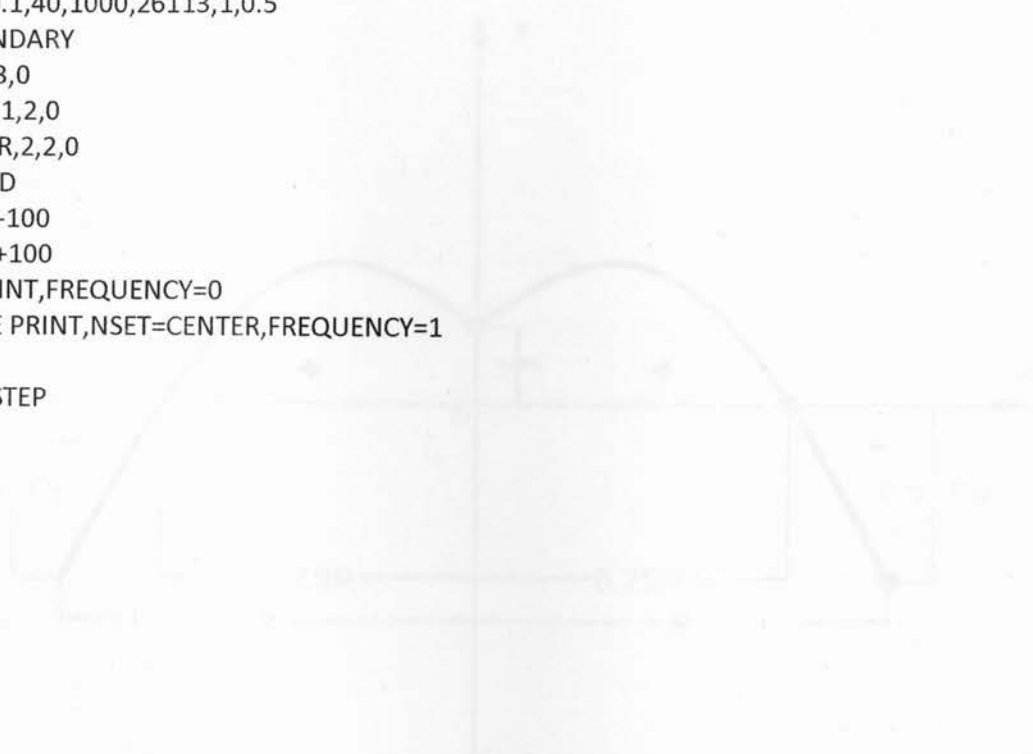
0,0,0,0,0,0

*NCOPY, OLD SET=BOT, CHANGENU=18000, NEW SET=NALL,SHIFT

0.003393,0,2.700000
0,0,0,0,0,0,0
*NCOPY, OLD SET=BOT, CHANGENU=20000, NEW SET=NALL,SHIFT
0.003566,0,3.000000
0,0,0,0,0,0,0
*NCOPY, OLD SET=BOT, CHANGENU=22000, NEW SET=NALL,SHIFT
0.003684,0,3.300000
0,0,0,0,0,0,0
*NCOPY, OLD SET=BOT, CHANGENU=24000, NEW SET=NALL,SHIFT
0.003743,0,3.600000
0,0,0,0,0,0,0
*NCOPY, OLD SET=BOT, CHANGENU=26000, NEW SET=NALL,SHIFT
0.003743,0,3.900000
0,0,0,0,0,0,0
*NCOPY, OLD SET=BOT, CHANGENU=28000, NEW SET=NALL,SHIFT
0.003684,0,4.200000
0,0,0,0,0,0,0
*NCOPY, OLD SET=BOT, CHANGENU=30000, NEW SET=NALL,SHIFT
0.003566,0,4.500000
0,0,0,0,0,0,0
*NCOPY, OLD SET=BOT, CHANGENU=32000, NEW SET=NALL,SHIFT
0.003393,0,4.800000
0,0,0,0,0,0,0
*NCOPY, OLD SET=BOT, CHANGENU=34000, NEW SET=NALL,SHIFT
0.003166,0,5.100000
0,0,0,0,0,0,0
*NCOPY, OLD SET=BOT, CHANGENU=36000, NEW SET=NALL,SHIFT
0.002889,0,5.400000
0,0,0,0,0,0,0
*NCOPY, OLD SET=BOT, CHANGENU=38000, NEW SET=NALL,SHIFT
0.002567,0,5.700000
0,0,0,0,0,0,0
*NCOPY, OLD SET=BOT, CHANGENU=40000, NEW SET=NALL,SHIFT
0.002204,0,6.000000
0,0,0,0,0,0,0
*NCOPY, OLD SET=BOT, CHANGENU=42000, NEW SET=NALL,SHIFT
0.001807,0,6.300000
0,0,0,0,0,0,0
*NCOPY, OLD SET=BOT, CHANGENU=44000, NEW SET=NALL,SHIFT
0.00138,0,6.600000
0,0,0,0,0,0,0
*NCOPY, OLD SET=BOT, CHANGENU=46000, NEW SET=NALL,SHIFT
0.000933,0,6.900000
0,0,0,0,0,0,0
*NCOPY, OLD SET=BOT, CHANGENU=48000, NEW SET=NALL, SHIFT
0.00047,0,7.200000
0,0,0,0,0,0,0
*NCOPY, OLD SET=BOT, CHANGENU=50000, NEW SET=TOP, SHIFT

```
0,0,7.500000
0,0,0,0,0,0
*NSET,NSET=CENTER,GENERATE
113,50113,2000
*ELEMENT, TYPE=C3D6
1,101,102,113,2101,2102,2113
2,102,103,113,2102,2103,2113
3,103,104,113,2103,2104,2113
4,104,105,113,2104,2105,2113
5,105,106,113,2105,2106,2113
6,106,107,113,2106,2107,2113
7,107,108,113,2107,2108,2113
8,108,109,113,2108,2109,2113
9,109,110,113,2109,2110,2113
10,110,111,113,2110,2111,2113
11,111,112,113,2111,2112,2113
12,112,101,113,2112,2101,2113
*ELGEN, ELSET=ELSET1
1,25,2000,1000
2,25,2000,1000
3,25,2000,1000
4,25,2000,1000
5,25,2000,1000
6,25,2000,1000
7,25,2000,1000
8,25,2000,1000
9,25,2000,1000
10,25,2000,1000
11,25,2000,1000
12,25,2000,1000
*ELEMENT,TYPE=C3D8
101,101,301,302,102,2101,2301,2302,2102
112,112,312,301,101,2112,2312,2301,2101
*ELGEN
101,4,200,100
112,4,200,100
*ELGEN, ELSET=ELSET2
101,11,1,1,25,2000,1000
112,25,2000,1000
*ELGEN,ELSET=ELSET3
201,11,1,1,25,2000,1000
212,25,2000,1000
*ELGEN,ELSET=ELSET4
301,11,1,1,25,2000,1000
312,25,2000,1000
*ELGEN,ELSET=ELSET5
401,11,1,1,25,2000,1000
412,25,2000,1000
```

```
*ELSET,ELSET=ELALL
ELSET1,ELSET2,ELSET3,ELSET4,ELSET5
*SOLID SECTION,ELSET=ELALL, MATERIAL=STEEL
*MATERIAL,NAME=STEEL
*ELASTIC
2.9008E7,0.3
*PLASTIC
50038
*STEP,NLGEOM,INC=50
*STATIC, RIKS
0.1,1,0.1,40,1000,26113,1,0.5
*BOUNDARY
113,1,3,0
50113,1,2,0
CENTER,2,2,0
*CLOAD
TOP,3,-100
Bot,3,+100
*EL PRINT,FREQUENCY=0
*NODE PRINT,NSET=CENTER,FREQUENCY=1
u1
*END STEP
```

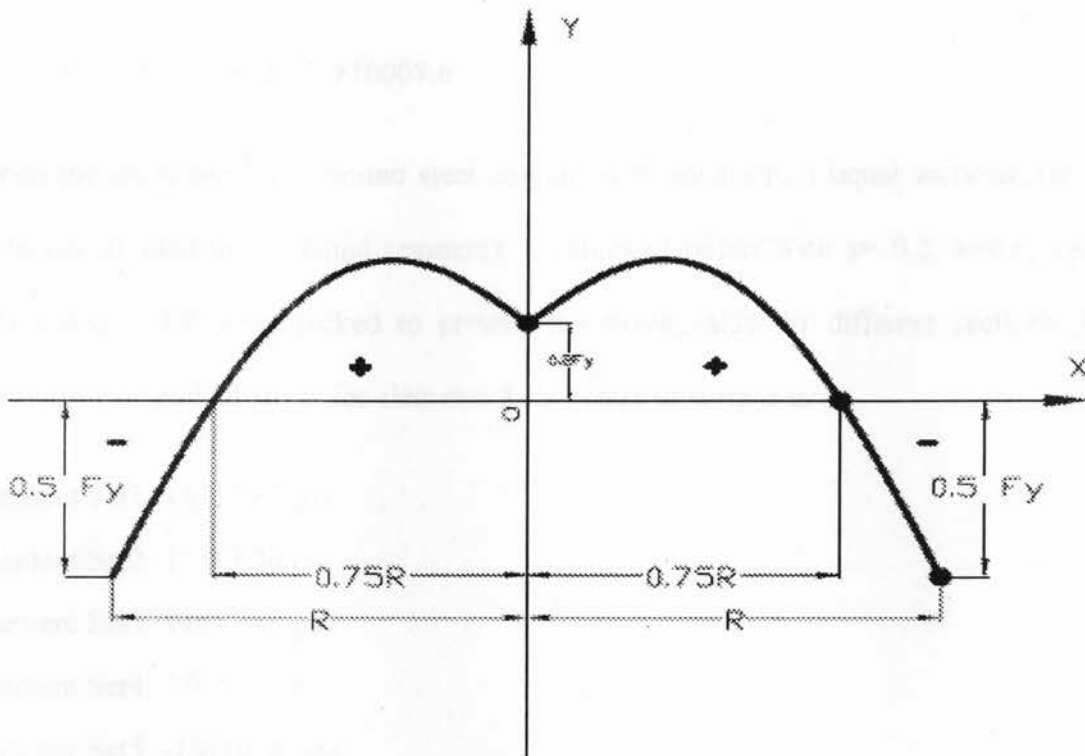


Appendix F:

Sample calculation of symmetrical residual stress from Roy's study (Roy, 2008):

For $R=2$ inch steel column, $F_y=345$ MPa=50,038 psi

From the result of Roy's study, distribution of symmetrical residual stress has typical profile as shown below:



Based on the assumption, the second order polynomial curve goes through 3 points:

Point1: $(0, 0.2F_y) = (0, 100, 07.6)$

Point2: $(0.75R, 0) = (1.5, 0)$

Point3: $(R, -0.5F_y) = (2, -25, 019)$

The equation of the parabola can be developed by substituting these 3 points in and is listed below:

$$y = -21683.13x^2 + 25852.97x + 10007.6$$

Since the cross-section of round steel column is divided into 5 equal sections, (ie: the radius is divided into 5 equal segment), y values of points with $x = 0.2$, $x = 0.6$, $x = 1.0$, $x = 1.4$ and $x = 1.8$ were picked to present the stress value for different sections. The symmetrical residual stress for elements from centre to surface is:

Element Set1: 14310.87 psi

Element Set2: 17713.46 psi

Element Set3: 14177.44 psi

Element Set4: 3702.82 psi

Element Set5: -13710.40 psi

Appendix G:

*HEADING

ULTIMATE STRENGTH OF A COLUMN with NON-SYMMETRICAL RESIDUAL STRESSES

*PREPRINT, ECHO=YES, MODEL=NO, HISTORY=NO

*NODE

1,-0.5625,-0.375,0

5,-0.5625,0.375,0

31,0.5625,-0.375,0

35,0.5625,0.375,0

36,-0.375,-0.5625,0

40,0.375,-0.5625,0

41,-0.375,0.5625,0

45,0.375,0.5625,0

*NGEN,NSET=LEFT

1,5,1

*NGEN,NSET=RIGHT

31,35,1

*NFILL,NSET=SQUARE

LEFT,RIGHT,6,5

*NGEN,NSET=DOWN

36,40,1

*NGEN,NSET=UP

41,45,1

*NODE,NSET=EDGE

46,0,0.75,0

47,0.1875,0.726184,0

48,0.375,0.649519,0

49,0.496078,0.5625,0

50,0.5625,0.496078,0

51,0.649519,0.375,0

52,0.726184,0.1875,0

53,0.75,0,0

54,0.726184,-0.1875,0

55,0.649519,-0.375,0

56,0.5625,-0.496078,0

57,0.496078,-0.5625,0

58,0.375,-0.649519,0

59,0.1875,-0.726184,0

60,0,-0.75,0

61,-0.1875,-0.726184,0

62,-0.375,-0.649519,0

63,-0.496078,-0.5625,0

64,-0.5625,-0.496078,0

65,-0.649519,-0.375,0

66,-0.726184,-0.1875,0

67,-0.75,0,0

68,-0.726184,0.1875,0

69,-0.649519,0.375,0
70,-0.5625,0.496078,0
71,-0.496078,0.5625,0
72,-0.375,0.649519,0
73,-0.1875,0.726184,0
*NSET,NSET=BOT
SQUARE,DOWN,UP,EDGE
*NCOPY, OLD SET=BOT, CHANGENU=2000, NEW SET=NALL, SHIFT
0.00188,0,0.300000
0,0,0,0,0,0
*NCOPY, OLD SET=BOT, CHANGENU=4000, NEW SET=NALL,SHIFT
0.00373,0,0.600000
0,0,0,0,0,0
*NCOPY, OLD SET=BOT, CHANGENU=6000, NEW SET=NALL,SHIFT
0.005522,0,0.900000
0,0,0,0,0,0
*NCOPY, OLD SET=BOT, CHANGENU=8000, NEW SET=NALL,SHIFT
0.007226,0,1.200000
0,0,0,0,0,0
*NCOPY, OLD SET=BOT, CHANGENU=10000, NEW SET=NALL,SHIFT
0.008817,0,1.500000
0,0,0,0,0,0
*NCOPY, OLD SET=BOT, CHANGENU=12000, NEW SET=NALL,SHIFT
0.010268,0,1.800000
0,0,0,0,0,0
*NCOPY, OLD SET=BOT, CHANGENU=14000, NEW SET=NALL,SHIFT
0.011558,0,2.100000
0,0,0,0,0,0
*NCOPY, OLD SET=BOT, CHANGENU=16000, NEW SET=NALL,SHIFT
0.012665,0,2.400000
0,0,0,0,0,0
*NCOPY, OLD SET=BOT, CHANGENU=18000, NEW SET=NALL,SHIFT
0.013572,0,2.700000
0,0,0,0,0,0
*NCOPY, OLD SET=BOT, CHANGENU=20000, NEW SET=NALL,SHIFT
0.014266,0,3.000000
0,0,0,0,0,0
*NCOPY, OLD SET=BOT, CHANGENU=22000, NEW SET=NALL,SHIFT
0.014734,0,3.300000
0,0,0,0,0,0
*NCOPY, OLD SET=BOT, CHANGENU=24000, NEW SET=NALL,SHIFT
0.01497,0,3.600000
0,0,0,0,0,0
*NCOPY, OLD SET=BOT, CHANGENU=26000, NEW SET=NALL,SHIFT
0.01497,0,3.900000
0,0,0,0,0,0
*NCOPY, OLD SET=BOT, CHANGENU=28000, NEW SET=NALL,SHIFT
0.014734,0,4.200000

0,0,0,0,0,0
 *NCOPY, OLD SET=BOT, CHANGENU=30000, NEW SET=NALL,SHIFT
 0.014266,0,4.500000
 0,0,0,0,0,0
 *NCOPY, OLD SET=BOT, CHANGENU=32000, NEW SET=NALL,SHIFT
 0.013572,0,4.800000
 0,0,0,0,0,0
 *NCOPY, OLD SET=BOT, CHANGENU=34000, NEW SET=NALL,SHIFT
 0.012665,0,5.100000
 0,0,0,0,0,0
 *NCOPY, OLD SET=BOT, CHANGENU=36000, NEW SET=NALL,SHIFT
 0.011558,0,5.400000
 0,0,0,0,0,0
 *NCOPY, OLD SET=BOT, CHANGENU=38000, NEW SET=NALL,SHIFT
 0.010268,0,5.700000
 0,0,0,0,0,0
 *NCOPY, OLD SET=BOT, CHANGENU=40000, NEW SET=NALL,SHIFT
 0.008817,0,6.000000
 0,0,0,0,0,0
 *NCOPY, OLD SET=BOT, CHANGENU=42000, NEW SET=NALL,SHIFT
 0.007226,0,6.300000
 0,0,0,0,0,0
 *NCOPY, OLD SET=BOT, CHANGENU=44000, NEW SET=NALL,SHIFT
 0.005522,0,6.600000
 0,0,0,0,0,0
 *NCOPY, OLD SET=BOT, CHANGENU=46000, NEW SET=NALL,SHIFT
 0.00373,0,6.900000
 0,0,0,0,0,0
 *NCOPY, OLD SET=BOT, CHANGENU=48000, NEW SET=NALL, SHIFT
 0.00188,0,7.200000
 0,0,0,0,0,0
 *NCOPY, OLD SET=BOT, CHANGENU=50000, NEW SET=TOP, SHIFT
 0,0,7.500000
 0,0,0,0,0,0
 *NSET,NSET=CENTER,GENERATE
 18,50018,2000
 *ELEMENT,TYPE=C3D8
 1,1,6,7,2,2001,2006,2007,2002
 25,36,37,11,6,2036,2037,2011,2006
 26,37,38,16,11,2037,2038,2016,2011
 27,38,39,21,16,2038,2039,2021,2016
 28,39,40,26,21,2039,2040,2026,2021
 29,10,15,42,41,2010,2015,2042,2041
 30,15,20,43,42,2015,2020,2043,2042
 31,20,25,44,43,2020,2025,2044,2043
 32,25,30,45,44,2025,2030,2045,2044
 33,43,44,47,46,2043,2044,2047,2046
 34,44,45,48,47,2044,2045,2048,2047

35,34,52,51,35,2034,2052,2051,2035
36,33,53,52,34,2033,2053,2052,2034
37,32,54,53,33,2032,2054,2053,2033
38,31,55,54,32,2031,2055,2054,2032
39,59,58,40,39,2059,2058,2040,2039
40,60,59,39,38,2060,2059,2039,2038
41,61,60,38,37,2061,2060,2038,2037
42,62,61,37,36,2062,2061,2037,2036
43,65,1,2,66,2065,2001,2002,2066
44,66,2,3,67,2066,2002,2003,2067
45,67,3,4,68,2067,2003,2004,2068
46,68,4,5,69,2068,2004,2005,2069
47,41,42,73,72,2041,2042,2073,2072
48,42,43,46,73,2042,2043,2046,2073
57,30,35,49,45,2030,2035,2049,2045
58,40,57,31,26,2040,2057,2031,2026
59,63,36,6,1,2063,2036,2006,2001
60,5,10,41,71,2005,2010,2041,2071
*ELGEN
1,6,5,1,4,1,6
*ELEMENT, TYPE=C3D6
49,45,49,48,2045,2049,2048
50,35,51,50,2035,2051,2050
51,56,55,31,2056,2055,2031
52,58,57,40,2058,2057,2040
53,62,36,63,2062,2036,2063
54,64,1,65,2064,2001,2065
55,69,5,70,2069,2005,2070
56,71,41,72,2071,2041,2072
61,35,50,49,2035,2050,2049
62,57,56,31,2057,2056,2031
63,64,63,1,2064,2063,2001
64,5,71,70,2005,2071,2070
*ELGEN, ELSET=ELSET1
55,25,2000,1000
46,25,2000,1000
45,25,2000,1000
44,25,2000,1000
43,25,2000,1000
54,25,2000,1000
*ELGEN, ELSET=ELSET2
56,25,2000,1000
64,25,2000,1000
60,25,2000,1000
19,25,2000,1000
13,25,2000,1000
7,25,2000,1000
1,25,2000,1000

59,25,2000,1000
63,25,2000,1000
53,25,2000,1000
*ELGEN, ELSET=ELSET3
47,25,2000,1000
29,25,2000,1000
20,25,2000,1000
14,25,2000,1000
8,25,2000,1000
2,25,2000,1000
25,25,2000,1000
42,25,2000,1000
*ELGEN, ELSET=ELSET4
48,25,2000,1000
30,25,2000,1000
21,25,2000,1000
15,25,2000,1000
9,25,2000,1000
3,25,2000,1000
26,25,2000,1000
41,25,2000,1000
*ELGEN, ELSET=ELSET5
33,25,2000,1000
31,25,2000,1000
22,25,2000,1000
16,25,2000,1000
10,25,2000,1000
4,25,2000,1000
27,25,2000,1000
40,25,2000,1000
*ELGEN, ELSET=ELSET6
34,25,2000,1000
32,25,2000,1000
23,25,2000,1000
17,25,2000,1000
11,25,2000,1000
5,25,2000,1000
28,25,2000,1000
39,25,2000,1000
*ELGEN, ELSET=ELSET7
49,25,2000,1000
57,25,2000,1000
61,25,2000,1000
24,25,2000,1000
18,25,2000,1000
12,25,2000,1000
6,25,2000,1000
58,25,2000,1000

```
62,25,2000,1000
52,25,2000,1000
*ELGEN, ELSET=ELSET8
50,25,2000,1000
35,25,2000,1000
36,25,2000,1000
37,25,2000,1000
38,25,2000,1000
51,25,2000,1000
*ELSET,ELSET=ELALL
ELSET1,ELSET2,ELSET3,ELSET4,ELSET5,ELSET6,ELSET7,ELSET8
*SOLID SECTION,ELSET=ELALL, MATERIAL=STEEL
*MATERIAL,NAME=STEEL
*ELASTIC
2.9008E7,0.3
*PLASTIC
50038
*STEP,NLGEOM,INC=50
*STATIC, RIKS
0.1,1,0.1,40,1000,26018,1,0.5
*BOUNDARY
18,1,3,0
50018,1,2,0
CENTER,2,2,0
*CLOAD
TOP,3,-100
BOT,3,+100
*EL PRINT,FREQUENCY=0
*NODE PRINT,NSET=CENTER,FREQUENCY=1
u1
*END STEP
```